

Train and You'll Miss It: Interactive Model Iteration with Weak Supervision and Pre-Trained Embeddings

Mayee F. Chen* Daniel Y. Fu*† Frederic Sala Sen Wu Ravi Teja Mullapudi
 Fait Poms Kayvon Fatahalian Christopher Ré
 {mfchen, danfu, fredsala, senwu, fpoms, kayvonf, chrismre}@cs.stanford.edu,
 mullapudi@cs.cmu.edu

Abstract

Our goal is to enable machine learning systems to be trained interactively. This requires models that perform well and train quickly, without large amounts of hand-labeled data. We take a step forward in this direction by borrowing from weak supervision (WS), wherein models can be trained with noisy sources of signal instead of hand-labeled data. But WS relies on training downstream deep networks to extrapolate to unseen data points, which can take hours or days. Pre-trained embeddings can remove this requirement. We do not use the embeddings as features as in transfer learning (TL), which requires fine-tuning for high performance, but instead use them to define a distance function on the data and extend WS source votes to nearby points. Theoretically, we provide a series of results studying how performance scales with changes in source coverage, source accuracy, and the Lipschitzness of label distributions in the embedding space, and compare this rate to standard WS without extension and TL without fine-tuning. On six benchmark NLP and video tasks, our method outperforms WS without extension by 4.1 points, TL without fine-tuning by 12.8 points, and traditionally-supervised deep networks by 13.1 points, and comes within 0.7 points of state-of-the-art weakly-supervised deep networks—all while training in less than half a second.

1 Introduction

The introduction of the interactive console in 1962 revolutionized how people write computer programs [10]. Machine learning similarly stands to benefit from enabling *programmatically-interactive* model iteration cycles—training models, inspecting their results, and fixing failure modes in seconds, instead of hours or days. This requires models that perform well and train quickly, without requiring large amounts of hand-labeled data. Modern deep learning models can achieve high performance, but only at the cost of heavy training over large amounts of labeled data to optimize feature representations, precluding the possibility of such interactive timescales. In this paper, we build models that can be iterated on interactively and achieve high performance without having to optimize features through training.

To do so, we borrow from work in weak supervision (WS), which enables more interactive interfaces for model iteration. WS methods automatically generate probabilistic labels for training data from multiple weak sources—such as heuristics, external knowledge bases, and user-defined functions [23, 50, 15, 14, 28, 41, 44, 30, 13, 43, 72, 25] instead of relying on hand labels. WS has been used throughout industry [58, 53, 5, 59] and academia [19, 55] to enable more interactive model iteration; instead of adjusting model behavior by hand-labeling training data, users instead write heuristics or tweak existing sources to change the training labels.

The WS probabilistic labels can be used directly as final model predictions, but can have trouble extrapolating to unseen data points. WS frameworks often train downstream deep networks to achieve

*Denotes equal contribution. †Corresponding author.

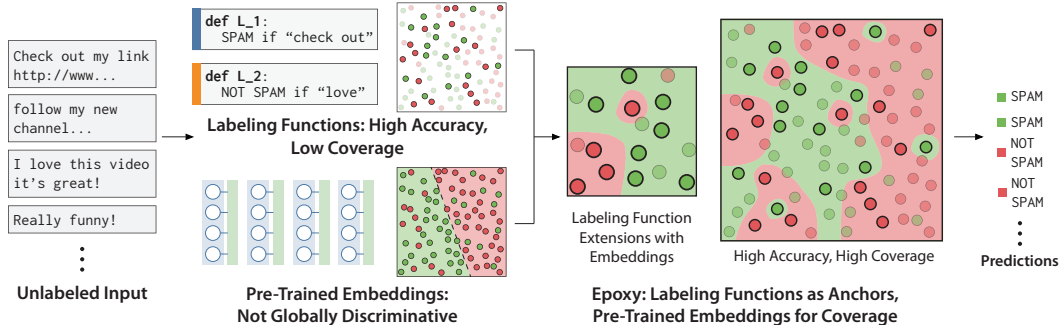


Figure 1: Weak sources may have high accuracy but only cover a limited subset of the data. Pre-trained embeddings may not be globally discriminative without fine-tuning. EPOXY combines both by using pre-trained embeddings to locally extend labeling sources, achieving high overall performance.

good performance in these cases. Deep networks can pull out more general signals from the data than are encoded in the weak sources, which often have low coverage over the dataset and thus do not extrapolate well on their own. Figure 1 (middle top) shows a representative example. In text applications, deep networks can find synonyms to user-provided key words or relax word order, whereas user-provided heuristic functions often encode specific phrases. But training these deep networks can take hours or days, slowing down model iteration past interactive timescales.

How can we get the interactivity benefits of programmatic WS without having to train deep networks for good performance? The popularity of transfer learning (TL) suggests that using deep networks pre-trained on large datasets can reduce training costs [17, 16, 33]. But TL often requires fine-tuning to achieve high accuracies—since pre-trained embeddings may not contain enough information to be globally discriminative (Figure 1 middle bottom). Although fine-tuning is cheaper than training from scratch, it still requires many iterations of gradient descent.

We propose a different mechanism for using pre-trained embeddings to enable high-quality WS without training a deep network. Although pre-trained embeddings might not be sufficiently discriminative to use as features alone, we observe that they can often be used to create a sufficiently-reliable local notion of distance between points (essentially a type of kernel). We use this distance notion to smoothly transfer source votes to points that are nearby in embedding space (Figure 1 right)—exploiting the idea that nearby points in a relevant embedding space should have similar labels. This mechanism is similar to semi-supervised techniques like label propagation [74, 27], but we use the machinery of WS to anchor on weakly-labeled points instead of assuming gold labels (and we do not tune the embeddings). Perhaps surprisingly, our approach, named EPOXY, can sometimes recover the performance of state-of-the-art weakly-supervised downstream deep networks, and outperform traditionally-supervised deep networks—without having to rely on an expensive training procedure.

Theoretically, we provide a sequence of results evaluating how much signal we can extract from pre-trained embeddings using EPOXY. First, we define a notion of probabilistic Lipschitzness [35] to describe the label space’s smoothness, with which we can tightly characterize the improvement in rate of convergence and generalization error of EPOXY in the size of the (unlabeled) data over WS without source extensions. We show that improvement depends on two factors: the increase in coverage from extending weak labels, and the accuracy of the extension. Next, we show how the Lipschitzness of the task label distribution is related to the intrinsic quality of the model used to produce the pre-trained embedding, and we use this connection to bound how close we are to the performance of such models. Finally, we describe the conditions under which our method outperforms TL without fine-tuning; we do so by viewing the weak sources as an ensemble of specialized models.

We empirically validate EPOXY on six benchmark NLP and video applications that have been used to evaluate previous state-of-the-art weak supervision frameworks (and thus have weak sources readily available) [52, 20]. EPOXY outperforms WS without source extensions and without training a downstream deep network by 4.1 points, and outperforms non-finetuned TL by 12.8 points. EPOXY achieves training cycles of less than half a second—but comes within 0.7 points of training deep networks with state-of-the-art weak supervision techniques, which themselves outperform fully-supervised deep network baselines by 13.8 points.

Algorithm 1 Labeling Function Extension Method

Input: Unlabeled dataset $D = \{X_i\}_{i=1}^n$, labeling functions $\lambda = \lambda_1, \dots, \lambda_m$, embedding distance function d_Z , threshold radii $r \in \mathbb{R}^m$, weighting function W .
Returns: $\lambda_1, \dots, \bar{\lambda}_m$
for $\lambda_j \in \lambda, X_i \in D$ **do**
 if $\lambda_j(X_i) \neq 0$ **then**
 $\bar{\lambda}_j(X_i) := \lambda_j(X_i)$
 else
 Compute the set of X_i 's labeled neighbors, $N_{r_j}(X_i) = \{X \in \text{supp}(\lambda_j) : d_Z(X, X_i) \leq r_j\}$.
 if $|N_{r_j}(X_i)| \neq 0$ **then**
 Assign $\bar{\lambda}_j(X_i) = W(N_{r_j}(X_i))$.
 else
 X_i is too far from $\text{supp}(\lambda_j)$, so the new labeling function still abstains with $\bar{\lambda}_j(X_i) = 0$.
end for

2 Preliminaries

We provide necessary background on weak supervision and pre-trained deep networks. A more in-depth discussion is presented in the related work (Section 6).

Weakly-supervised machine learning. In WS [51, 52, 50], practitioners programmatically generate training labels from multiple noisy label sources. For example, a practitioner trying to classify comments as spam could write heuristics looking for key words like “check out” (comments that say “check out my channel” are likely to be spam). Sources can vote or abstain on individual points (while “check out” is a strong signal for *spam*, its absence does not mean the comment is *not spam*).

Formally, let $X = [X^1, X^2, \dots, X^T] \in \mathcal{X}$ be a vector of T related elements (e.g., contiguous frames in a video) and $Y = [Y^1, Y^2, \dots, Y^T] \in \mathcal{Y}$ be the vector of *unobserved* true task labels (we refer to each Y^i as a task), with (X, Y) drawn from some distribution \mathcal{D} . Let there be m weak sources λ , each voting or abstaining per X via a *labeling function* $\lambda_j : \mathcal{X} \rightarrow \mathcal{Y} \cup \{0\}$ for all $j = 1, \dots, m$ ($\lambda_j(X) = 0$ is an abstain). Let λ'_j index abstentions, with $\lambda'_j(X) = 0$ if $\lambda_j(X) = 0$ and $\lambda'_j(X) = 1$ otherwise. Let $\text{supp}(\lambda_j)$ be the points λ_j votes on, with *coverage* the proportional size of $\text{supp}(\lambda_j)$, and *minimal overlap* o_{\min} be $o_{\min} = \min_i \max_{j:j \neq i} \Pr(X \in \text{supp}(\lambda_i) \cap \text{supp}(\lambda_j))$.

The goal is to learn the joint distribution $P(Y, \lambda)$, called the *label model*, to combine votes into element-wise probabilistic labels by applying the m sources to an unlabeled dataset $D = \{X_i\}_{i=1}^n$. The label model can be used directly for inference (i.e., the probabilistic labels are the final predictions) but is only useful on points in the support of the labeling functions. For better extrapolation, the labels are used to train an end model $f_w \in \mathcal{F} : \mathcal{X} \rightarrow \mathcal{Y}$.

Pre-trained networks. Formally, we treat pre-trained networks as mapping $g : \mathcal{X} \rightarrow \mathcal{Z}$ from data points into an embedding space \mathcal{Z} . Fine-tuning changes this mapping during training; transfer learning without fine-tuning learns a function $f_z : \mathcal{Z} \rightarrow \mathcal{Y}$. We associate with \mathcal{Z} a distance function $d_Z : \mathcal{Z} \times \mathcal{Z} \rightarrow \mathbb{R}$, and for convenience write $d_Z(X_1, X_2)$ for $d_Z(g(X_1), g(X_2))$. To characterize the behavior of label distributions with respect to the embedding space, we adapt the idea of conditional probabilistic Lipschitzness in [35, 47] to present a variant of probabilistic bi-Lipschitzness:

Definition 1. ((L, M) -Lipschitzness. Define the metric space (\mathcal{Z}, d_Z) and functions $L, M : \mathbb{R} \rightarrow [0, 1]$. For $V \in \{\lambda'_1, \dots, \lambda'_m, Y\}$, we say that the function V is (L, M) -Lipschitz if for all $r > 0$,

$$L(r) \leq P_{X_1, X_2}(V(X_1) \neq V(X_2) \mid d_Z(X_1, X_2) \leq r) \leq M(r),$$

where $Y(X_1) = Y_1, Y(X_2) = Y_2$, and $(X_1, Y_1), (X_2, Y_2) \sim \mathcal{D}$.

3 Improving Label Model Performance with Pre-trained Embeddings

We describe EPOXY. Our goal is to combine pre-trained embeddings and noisy labeling functions to approach the performance of a deep network without the need for fine-tuning. As in the standard WS approach, we are given labeling functions $\lambda = \lambda_1, \dots, \lambda_m$ and an unlabeled dataset $D = \{X_i\}_{i=1}^n$. Instead of learning $P(Y, \lambda)$ directly from these inputs, we add an extension stage to generate extended labeling functions $\bar{\lambda}$, and then learn $P(Y, \bar{\lambda})$ using WS techniques.

Extension stage. In the *extension* stage, we examine the output of λ_j . If it votes on X_i , e.g. $X_i \in \text{supp}(\lambda_j)$, the vote is unchanged. If λ_j abstains, we use pre-trained embeddings to potentially produce a vote on X_i . To do so, we use an *extension radius* r_j for each labeling function λ_j . The extension process is simple—if X_i is not labeled by λ_j , we search for the neighborhood of points labeled by λ_j within a radius of r_j from X_i , which we denote as the set $N_{r_j}(X_i)$, and assign to X_i the thresholded output of the function $W(N_{r_j}(X_i)) = \sum_{X_k \in N_{r_j}(X_i)} w_k \lambda_j(X_k)$ for some weighting rule. The newly labeled area is now defined as $B_r(\lambda_j) = \{X_i \notin \text{supp}(\lambda_j) : \exists X_k \in \text{supp}(\lambda_j) \text{ s.t. } d_{\mathcal{Z}}(X_i, X_k) \leq r_j\}$, while in other areas we maintain the abstention. There are multiple choices for the weighting rule, some of which provide strong theoretical guarantees as described in in Section 4. In practice, we observe that simple rules such as 1-nearest neighbor yield excellent performance. Afterwards, we have extended labeling functions $\bar{\lambda}_i$, and we can use any WS technique that uses the interface described in the background.¹ This procedure is summarized in Algorithm 1.

4 Theoretical Analysis

Now we analyze our method for improving label model generalization. We bound the generalization lift and rate improvement of our method over standard WS in terms of the Lipschitzness of our labels. Next, we connect label Lipschitzness with the intrinsic quality of the pre-trained model used for the embeddings. Finally, we bound the generalization gap between EPOXY and an end model trained on the embeddings, and we describe the conditions under which our method outperforms transfer learning (TL). We present our proofs and synthetic experiments in the Appendix.

Comparison to standard WS. We characterize the minimum improvement and convergence rate of generalization error for EPOXY versus WS label model without source extensions in terms of two factors: accuracy and coverage. For simplicity, we use a single class-balanced task $Y \in \{-1, 1\}$. We assume that Y is (L_Y, M_Y) -Lipschitz, and each labeling function (LF) is $(L_{\lambda'_i}, M_{\lambda'_i})$ -Lipschitz. We consider the case of extending one LF λ_i whose accuracy is uniform on its support. The analysis for more general cases is found in the Appendix.

The first quantity of interest is the *accuracy* of an extended labeling function. Define the accuracy of the original λ_i to be $a_i := \Pr(\lambda_i = Y | \lambda_i \neq 0)$, $p_i = \Pr(X \in \text{supp}(\lambda_i))$ for the support of λ_i , and $p_{d(r)} = \Pr(d_{\mathcal{Z}}(X, X') \leq r)$. We can express the *extended accuracy* \bar{a}_i as a function of a_i .

Proposition 1. *Denote the extended accuracy of $\bar{\lambda}_i$ with threshold radius r to be $\bar{a}_i := \Pr(\bar{\lambda}_i = Y | \bar{\lambda}_i \neq 0)$. There exists a weighting rule such that*

$$\bar{a}_i \geq a_i - (2a_i - 1) \frac{M_Y(r)}{p_i^2(1 + L_{\lambda'_i}(r)p_{d(r)})}.$$

The accuracy of the extended LF is dependent on the Lipschitzness of the task and the original LF accuracy. Assuming that $a_i > 0.5$, i.e. the LF votes better than random, the extended accuracy roughly gets worse as the ratio $M_Y(r)/L_{\lambda'_i}(r)$ increases, as we would expect.

The other quantity of interest is how much we extend the *coverage* of LFs. As coverage increases, there are two effects. First, more points are labeled, resulting in potentially greater generalization lift. Second, the supports of extended labeling functions will overlap more, resulting in better estimation of accuracy parameters for the WS label model. Recall our definition of o_{\min} . Define $L_{\min} = \min_{\lambda'_i, r_i} L_{\lambda'_i}(r_i)$ and $r_{\min} = \min_i r_i$. The increase in the minimum overlap of supports o_{\min} after extending depends on L_{\min} and r_{\min} , which thus controls estimation error.

We can now compare the generalization error of EPOXY versus standard WS in terms of rates and asymptotic risk. Define the risk of a model f as $\mathcal{R}(f) = \mathbb{E}_{(X,Y) \sim \mathcal{D}} [\ell(f(X), Y)]$, where ℓ is a loss function. In WS, the output is a probabilistic label \tilde{Y} estimated using our LFs λ . The label model risk is $\mathcal{R}(f_{WS})$, where $f_{WS}(X) = 2 \Pr(\tilde{Y} = 1 | \lambda = \lambda_1(X), \dots, \lambda_m(X)) - 1$. We have similar definitions using $\bar{\lambda}$ for $\mathcal{R}(f_E)$ for EPOXY and we take the loss for both models to be $\ell(Y', Y) = \frac{1}{2} |Y - Y'|$. Next, $c_p = \min_X \Pr(\lambda = \lambda(X))$, e_{\min} is a lower bound on $\mathbb{E}[\lambda_i Y | \lambda_i \neq 0]$, c_1 is a lower bound on $\mathbb{E}[\lambda_i \lambda_j | \lambda_i, \lambda_j \neq 0]$, and $c_2 = \mathbb{E}[\Pr(Y = 1 | \lambda = \lambda(X))]$. Similar definitions hold for \bar{c}_p and other terms using $\bar{\lambda}$.

¹In the appendix, we review in more detail the choice used in our implementation and experimental setup.

Theorem 1. Define $\varepsilon_n = \sqrt{\frac{\log(2/\delta)}{2n}}$. With probability $\geq 1 - \delta$, the estimation error of EPOXY is

$$\mathbb{E} \left[|\mathcal{R}(f_E) - \mathcal{R}(\hat{f}_E)| \right] \leq \frac{1}{\bar{c}_p - \varepsilon_n} \left(\frac{81\sqrt{\pi}}{2\bar{e}_{\min}\bar{c}_1^2} \cdot \frac{m}{\sqrt{n \cdot o_{\min}(1 + (2L_{\min} - L_{\min}^2)p_{d(r_{\min})})}} + \varepsilon_n \bar{c}_2 \right),$$

while for WS it is

$$\mathbb{E} \left[|\mathcal{R}(f_{WS}) - \mathcal{R}(\hat{f}_{WS})| \right] \leq \frac{1}{c_p - \varepsilon_n} \left(\frac{81\sqrt{\pi}}{2e_{\min}c_1^2} \cdot \frac{m}{\sqrt{n \cdot o_{\min}}} + \varepsilon_n c_2 \right).$$

When λ_i is extended using threshold radius r and the same weighting rule as in Prop. 1, the asymptotic improvement in generalization error is at least

$$\mathcal{R}(f_{WS}) - \mathcal{R}(f_E) \geq L_{\lambda'_i}(r)p_{d(r)}p_i \left(\frac{1}{2}(C+1)(\tilde{a}_i\bar{a}_i + (1-\tilde{a}_i)(1-\bar{a}_i)) - C \right),$$

where $\tilde{a}_i \geq \bar{a}_i - (2a_i - 1) \frac{M_Y(r)}{L_{\lambda'_i}(r)p_{d(r)}p_i^2(1+L_{\lambda'_i}(r)p_{d(r)})}$ is the accuracy of $\bar{\lambda}_i$ over $B_r(\lambda_i)$, and C is a constant lower bounding the performance of the other labeling functions.

The convergence rate of EPOXY has asymptotic improvement of $\sqrt{1 + (2L_{\min} - L_{\min}^2)p_{d(r_{\min})}}$ over standard WS, which increases as the threshold radius increases. In the asymptotic case, we make the following observations about the generalization lift:

- The lift increases as the original accuracy a_i is increased, suggesting that the most accurate labeling functions should be extended.
- Given a fixed threshold radius, the lift decreases in $M_Y(r)$, suggesting that our extension method performs more poorly on less smooth embeddings.
- The lift improves as r increases due to $L_{\lambda'_i}(r)$ (more likely to extend to areas outside of support) and $p_{d(r)}$ (more points voted on), but the accuracies \tilde{a}_i and \bar{a}_i also become worse.

These insights imply that *there is a trade off between accuracy and coverage*. We illustrate this behavior and show how to set an approximate optimal radius in synthetic experiments (Appendix).

Comparison to models trained using the embeddings. Theorem 1 specifies the lift in terms of the Lipschitzness. How do we know what kind of Lipschitzness our embeddings-based approach will yield? We show the connection via a simple proposition. We write f_z for a model using the embeddings \mathcal{Z} . Below we implicitly take $\ell(f(X), Y)$ to be the 0/1 loss. Then,

Proposition 2. Suppose we have an embedding function g achieving risk $\mathcal{R}(f_z)$. Suppose also that the model class f_z satisfies $\Pr_{X_1, X_2}(f_z(X_1) \neq f_z(X_2) | d_{\mathcal{Z}}(X_1, X_2) \leq r) \leq M_{f_z}(r)$. Then, the labels Y have smoothness given by

$$\Pr_{X_1, X_2}(Y_1 \neq Y_2 | d_{\mathcal{Z}}(X_1, X_2) \leq r) \leq M_{f_z}(r) + 2\mathcal{R}(f_z).$$

This simple bound on smoothness inherited from an embedding-based model plugs in as the smoothness in Theorem 1. The key requirement is that the distance used to extend, $d_{\mathcal{Z}}$, is the same as that providing model smoothness (the $M_Y(r)$ above). Proposition 2 both explains when and why EPOXY produces a quality label model, and motivates its use (as opposed to simply extending one source).

An easy argument bounds the risk for a source $\bar{\lambda}_i$ with original accuracy a_i extended to cover all of \mathcal{X} . Suppose an embedding $Z = g(X)$ achieves a risk of $\mathcal{R}(f_z)$, and that the smallest radius needed to cover all of \mathcal{X} when extending λ_i is d_V . Then its risk is upper bounded as

$$\mathcal{R}(\bar{\lambda}_i) \leq 1 - a_i + (2a_i - 1) \frac{M_{f_z}(d_V) + 2\mathcal{R}(f_z)}{p_i^2(1 + L_{\lambda'_i}(d_V)p_{d(d_V)})}.$$

We note some implications: if λ_i is a low-quality source, with accuracy $a_i = 1/2$, then $\mathcal{R}(\bar{\lambda}_i) \leq 1$, which says nothing about the extension, as signal from the embeddings is washed out by the poor-quality source. If $a_i = 1$, our source is perfect on its support. Then the risk is a constant times

	Task (Embedding)	EPOXY	Interactive-Speed Baselines			Fully-Trained End Models		
			TS-NFT	WS-NFT	WS-LM	TS-FT	WS-FT	EPOXY-FT
NLP	Spam (BERT)	89.6	78.5	87.2	83.6	76.7	90.0	94.1
	Weather (BERT)	82.0	71.6	74.4	78.0	71.2	85.6	86.8
	Spouse (BERT)	<u>48.4</u>	17.7	17.5	47.0	20.4	49.6	51.3
Video	Basketball (RN-101)	<u>31.3</u>	18.8	16.8	27.9	26.8	35.8	36.7
	Commercial (RN-101)	<u>90.1</u>	73.6	75.5	88.4	90.9	92.5	93.0
	Tennis (RN-101)	<u>82.9</u>	76.7	79.5	82.0	57.6	82.9	83.1
	Basketball (BiT-M)	<u>42.5</u>	22.8	23.2	27.9	29.1	33.8	45.8
	Commercial (BiT-M)	<u>91.8</u>	71.7	73.8	88.4	93.2	93.7	94.4
	Tennis (BiT-M)	<u>83.1</u>	75.5	79.0	82.0	47.5	83.7	83.8
	Average Training Time (s)	0.5	1.2	5.7	0.1	1,243.0	5,354.1	4,995.0

Table 1: EPOXY performance and training time compared to baselines. Scores are F1 except for Spam and Weather (accuracy) and are averaged across five random seeds; best score in bold, best interactive-speed model underlined. Interactive-speed baselines include transfer learning without fine-tuning using traditional hand labels (TS-NFT) and WS probabilistic labels (WS-NFT), as well as WS label model (WS-LM). Fully-trained end models use traditional supervision (TS-FT), WS labels (WS-FT), and EPOXY-generated labels (EPOXY-FT).

the risk of the embedding-based model, with an additive term and scaling coming from the model smoothness and the radius. If we have a large representative support, driving $d_V \rightarrow 0$ and thus $M_{f_z}(d_V), L_{\lambda'_i}(d_V) \rightarrow 0$, the risk of the extended source is $2\mathcal{R}(f_z)$. This reproduces a learned model, without training—but such cases are rare, *motivating extensions of varying radii*.

Comparison to end models. While we may not be able to match the performance of a fully-trained deep neural network as an end model, we hope to approach it, and potentially even outperform more limited models. The next result uses the machinery built so far to derive conditions for the latter.

The intuition is to compare a model f_z from a class with fixed capacity trained over data from \mathcal{D} with an ensemble of m *specialized* models f_i each specialized to a distribution \mathcal{D}_i defined on a subspace \mathcal{X}_i . Intuitively, the risk of a specialized model, $\mathcal{R}(f_i)$, can be lower than $\mathcal{R}(f_z)$ when restricted to \mathcal{X}_i . When this happens, we expect the ensemble model’s risk to be superior.

We can relate extended sources to specialized models with Proposition 2, and use EPOXY instead of emsembling the sources, where each $\text{supp}(\bar{\lambda}_i) \supseteq \mathcal{X}_i$.

Theorem 2. *Let $f_i, 1 \leq i \leq m$ be defined as above. Define $p = \Pr(Y = 1)$, the max odds to be $b = \max\{\frac{p}{1-p}, \frac{1-p}{p}\}$, and $\mathcal{X}_0 = \{X : X \notin \bigcup_{i=1}^m \text{supp}(\lambda_i)\}$. Then,*

$$\mathcal{R}(f_E) \leq 2b \cdot \mathbb{E}_{\mathcal{D}_i} \left[1 - a_i + (2a_i - 1) \frac{M_{f_i}(r_i) + 2\mathcal{R}(f_i)}{p_i^2(1 + L_{\lambda'_i}(r_i)p_{d(r_i)})} \right] + 2\Pr(X \in \mathcal{X}_0)p(1-p).$$

Consequently, setting the right-hand expression to be less than $\mathcal{R}(f_z)$ gives us a condition characterizing when EPOXY beats an end model. That is, as long as the (average) specialization offers improved performance and the loss when passing from the specialized model to the extended source is smaller than this improvement, EPOXY outperforms an end model. As we shall see, this does not typically occur for a fully-trained deep model, but does for the TL without fine-tuning.

5 Evaluation

We evaluate EPOXY on benchmark WS tasks. We compare EPOXY’s performance against WS without label extension, against TL without fine-tuning, and against fully-trained deep networks, discuss ablations on optimizing r_i , and evaluate runtime.

Datasets. We evaluate EPOXY on six benchmark NLP and video analysis tasks that have been used to evaluate previous state-of-the-art weak supervision systems [20, 52]. For the text datasets, we use pre-trained BERT embeddings for label extension; for the video datasets, we use ResNet-101 pre-trained on ImageNet and BiT-M with ResNet-50x1 backbone, a recently-released model designed for visual transfer learning [33]. We use cosine distance as the distance function for all tasks, and use

	BERT			RN-101 ImageNet			BiT-M RN-50x1		
	Spam	Weather	Spouse	Basketball	Commercial	Tennis	Basketball	Commercial	Tennis
WS-LM average LF coverage	16.2	8.8	3.8	49.2	54.5	66.9	49.2	54.5	66.9
EPOXY average LF coverage	22.9	9.0	7.7	63.4	80.8	72.5	57.0	84.7	74.7
$1 - d(PT, DN)$	0.735	0.677	0.248	0.562	0.284	0.113	0.907	0.559	0.408
EPOXY vs. WS-LM	+6.0	+4.0	+1.4	+3.4	+1.7	+0.9	+14.6	+3.4	+1.1
Average LF accuracy	82.8	75.4	58.6	59.3	92.3	81.9	59.3	92.3	81.9
LF accuracy vs. TS-NFT	+4.3	+3.8	+41.1	+42.5	+18.7	+5.2	+36.1	+20.6	+6.4
LF accuracy vs. WS-NFT	-4.4	+1.0	+40.9	+40.5	+16.8	+2.4	+36.5	+18.5	+2.9
EPOXY vs. TS-NFT	+11.1	+10.4	+30.7	+12.5	+16.5	+6.2	+19.7	+20.1	+7.6
EPOXY vs. WS-NFT	+2.4	+7.6	+30.9	+14.5	+14.6	+3.4	+25.7	+16.3	+3.6
N_{train}/N_{dev}	13.2	3.7	7.9	17.0	6.8	9.3	17.0	6.8	9.3
EPOXY vs. TS-FT	+12.9	+10.8	+28.0	+4.5	-0.8	+25.3	+13.4	-1.4	+25.0
EPOXY vs. WS-FT	-0.4	-3.6	-1.2	-4.5	-2.4	+0.0	+8.7	-1.9	-0.6

Table 2: EPOXY lift compared to baselines with explanatory metrics. Top: EPOXY improves over WS-LM by improving average coverage of the labeling functions. Lift is correlated with the quantity $1 - d(PT, DN)$, the similarity between pre-trained and fine-tuned embeddings for each task according to distance. Middle: EPOXY outperforms transfer learning without fine-tuning because the labeling sources are accurate on average over their support sets. Bottom: EPOXY outperforms training a deep network over a small collection of hand labels (TS-FT) because it uses more data, and approaches the performance of training a deep network over probabilistic labels (WS-FT).

1-nearest neighbor as the weighting rule. **Spam** classifies whether YouTube comments are spam [3], **Weather** classifies sentiment over Tweets about weather [2], and **Spouse** seeks to extract spouse relationships in a set of news articles [11]. **Basketball** identifies basketball videos from a subset of ActivityNet [9], **Commercial** identifies commercials in a corpus of TV News [21, 1], and **Tennis** identifies tennis rallies from broadcast footage. Each dataset consists of a large unlabeled training set, a smaller hand-labeled *development set* (train/dev split sizes from 187/50 points to 64,130/9,479 points), and a held-out test set. We use the unlabeled training set to train label models and end models, and use the development set for a) training of traditional supervision baselines, and b) hyperparameter tuning of the label and end models.

Baselines. For each task, we evaluate EPOXY against the WS label model from [20] without extensions (WS-LM) to evaluate how much lift our extensions provide; TL without fine-tuning, trained with both hand labels on the dev set (TS-NFT) and probabilistic labels (WS-NFT) on the training set, to evaluate against other models that can train at interactive speeds; and training deep networks with hand labels (TS-FT), probabilistic labels (WS-FT), and labels generated by EPOXY (EPOXY-FT) to see how close we can get to the performance of training a deep network (these approaches often use TL with fine-tuning, see Appendix for details). For TL without fine-tuning, we train a fully-connected layer over the embeddings. The Appendix contains details about the tasks and experimental setup, error analysis of each approach, and comparisons against other weak supervision frameworks [50] and approaches to TL without fine-tuning. Table 1 shows the performance and training time of EPOXY and these baselines on our datasets. In the subsequent sections, we compare EPOXY performance against baselines and explain the differences with explanatory metrics (Table 2).

5.1 Comparison Against WS Label Model

We compare the performance of EPOXY with the WS label model without label extensions. Table 2 (top) shows the lift of EPOXY compared to WS-LM, along with average per-labeling function coverage before and after extensions. EPOXY outperforms WS-LM on all six tasks because it increases labeling function coverage, allowing EPOXY to generate accurate predictions on more points (critically, improving recall, discussed in further detail in Appendix).

We also report the quantity $1 - d(PT, DN)$, which is the average cosine similarity between pre-trained embeddings and fine-tuned embeddings. This quantity measures how similar the pre-trained embeddings are to the fine-tuned embeddings according to our distance function, which helps explain lift of EPOXY over WS-LM. We find that there is a strong correlation between this metric and lift ($R^2 = 0.692$), helping to explain how well our method works. When this metric is high, we can extract more useful information out of the pre-trained embeddings via distance functions, as we do in EPOXY. Although this metric is informative for exploiting embeddings via distances, we note that it is not necessarily informative for predicting performance of using the embeddings as features

without fine-tuning. Fine-tuning can adjust the embeddings in ways that result in large changes to performance without affecting distance; we measure this effect in the Appendix.

5.2 Comparison Against TL Without Fine-Tuning

We now compare the performance of EPOXY against TL without fine-tuning. Unlike fully-trained deep networks, both approaches can train at programmatically-interactive speeds (less than 10 seconds on average, see Table 1 bottom). Table 2 (middle) shows the relative lift of EPOXY compared to TS-NFT and WS-NFT along with the average accuracy of labeling functions on their support sets (formally, average $P(\lambda_j(X_i) = Y_i | X_i \in \text{supp}(\lambda_j))$ for $j \in 1, \dots, m$). EPOXY can outperform non-finetuned models because the labeling functions are accurate on their support sets, whereas the limited-capacity TL models need to learn a global mapping from the pre-trained embeddings to the class label. As Theorem 2 suggests, this local specialization allows EPOXY to have higher overall performance.

5.3 Comparison Against Fully-Trained Deep Networks

We now compare the performance of EPOXY against fully-trained deep networks supervised both with traditional hand labels (TS-FT) and probabilistic labels (WS-FT). Table 2 (bottom) shows the relative lift of EPOXY compared to these baselines, along with the ratio of the size of the unlabeled training set to the labeled dev set. EPOXY can outperform the traditionally-supervised end model in many cases, since it has access to much more data (up to 17 times, labeled automatically). Meanwhile, it approaches the performance of a weakly-supervised end model, coming within one point of WS-FT in two tasks and outperforming in one case. We note that this lift can further improve the performance of training a deep network by using EPOXY to generate weak labels for an end model (reported as EPOXY-FT in Table 1).

5.4 Ablations

We summarize the results of ablations on properly optimizing the extension thresholds r_i (details in Appendix). First, we use a single threshold r for all labeling functions, instead of setting different thresholds for each labeling function. This results in a performance degradation in the EPOXY label model of 3.0 points on average. We also study performance from sweeping r_i and find that, for each task, performance improves as we increase r_i from 0, but degrades if the threshold is too large, demonstrating the accuracy-coverage trade off.

5.5 Runtime Evaluation

We measure EPOXY’s training time compared to other methods. All timing measurements were taken on a machine with an Intel Xeon E5-2690 v4 CPU with a Tesla P100-PCIE-16GB GPU. Table 1 (bottom row) reports the average training time in seconds of each method. EPOXY does not train a deep network, so it can run in less than half a second on average—enabling programmatically-interactive re-training cycles. In contrast, deep end models are much more expensive, requiring hours to train on average. The non-finetuned approaches (*-NFT) are much less expensive and train in seconds, but achieve lower performance scores than EPOXY. Both EPOXY and the non-finetuned transfer learning approaches require a one-time upfront cost for deep network inference to compute embeddings (exact timings in Appendix), which takes less than three minutes on average.

6 Related Work

Weak supervision is a broad set of techniques using weak sources of signal to supervise models, such as distant supervision [43, 12, 26, 63], co-training methods [6], pattern-based supervision [23] and feature annotation [42, 70, 39]. Recently, weak supervision frameworks have systematically integrated multiple noisy sources in two stages—first using a latent variable model to de-noise source votes, and then using a powerful end model to improve performance [51, 52, 4, 5, 22, 32, 58, 53, 20, 71, 57, 56, 7]. Our work focuses on removing this second stage from the pipeline to enable faster iteration cycles.

Transfer learning uses large datasets to learn useful feature representations that can be fine-tuned for downstream tasks [33, 17, 61, 49]. Transfer learning techniques for text applications typically

pre-train on large corpora of unlabeled data [17, 69, 18, 40, 36, 8, 48], while common applications of transfer learning to computer vision pre-train on both large supervised datasets such as ImageNet [16, 54] and large unsupervised or weakly-supervised datasets [29, 38, 64, 61, 41, 24]. Pre-trained embeddings have also been used as data point descriptors for similarity-based search algorithms, such as KNN search, to improve model performance [31, 46, 45, 73]. We view our work as complementary to these approaches, presenting another mechanism for using pre-trained networks.

Semi-supervised and few-shot learning approaches aim to learn good models for downstream tasks given a few labeled examples. Semi-supervised approaches like label propagation [74, 27] start from a few labeled examples and iteratively fine-tune representations on progressively larger datasets, while few-shot learning approaches such as meta-learning and metric learning aim to build networks that can be directly trained with a few labels [66, 60, 62]. Our work is inspired by these approaches for expanding signal from a subset of the data to the entire dataset using deep representations, but we do not assume that our labeling sources are perfect, and we do not tune the representation.

7 Conclusion

We study when it is possible to build weakly-supervised models without training a downstream deep network by using pre-trained embeddings to extend noisy labeling sources. We develop theoretical results characterizing how much information we can extract from distances between data points based on the probabilistic Lipschitzness of the embedding space, and empirically validate our method on six benchmark applications. As pre-trained networks grow increasingly larger and more powerful, we hope that our work inspires a variety of approaches to using pre-trained networks beyond fine-tuning.

Acknowledgments

We gratefully acknowledge the support of DARPA under Nos. FA86501827865 (SDH) and FA86501827882 (ASED); NIH under No. U54EB020405 (Mobilize), NSF under Nos. CCF1763315 (Beyond Sparsity), CCF1563078 (Volume to Velocity), and 1937301 (RTML); ONR under No. N000141712266 (Unifying Weak Supervision); the Moore Foundation, NXP, Xilinx, LETI-CEA, Intel, IBM, Microsoft, NEC, Toshiba, TSMC, ARM, Hitachi, BASF, Accenture, Ericsson, Qualcomm, Analog Devices, the Okawa Foundation, American Family Insurance, Google Cloud, Swiss Re, Brown Institute for Media Innovation, the HAI-AWS Cloud Credits for Research program, Department of Defense (DoD) through the National Defense Science and Engineering Graduate Fellowship (NDSEG) Program, and members of the Stanford DAWN project: Teradata, Facebook, Google, Ant Financial, NEC, VMWare, and Infosys. The U.S. Government is authorized to reproduce and distribute reprints for Governmental purposes notwithstanding any copyright notation thereon. Any opinions, findings, and conclusions or recommendations expressed in this material are those of the authors and do not necessarily reflect the views, policies, or endorsements, either expressed or implied, of DARPA, NIH, ONR, or the U.S. Government.

References

- [1] Internet archive: Tv news archive. <https://archive.org/details/tv>, 2018.
- [2] Weather sentiment: Dataset in crowdflower. <https://data.world/crowdflower/weather-sentiment>, 2018.
- [3] Túlio C Alberto, Johannes V Lochter, and Tiago A Almeida. Tubesppam: Comment spam filtering on youtube. In *2015 IEEE 14th International Conference on Machine Learning and Applications (ICMLA)*, pages 138–143. IEEE, 2015.
- [4] Stephen H Bach, Bryan He, Alexander Ratner, and Christopher Ré. Learning the structure of generative models without labeled data. In *ICML*, 2017.
- [5] Stephen H Bach, Daniel Rodriguez, Yintao Liu, Chong Luo, Haidong Shao, Cassandra Xia, Souvik Sen, Alex Ratner, Braden Hancock, Houman Alborzi, et al. Snorkel drybell: A case study in deploying weak supervision at industrial scale. In *Proceedings of the 2019 International Conference on Management of Data*, pages 362–375, 2019.

- [6] Avrim Blum and Tom Mitchell. Combining labeled and unlabeled data with co-training. In *Proceedings of the eleventh annual conference on Computational learning theory*, pages 92–100. ACM, 1998.
- [7] Benedikt Boecking and Artur Dubrawski. Pairwise feedback for data programming. In *Proceedings of NeurIPS 2019 Workshop on Learning with Rich Experience (LIRE)*, December 2019.
- [8] Tom B. Brown, Benjamin Mann, Nick Ryder, Melanie Subbiah, Jared Kaplan, Prafulla Dhariwal, Arvind Neelakantan, Pranav Shyam, Girish Sastry, Amanda Askell, Sandhini Agarwal, Ariel Herbert-Voss, Gretchen Krueger, Tom Henighan, Rewon Child, Aditya Ramesh, Daniel M. Ziegler, Jeffrey Wu, Clemens Winter, Christopher Hesse, Mark Chen, Eric Sigler, Mateusz Litwin, Scott Gray, Benjamin Chess, Jack Clark, Christopher Berner, Sam McCandlish, Alec Radford, Ilya Sutskever, and Dario Amodei. Language models are few-shot learners. *arXiv preprint arXiv:2005.14165*, 2020.
- [9] Fabian Caba Heilbron, Victor Escorcia, Bernard Ghanem, and Juan Carlos Nieves. Activitynet: A large-scale video benchmark for human activity understanding. In *Proceedings of the IEEE Conference on Computer Vision and Pattern Recognition*, pages 961–970, 2015.
- [10] Fernando J Corbató, Marjorie Merwin-Daggett, and Robert C Daley. An experimental time-sharing system. In *Proceedings of the May 1-3, 1962, spring joint computer conference*, pages 335–344, 1962.
- [11] David Corney, Dyaa Albakour, Miguel Martinez-Alvarez, and Samir Moussa. What do a million news articles look like? In *NewsIR@ ECIR*, pages 42–47, 2016.
- [12] Mark Craven, Johan Kumlien, et al. Constructing biological knowledge bases by extracting information from text sources. In *ISMB*, pages 77–86, 1999.
- [13] Alexander Philip Dawid and Allan M Skene. Maximum likelihood estimation of observer error-rates using the EM algorithm. *Applied statistics*, pages 20–28, 1979.
- [14] Mostafa Dehghani, Aliaksei Severyn, Sascha Rothe, and Jaap Kamps. Learning to learn from weak supervision by full supervision. In *NIPS workshop on Meta-Learning (MetaLearn 2017)*, 2017.
- [15] Mostafa Dehghani, Hamed Zamani, Aliaksei Severyn, Jaap Kamps, and W Bruce Croft. Neural ranking models with weak supervision. In *Proceedings of the 40th International ACM SIGIR Conference on Research and Development in Information Retrieval*, pages 65–74. ACM, 2017.
- [16] Jia Deng, Wei Dong, Richard Socher, Li-Jia Li, Kai Li, and Li Fei-Fei. Imagenet: A large-scale hierarchical image database. In *2009 IEEE conference on computer vision and pattern recognition*, pages 248–255. Ieee, 2009.
- [17] Jacob Devlin, Ming-Wei Chang, Kenton Lee, and Kristina Toutanova. Bert: Pre-training of deep bidirectional transformers for language understanding. *arXiv preprint arXiv:1810.04805*, 2018.
- [18] Li Dong, Nan Yang, Wenhui Wang, Furu Wei, Xiaodong Liu, Yu Wang, Jianfeng Gao, Ming Zhou, and Hsiao-Wuen Hon. Unified language model pre-training for natural language understanding and generation. In *Advances in Neural Information Processing Systems*, pages 13042–13054, 2019.
- [19] Jason Fries, Paroma Varma, Vincent S Chen, Ke Xiao, Heliodoro Tejeda, Priyanka Saha, Jared Dunnmon, Henry Chubb, Shiraz Maskatia, Madalina Fiterau, et al. Weakly supervised classification of aortic valve malformations using unlabeled cardiac mri sequences. *Nature communications*, 10:3111, 2019.
- [20] Daniel Y. Fu, Mayee F. Chen, Frederic Sala, Sarah M. Hooper, Kayvon Fatahalian, and Christopher Ré. Fast and three-rious: Speeding up weak supervision with triplet methods. *arXiv preprint arXiv:2002.11955*, 2020.
- [21] Daniel Y. Fu, Will Crichton, James Hong, Xinwei Yao, Haotian Zhang, Anh Truong, Avani Narayan, Maneesh Agrawala, Christopher Ré, and Kayvon Fatahalian. Rekall: Specifying video events using compositions of spatiotemporal labels. *arXiv preprint arXiv:1910.02993*, 2019.
- [22] Melody Y Guan, Varun Gulshan, Andrew M Dai, and Geoffrey E Hinton. Who said what: Modeling individual labelers improves classification. In *Thirty-Second AAAI Conference on Artificial Intelligence*, 2018.

- [23] Sonal Gupta and Christopher Manning. Improved pattern learning for bootstrapped entity extraction. In *Proceedings of the Eighteenth Conference on Computational Natural Language Learning*, pages 98–108, 2014.
- [24] Kaiming He, Haoqi Fan, Yuxin Wu, Saining Xie, and Ross Girshick. Momentum contrast for unsupervised visual representation learning. *arXiv preprint arXiv:1911.05722*, 2019.
- [25] Marti A Hearst. Automatic acquisition of hyponyms from large text corpora. In *Proceedings of the 14th conference on Computational linguistics-Volume 2*, pages 539–545. Association for Computational Linguistics, 1992.
- [26] Raphael Hoffmann, Congle Zhang, Xiao Ling, Luke Zettlemoyer, and Daniel S Weld. Knowledge-based weak supervision for information extraction of overlapping relations. In *Proceedings of the 49th Annual Meeting of the Association for Computational Linguistics: Human Language Technologies-Volume 1*, pages 541–550. Association for Computational Linguistics, 2011.
- [27] Ahmet Iscen, Giorgos Tolias, Yannis Avrithis, and Ondrej Chum. Label propagation for deep semi-supervised learning. In *Proceedings of the IEEE Conference on Computer Vision and Pattern Recognition*, pages 5070–5079, 2019.
- [28] Zhipeng Jia, Xingyi Huang, I Eric, Chao Chang, and Yan Xu. Constrained deep weak supervision for histopathology image segmentation. *IEEE transactions on medical imaging*, 36(11):2376–2388, 2017.
- [29] Armand Joulin, Laurens van der Maaten, Allan Jabri, and Nicolas Vasilache. Learning visual features from large weakly supervised data. In *European Conference on Computer Vision*, pages 67–84. Springer, 2016.
- [30] David R Karger, Sewoong Oh, and Devavrat Shah. Iterative learning for reliable crowdsourcing systems. In *Advances in neural information processing systems*, pages 1953–1961, 2011.
- [31] Urvashi Khandelwal, Omer Levy, Dan Jurafsky, Luke Zettlemoyer, and Mike Lewis. Generalization through memorization: Nearest neighbor language models. In *International Conference on Learning Representations*, 2019.
- [32] Ashish Khetan, Zachary C. Lipton, and Anima Anandkumar. Learning from noisy singly-labeled data. In *International Conference on Learning Representations*, 2018.
- [33] Alexander Kolesnikov, Lucas Beyer, Xiaohua Zhai, Joan Puigcerver, Jessica Yung, Sylvain Gelly, and Neil Houlsby. Large scale learning of general visual representations for transfer. *arXiv preprint arXiv:1912.11370*, 2019.
- [34] Daphne Koller and Nir Friedman. *Probabilistic graphical models: principles and techniques*. MIT press, 2009.
- [35] Shrinu Kushagra and Shai Ben-David. Information preserving dimensionality reduction. In Kamalika Chaudhuri, CLAUDIO GENTILE, and Sandra Zilles, editors, *Algorithmic Learning Theory*, pages 239–253. Cham, 2015. Springer International Publishing.
- [36] Zhenzhong Lan, Mingda Chen, Sebastian Goodman, Kevin Gimpel, Piyush Sharma, and Radu Soricut. Albert: A lite bert for self-supervised learning of language representations. *arXiv preprint arXiv:1909.11942*, 2019.
- [37] S. Lauritzen. *Graphical Models*. Clarendon Press, 1996.
- [38] Ang Li, Allan Jabri, Armand Joulin, and Laurens van der Maaten. Learning visual n-grams from web data. In *Proceedings of the IEEE International Conference on Computer Vision*, pages 4183–4192, 2017.
- [39] Percy Liang, Michael I Jordan, and Dan Klein. Learning from measurements in exponential families. In *Proceedings of the 26th annual international conference on machine learning*, pages 641–648. ACM, 2009.
- [40] Yinhan Liu, Myle Ott, Naman Goyal, Jingfei Du, Mandar Joshi, Danqi Chen, Omer Levy, Mike Lewis, Luke Zettlemoyer, and Veselin Stoyanov. Roberta: A robustly optimized bert pretraining approach. *arXiv preprint arXiv:1907.11692*, 2019.
- [41] Dhruv Mahajan, Ross Girshick, Vignesh Ramanathan, Kaiming He, Manohar Paluri, Yixuan Li, Ashwin Bharambe, and Laurens van der Maaten. Exploring the limits of weakly supervised pretraining. In *Proceedings of the European Conference on Computer Vision (ECCV)*, pages 181–196, 2018.

- [42] Gideon S Mann and Andrew McCallum. Generalized expectation criteria for semi-supervised learning with weakly labeled data. *Journal of machine learning research*, 11(Feb):955–984, 2010.
- [43] Mike Mintz, Steven Bills, Rion Snow, and Dan Jurafsky. Distant supervision for relation extraction without labeled data. In *Proceedings of the Joint Conference of the 47th Annual Meeting of the ACL and the 4th International Joint Conference on Natural Language Processing of the AFNLP: Volume 2-Volume 2*, pages 1003–1011. Association for Computational Linguistics, 2009.
- [44] Feng Niu, Ce Zhang, Christopher Ré, and Jude W Shavlik. Deepdive: Web-scale knowledge-base construction using statistical learning and inference. *VLDS*, 12:25–28, 2012.
- [45] Emin Orhan. A simple cache model for image recognition. In *Advances in Neural Information Processing Systems*, pages 10107–10116, 2018.
- [46] Nicolas Papernot and Patrick McDaniel. Deep k-nearest neighbors: Towards confident, interpretable and robust deep learning. *arXiv preprint arXiv:1803.04765*, 2018.
- [47] Anastasia Pentina and Shai Ben-David. Multi-task kernel learning based on probabilistic lipschitzness. In *Conf. Algorithmic Learning Theory (ALT)*, pages 682–701, 2018.
- [48] Alec Radford, Jeffrey Wu, Rewon Child, David Luan, Dario Amodei, and Ilya Sutskever. Language models are unsupervised multitask learners. *OpenAI Blog*, 1(8):9, 2019.
- [49] Colin Raffel, Noam Shazeer, Adam Roberts, Katherine Lee, Sharan Narang, Michael Matena, Yanqi Zhou, Wei Li, and Peter J Liu. Exploring the limits of transfer learning with a unified text-to-text transformer. *arXiv preprint arXiv:1910.10683*, 2019.
- [50] A. J. Ratner, B. Hancock, J. Dunnmon, F. Sala, S. Pandey, and C. Ré. Training complex models with multi-task weak supervision. In *Proceedings of the AAAI Conference on Artificial Intelligence*, Honolulu, Hawaii, 2019.
- [51] A. J. Ratner, Christopher M. De Sa, Sen Wu, Daniel Selsam, and C. Ré. Data programming: Creating large training sets, quickly. In *Proceedings of the 29th Conference on Neural Information Processing Systems (NIPS 2016)*, Barcelona, Spain, 2016.
- [52] Alexander Ratner, Stephen H. Bach, Henry Ehrenberg, Jason Fries, Sen Wu, and Christopher Ré. Snorkel: Rapid training data creation with weak supervision. In *Proceedings of the 44th International Conference on Very Large Data Bases (VLDB)*, Rio de Janeiro, Brazil, 2018.
- [53] Christopher Ré, Feng Niu, Pallavi Gudipati, and Charles Srisuwananukorn. Overton: A data system for monitoring and improving machine-learned products. In *Proceedings of the 10th Annual Conference on Innovative Data Systems Research*, 2020.
- [54] Olga Russakovsky, Jia Deng, Hao Su, Jonathan Krause, Sanjeev Satheesh, Sean Ma, Zhiheng Huang, Andrej Karpathy, Aditya Khosla, Michael Bernstein, et al. Imagenet large scale visual recognition challenge. *International journal of computer vision*, 115(3):211–252, 2015.
- [55] Khaled Saab, Jared Dunnmon, Christopher Ré, Daniel Rubin, and Christopher Lee-Messer. Weak supervision as an efficient approach for automated seizure detection in electroencephalography. *npj Digital Medicine*, 3(1):1–12, 2020.
- [56] Esteban Safranchik, Shiyong Luo, and Stephen H Bach. Weakly supervised sequence tagging from noisy rules. In *Thirty-Fourth AAAI Conference on Artificial Intelligence*, 2020.
- [57] Frederic Sala, Paroma Varma, Jason Fries, Daniel Y. Fu, Shiori Sagawa, Saelig Khattar, Ashwini Ramamoorthy, Ke Xiao, Kayvon Fatahalian, James Priest, and Christopher Ré. Multi-resolution weak supervision for sequential data. In *Advances in Neural Information Processing Systems* 32, pages 192–203, 2019.
- [58] Ying Sheng, Nguyen Ha Vo, James B. Wendt, Sandeep Tata, and Marc Najork. Migrating a privacy-safe information extraction system to a software 2.0 design. In *Proceedings of the 10th Annual Conference on Innovative Data Systems Research*, 2020.
- [59] Kai Shu, Subhabrata (Subho) Mukherjee, Guoqing Zheng, Ahmed Hassan Awadallah, Milad Shokouhi, and Susan Dumais. Learning with weak supervision for email intent detection. In *ACM SIGIR Conference on Research and Development in Information Retrieval*. ACM, July 2020.

- [60] Jake Snell, Kevin Swersky, and Richard Zemel. Prototypical networks for few-shot learning. In *Advances in neural information processing systems*, pages 4077–4087, 2017.
- [61] Chen Sun, Abhinav Shrivastava, Saurabh Singh, and Abhinav Gupta. Revisiting unreasonable effectiveness of data in deep learning era. In *Proceedings of the IEEE international conference on computer vision*, pages 843–852, 2017.
- [62] Flood Sung, Yongxin Yang, Li Zhang, Tao Xiang, Philip HS Torr, and Timothy M Hospedales. Learning to compare: Relation network for few-shot learning. In *Proceedings of the IEEE Conference on Computer Vision and Pattern Recognition*, pages 1199–1208, 2018.
- [63] Shingo Takamatsu, Issei Sato, and Hiroshi Nakagawa. Reducing wrong labels in distant supervision for relation extraction. In *Proceedings of the 50th Annual Meeting of the Association for Computational Linguistics: Long Papers-Volume 1*, pages 721–729. Association for Computational Linguistics, 2012.
- [64] Bart Thomee, David A Shamma, Gerald Friedland, Benjamin Elizalde, Karl Ni, Douglas Poland, Damian Borth, and Li-Jia Li. Yfcc100m: The new data in multimedia research. *Communications of the ACM*, 59(2):64–73, 2016.
- [65] P. Varma, F. Sala, A. He, A. J. Ratner, and C. Ré. Learning dependency structures for weak supervision models. In *Proceedings of the 36th International Conference on Machine Learning (ICML 2019)*, 2019.
- [66] Oriol Vinyals, Charles Blundell, Timothy Lillicrap, Daan Wierstra, et al. Matching networks for one shot learning. In *Advances in neural information processing systems*, pages 3630–3638, 2016.
- [67] Martin J Wainwright and Michael I Jordan. Graphical models, exponential families, and variational inference. *Foundations and Trends® in Machine Learning*, 1(1-2):1–305, 2008.
- [68] Thomas Wolf, Lysandre Debut, Victor Sanh, Julien Chaumond, Clement Delangue, Anthony Moi, Pierric Cistac, Tim Rault, R’emi Louf, Morgan Funtowicz, and Jamie Brew. Huggingface’s transformers: State-of-the-art natural language processing. *ArXiv*, abs/1910.03771, 2019.
- [69] Zhilin Yang, Zihang Dai, Yiming Yang, Jaime Carbonell, Russ R Salakhutdinov, and Quoc V Le. Xlnet: Generalized autoregressive pretraining for language understanding. In *Advances in neural information processing systems*, pages 5754–5764, 2019.
- [70] Omar F Zaidan and Jason Eisner. Modeling annotators: A generative approach to learning from annotator rationales. In *Proceedings of the Conference on Empirical Methods in Natural Language Processing*, pages 31–40. Association for Computational Linguistics, 2008.
- [71] Eric Zhan, Stephan Zheng, Yisong Yue, Long Sha, and Patrick Lucey. Generating multi-agent trajectories using programmatic weak supervision. In *7th International Conference on Learning Representations, ICLR 2019, New Orleans, LA, USA, May 6-9, 2019*, 2019.
- [72] Ce Zhang, Christopher Ré, Michael Cafarella, Christopher De Sa, Alex Ratner, Jaeho Shin, Feiran Wang, and Sen Wu. DeepDive: Declarative knowledge base construction. *Commun. ACM*, 60(5):93–102, 2017.
- [73] Jake Zhao and Kyunghyun Cho. Retrieval-augmented convolutional neural networks for improved robustness against adversarial examples. *arXiv preprint arXiv:1802.09502*, 2018.
- [74] Xiaojin Zhu and Zoubin Ghahramani. Learning from labeled and unlabeled data with label propagation. 2002.

Appendix

First, we provide a glossary of terms and notation that we use throughout this paper for easy summary (Section A). Next, we give details about the label model we use after extending our labeling functions (Section B). Next, we give the proofs of each theorem (Section C). Then we give additional experimental details (Section D) and present further evaluation (Section E).

A Glossary

The glossary is given in Table 3 below.

Symbol	Used for
X	Unlabeled data vector, $X = [X^1, X^2, \dots, X^T] \in \mathcal{X}$.
Y	Latent, ground-truth task label vector $[Y^1, Y^2, \dots, Y^T] \in \mathcal{Y} = \{-1, +1\}$.
\mathcal{D}	Distribution from which (X, Y) data points are sampled i.i.d.
m	Number of weak supervision labeling functions.
λ_i	Labeling function $\lambda_i : \mathcal{X} \rightarrow \mathcal{Y} \cup \{0\}$; all m labels per X collectively denoted λ .
o_{\min}	The minimal overlap between pairs of labeling functions used for parameter recovery, $\min_i \max_{j:j \neq i} \Pr(X \in \text{supp}(\lambda_i) \cap \text{supp}(\lambda_j))$.
D	Unlabeled dataset $\{X_i\}_{i=1}^n$ that λ is applied to in order to produce labels.
n	Number of data vectors.
g	Mapping from \mathcal{X} to embedding space \mathcal{Z} .
\mathcal{Z}	The embedding space corresponding to the pre-trained network.
f_z	A classifier $f_z : \mathcal{Z} \rightarrow \mathcal{Y}$ that uses the embeddings in \mathcal{Z} (i.e. transfer learning without fine-tuning).
d_Z	A given distance function on the embedding space \mathcal{Z} .
$M_Y(r)$	An upper bound on $\Pr(Y_1 \neq Y_2 d_Z(X_1, X_2) \leq r)$.
$L_{\lambda'_i}(r)$	A lower bound on $\Pr(\lambda_i(X_1) = 0, \lambda_i(X_2) \neq 0 d_Z(X_1, X_2) \leq r)$.
$\tilde{\lambda}$	The set of extended labeling functions.
\mathbf{r}	Threshold radii, where each r_i specifies how much to extend λ_i .
$N_{r_j}(X)$	The points in the support of λ_j that are within r_j of X .
W	Weighing rule $W(N_{r_j}(X))$ used to assign labels to extended points based on neighbors in $\text{supp}(\lambda_j)$.
$B_r(\lambda_j)$	The set of newly labeled points $\{X_i \notin \text{supp}(\lambda_j) : \exists X_k \in \text{supp}(\lambda_j) \text{ s.t. } d_Z(X_i, X_k) \leq r_j\}$.
a_i	Accuracy of original labeling function $\Pr(\lambda_i = Y \lambda_i \neq 0)$.
\bar{a}_i	Accuracy of extended labeling function $\Pr(\tilde{\lambda}_i = Y \tilde{\lambda}_i \neq 0)$.
p_i	Relative size of λ_i 's support set, $\Pr(X \in \text{supp}(\lambda_i))$.
$p_d(r)$	Proportion of points within r of each other, $\Pr(d_Z(X, X') \leq r)$.
L_{\min}	Minimum value of $L_{\lambda'_i}(r_i)$ across all $i = 1, \dots, m$.
r_{\min}	Smallest extension radius $r_{\min} = \min_i r_i$.

Table 3: Glossary of variables and symbols used in this paper.

B Additional Algorithmic Details

We present an overview of the weak supervision model used after extending our labeling functions via Algorithm 1 (Section B.1). Then, we discuss some of the basic properties of this model that are important for our theoretical results (Section B.2). Since this model applies to both the extended labeling functions and original labeling functions, we use λ for simplicity in this section.

B.1 Probabilistic label model

Recall that the goal of weak supervision is to combine noisy sources λ on an unlabeled dataset to produce probabilistic labels \tilde{Y} . We review the modeling and parameter recovery method presented in [20]. We first describe our choice of probabilistic graphical model based on the extended labeling functions. Then, we discuss how to recover parameters of the graphical model. Finally, we explain how to perform inference with the recovered parameters to generate probabilistic labels on the data.

Binary Ising Model In the standard weak supervision setting, we have a set of labeling functions $\lambda = \lambda_1, \dots, \lambda_m$ that vote or abstain on $Y = [Y^1, \dots, Y^T]$. Each labeling function λ_i produces a vote on one element of Y , which we denote as $Y^{\text{dep}}(i)$. Therefore, we can view λ and Y as random variables that are functions of X , where the labeling functions are independent of each other conditioned on Y . Let the graph $G_{\text{dep}} = (\{Y, \lambda\}, E_{\text{dep}})$ specify the dependencies between the noisy labeling functions and the task labels, using standard technical notions from the PGM literature [34, 37, 67]. In particular, the lack of an edge in G_{dep} between a pair of variables indicates independence conditioned on a separator set of variables [37], and there exists an edge between each λ_i and $Y^{\text{dep}}(i)$. We assume that G_{dep} is user-provided, although it can be estimated directly from the votes of the labeling functions [65]. We also assume that we are provided with the class balance prior $\Pr(Y)$, although this can also be learned from the data [50].

We augment the dependency graph G_{dep} to produce a binary Ising model. To incorporate behavior when sources abstain, we represent the outputs of each labeling function λ_i using a pair of binary random variables, $(v_i^1, v_i^{-1}) \in \{-1, +1\}$. More formally, when $\lambda_i = 1$, we set $(v_i^1, v_i^{-1}) = (1, -1)$; when $\lambda_i = -1$, we set them to $(-1, 1)$, and when $\lambda_i = 0$, we set them with equal probability to $(1, 1)$ or $(-1, -1)$. This allows us to encode abstaining behavior with $v_i^1 v_i^{-1} = 1$ implying $\lambda_i = 0$. We thus have edges from v_i^1 and v_i^{-1} to $Y^{\text{dep}}(i)$, as well as an edge between v_i^1 and v_i^{-1} . Using this augmentation, we have a new graph $G = (V, E)$ based on G_{dep} , where $V = \{Y, v\}$, that follows a binary Ising model. The joint distribution among Y and v is

$$f_G(Y, v) = \frac{1}{Z} \exp \left(\sum_{k=1}^T \theta_{Y_k} Y_k + \sum_{(Y_k, Y_l) \in E} \theta_{Y_k, Y_l} Y_k Y_l + \sum_{i=1}^m \theta_i (v_i^1 - v_i^{-1}) Y^{\text{dep}}(i) + \sum_{i=1}^m \theta_{i,i} v_i^1 v_i^{-1} \right) \quad (1)$$

where Z corresponds to the cumulant function and θ parametrizes this density function. In this graphical model, θ_{Y_k} and θ_{Y_k, Y_l} are parameters corresponding to the prior $\Pr(Y)$. θ_i parametrizes the edges between the labeling functions and the task label, hence corresponding to the accuracy of the labeling function. $\theta_{i,i}$ between each v_i^1, v_i^{-1} represents the abstain rate.

Parameter Recovery We now explain how to recover the unknown accuracy parameters of this graphical model using an efficient method-of-moments based approach from [20]. In particular, we use the following independence property:

Proposition 3. $\lambda_i Y^{\text{dep}}(i) \perp\!\!\!\perp \lambda_j Y^{\text{dep}}(j) | \lambda_i, \lambda_j \neq 0$ for all $i \neq j \in 1, \dots, m$.

Proof. To see how this holds true, denote $S = \{Y^k \in Y : \lambda_i \perp\!\!\!\perp \lambda_j | Y^k\}$, e.g. Y^k is a variable on the path from λ_i to λ_j in G_{dep} . Then, marginalizing over $V \setminus \{S \cup (v_i^1, v_i^{-1}), (v_j^1, v_j^{-1})\}$ and conditioning on $\lambda_i, \lambda_j \neq 0$, e.g. $v_i^1 \neq v_i^{-1}, v_j^1 \neq v_j^{-1}$, we use (1) to get

$$\Pr(S, (v_i^1, v_i^{-1}), (v_j^1, v_j^{-1}) | v_i^1 \neq v_i^{-1}, v_j^1 \neq v_j^{-1}) = \frac{1}{Z_{ij}} \exp \left(\sum_{Y_k \in S} \theta_{Y_k} Y_k + \sum_{(Y_k, Y_l) \in S} \theta_{Y_k, Y_l} Y_k Y_l + \theta_i (v_i^1 - v_i^{-1}) Y^{\text{dep}}(i) + \theta_j (v_j^1 - v_j^{-1}) Y^{\text{dep}}(j) \right)$$

for some different cumulant function Z_{ij} . Moreover, $v_i^1 - v_i^{-1}$ and $v_j^1 - v_j^{-1}$ are always equal to -2 or 2 since this probability is conditioned on $\lambda_i, \lambda_j \neq 0$. Then, by setting $\theta'_i = 2\theta_i$ and $\theta'_j = 2\theta_j$, we can write this density function directly in terms of λ_i and λ_j :

$$\Pr(S, \lambda_i, \lambda_j | \lambda_i, \lambda_j \neq 0) = \frac{1}{Z_{ij}} \exp \left(\sum_{Y_k \in S} \theta_{Y_k} Y_k + \sum_{(Y_k, Y_l) \in S} \theta_{Y_k, Y_l} Y_k Y_l + \theta'_i \lambda_i Y^{\text{dep}}(i) + \theta'_j \lambda_j Y^{\text{dep}}(j) \right).$$

Then, by Proposition 1 of [20], we know that $\lambda_i Y^{\text{dep}}(i)$ and $\lambda_j Y^{\text{dep}}(j)$ are independent conditioned on $\lambda_i, \lambda_j \neq 0$. \square

Based on this independence property, we can say that

$$\mathbb{E} [\lambda_i Y^{\text{dep}}(i) | \lambda_i \neq 0] \cdot \mathbb{E} [\lambda_j Y^{\text{dep}}(i) | \lambda_j \neq 0] = \mathbb{E} [\lambda_i \lambda_j | \lambda_i, \lambda_j \neq 0].$$

This is because $Y^{\text{dep}}(i)^2$ is always equal to 1, and $\mathbb{E} [\lambda_i Y^{\text{dep}}(i) | \lambda_i, \lambda_j \neq 0]$ is equal to $\mathbb{E} [\lambda_i Y^{\text{dep}}(i) | \lambda_i \neq 0]$ since λ_i and λ_j are conditionally independent given $Y^{\text{dep}}(i)$. While $\mathbb{E} [\lambda_i Y^{\text{dep}}(i) | \lambda_i \neq 0]$, $\mathbb{E} [\lambda_j Y^{\text{dep}}(i) | \lambda_j \neq 0]$ correspond to the unknown accuracies of labeling functions, their product is observable. If we are able to introduce a third λ_k that is conditionally independent of λ_i and λ_j given the same Y , we have a system of three equations that can be solved using observable pairwise products that represent the rates of agreement between labeling functions. Then, we can use [20]’s *triplet method* to recover these expectations, which we denote as $a_i^E = \mathbb{E} [\lambda_i Y^{\text{dep}}(i) | \lambda_i \neq 0]$.

Inference These expectations can be converted into marginal clique probabilities of the form $\mu_{y,i}(X) := \Pr(Y^{\text{dep}}(i) = y, \lambda_i = \lambda_i(X))$ based on a simple linear transformation using observable probabilities and the distribution prior $\Pr(Y)$. The overall joint probability can be written as a product over these marginal clique probabilities using a junction tree representation based on the maximal cliques and separator sets of G_{dep} . Because all labeling functions are conditionally independent given Y and each labeling function only votes on one task, all maximal cliques are either of the form $\mu_{y,i}$ or $\mu_{y,C} := \Pr(Y_C = y_C)$, where $C \in \mathcal{C}$, and \mathcal{C} is the set of maximal cliques on Y . Furthermore, all separator sets are singletons on elements of Y , which we express as $\mu_{y,j} := \Pr(Y_j = y_j)$. Then we can write the recovered distribution as

$$\Pr_{\mu}(Y = y, \boldsymbol{\lambda} = \boldsymbol{\lambda}(X)) = \frac{\prod_{i=1}^m \mu_{y,i}(X) \prod_{C \in \mathcal{C}} \mu_{y,C}}{\prod_{j=1}^T \mu_{y,j}^{d(Y^j)-1}}, \quad (2)$$

where $d(Y^j)$ is the degree of Y^j in G_{dep} . Then the probabilistic label \tilde{Y} on a data point X can be computed using $\Pr_{\mu}(\tilde{Y} = 1 | \boldsymbol{\lambda} = \boldsymbol{\lambda}(X))$ based on (2).

B.2 Properties of the graphical model for section 4

We now discuss some properties of the single-task version of the graphical model in (1). These properties, which can also be shown for $T > 1$, are used in proving the bounds presented in section 4 and also allow us to concisely write out the WS algorithm used for our theoretical results (Algorithm 2).

First, when $T = 1$, (1) can be rewritten as

$$f_G(Y, \mathbf{v}) = \frac{1}{Z} \exp \left(\theta_Y Y + \sum_{i=1}^m \theta_i (v_i^1 - v_i^{-1}) Y + \sum_{i=1}^m \theta_{i,i} v_i^1 v_i^{-1} \right), \quad (3)$$

and (2) becomes simpler:

$$\Pr_{\mu}(Y = y, \boldsymbol{\lambda} = \boldsymbol{\lambda}(X)) = \frac{\prod_{i=1}^m \mu_{y,i}(X)}{\Pr(Y = y)^{m-1}} = \prod_{i=1}^m \Pr(\lambda_i = \lambda_i(X) | Y = y) \Pr(Y = y). \quad (4)$$

We present a symmetry property on the accuracies.

Lemma 1. *For any labeling function λ_i with accuracy a_i ,*

$$\begin{aligned} \Pr(\lambda_i = 1 | Y = 1, \lambda_i \neq 0) &= \Pr(\lambda_i = -1 | Y = -1, \lambda_i \neq 0) = a_i \\ \Pr(\lambda_i = -1 | Y = 1, \lambda_i \neq 0) &= \Pr(\lambda_i = 1 | Y = -1, \lambda_i \neq 0) = 1 - a_i. \end{aligned}$$

Proof. We can write the marginal distribution of $\Pr(Y, \lambda_i | \lambda_i \neq 0)$ as

$$\Pr(Y, \lambda_i | \lambda_i \neq 0) = \frac{1}{Z_i} \exp(\theta_Y + \theta_i \lambda_i Y).$$

By Proposition 2 of [20], we know that $\lambda_i Y \perp\!\!\!\perp Y | \lambda_i \neq 0$. This means that

$$\Pr(\lambda_i Y = 1, Y = 1 | \lambda_i \neq 0) = \Pr(\lambda_i Y = 1 | \lambda_i \neq 0) \cdot \Pr(Y = 1 | \lambda_i \neq 0)$$

Dividing both sides by $\Pr(Y = 1 | \lambda_i \neq 0)$, we get

$$\begin{aligned} \Pr(\lambda_i Y = 1 | Y = 1, \lambda_i \neq 0) &= \Pr(\lambda_i Y = 1 | \lambda_i \neq 0) \\ \Rightarrow \Pr(\lambda_i = 1 | Y = 1, \lambda_i \neq 0) &= a_i \end{aligned}$$

Repeating this calculation with $\Pr(\lambda_i Y = 1, Y = -1 | \lambda_i \neq 0)$ gives us $\Pr(\lambda_i = -1 | Y = -1, \lambda_i \neq 0) = a_i$. We do the same again with $\Pr(\lambda_i Y = -1, Y = -1 | \lambda_i \neq 0)$ and $\Pr(\lambda_i Y = -1, Y = 1 | \lambda_i \neq 0)$ to get the second equation by noting that $\Pr(\lambda_i Y = -1 | \lambda_i \neq 0) = 1 - a_i$. \square

Next, our graphical model assumes that abstaining sources do not affect the label Y .

Lemma 2. *For any labeling function λ_i ,*

$$\Pr(Y = y, \lambda_i = 0) = \Pr(Y = y) \cdot \Pr(\lambda_i = 0)$$

Proof. By definition, we can write $\Pr(Y = y, \lambda_i = 0)$ as $\Pr(Y = y, v_i^1 v_i^{-1} = 1)$. Using Proposition 2 of [20], we have that $v_i^1 v_i^{-1} \perp\!\!\!\perp Y$, and therefore

$$\Pr(Y = y, v_i^1 v_i^{-1} = 1) = \Pr(Y = y) \Pr(v_i^1 v_i^{-1} = 1) = \Pr(Y = y) \Pr(\lambda_i = 0)$$

Note that this property means that $\Pr(Y = y | \lambda_i = 0) = \Pr(Y = y | \lambda_i \neq 0) = \Pr(Y = y)$. \square

Using these two properties, the output of the probabilistic label model is a simple expression in terms of the accuracies of labeling functions. By Lemmas 1 and 2, we know that

$$\begin{aligned} \Pr(\lambda_i Y = \lambda_i(X) \cdot y | \lambda_i \neq 0) &= \Pr(\lambda_i = \lambda_i(X) | Y = y, \lambda_i \neq 0) = \frac{\Pr(\lambda_i = \lambda_i(X), Y = y, \lambda_i \neq 0)}{\Pr(Y = y, \lambda_i \neq 0)} \\ &= \frac{\Pr(\lambda_i = \lambda_i(X), Y = y)}{\Pr(Y = y) \Pr(\lambda_i \neq 0)} = \frac{\Pr(\lambda_i = \lambda_i(X) | Y = y)}{\Pr(\lambda_i \neq 0)}. \end{aligned}$$

$\Pr(\lambda_i = \lambda_i(X) | Y = y)$ is the probability used in (4), so we are able to easily use the accuracy a_i to compute probabilistic labels. We now summarize this method of learning the label model for $T = 1$ in Algorithm 2, which is also the algorithm used for the bounds stated in section 4. Note that in order to reduce estimation error, we select triplets i, j, k that have the largest possible overlaps in their support sets.

C Proofs

C.1 Proposition 1 Proof

Bounding the accuracy can be viewed through the following extension procedure: for each $X \in \text{supp}(\bar{\lambda}_i)$, we choose an $X' \in \text{supp}(\lambda_i)$ and assign $\bar{\lambda}_i(X) = \lambda_i(X')$. The method for choosing X' is as follows: we select the set of neighbors $N(X)$ in $\text{supp}(\lambda_i)$ within radius r of X , choose some $x_j \in N(X)$ using the pdf of X conditioned on $N(X)$, and set $X' = x_j$. Define $\mathcal{N} = \{N(X)\}$ to be the set of all possible neighbors. We can now write \bar{a}_i using our procedure:

$$\begin{aligned} \bar{a}_i &= \Pr(\bar{\lambda}_i(X) Y = 1 | \bar{\lambda}_i(X) \neq 0) \\ &= \sum_{k \in \mathcal{N}} \Pr(\bar{\lambda}_i(X) Y = 1 | \bar{\lambda}_i(X) \neq 0, N(X) = k) \Pr(N(X) = k | \bar{\lambda}_i(X) \neq 0) \\ &= \sum_{k \in \mathcal{N}} \Pr(\bar{\lambda}_i(X) Y = 1 | \bar{\lambda}_i(X) \neq 0, N(X) = k, X' \in k) \Pr(X' \in k | N(X) = k, \bar{\lambda}_i(X) \neq 0) \\ &\quad \times \Pr(N(X) = k | \bar{\lambda}_i(X) \neq 0). \end{aligned}$$

Algorithm 2 Label Model (Single Task)

Input: Labeling functions $\lambda = \lambda_1, \dots, \lambda_m$, prior $\Pr(Y)$, unlabeled dataset $D = \{X_i\}_{i=1}^n$.
Returns: $\Pr(\tilde{Y} = 1 | \lambda = \lambda(X))$
for $\lambda_i \in \lambda$ **do**
 Choose λ_j, λ_k that have the largest minimum overlap among pairs of $\lambda_i, \lambda_j, \lambda_k$.
 $\hat{a}_i^E \leftarrow \sqrt{|\hat{\mathbb{E}}[\lambda_i \lambda_j] \cdot \hat{\mathbb{E}}[\lambda_i \lambda_k] / \hat{\mathbb{E}}[\lambda_j \lambda_k]|}$ using observable estimates from D .
 Convert \hat{a}_i^E into a probability $\hat{a}_i = \frac{1}{2}(\hat{a}_i^E + 1)$.
 if $\lambda_i(X) = 1$ **then**
 $\Pr_{\hat{\mu}}(\lambda_i = \lambda_i(X) | Y = 1) = \hat{a}_i \Pr(\lambda_i \neq 0)$.
 else if $\lambda_i(X) = -1$ **then**
 $\Pr_{\hat{\mu}}(\lambda_i = \lambda_i(X) | Y = 1) = (1 - \hat{a}_i) \Pr(\lambda_i \neq 0)$.
 else
 $\Pr_{\hat{\mu}}(\lambda_i = \lambda_i(X) | Y = 1) = \Pr(\lambda_i = 0)$.
 Compute $\Pr_{\hat{\mu}}(\tilde{Y} = 1 | \lambda = \lambda(X)) = \prod_{i=1}^m \Pr_{\hat{\mu}}(\lambda_i = \lambda_i(X) | Y = 1) \Pr(Y = 1) / \Pr(\lambda = \lambda(X))$.

Note that $\Pr(X' \in k | N(X) = k, \bar{\lambda}_i(X) \neq 0)$ is equal to 1, since X' is always chosen from k if X 's neighbors are k . So we now have

$$\begin{aligned} \bar{a}_i &= \sum_{k \in \mathcal{N}} \Pr(\bar{\lambda}_i(X)Y = 1 | \bar{\lambda}_i(X) \neq 0, N(X) = k, X' \in k) \Pr(N(X) = k | \bar{\lambda}_i(X) \neq 0) \\ &= \sum_{k \in \mathcal{K}} \sum_{x_j \in k} \Pr(\bar{\lambda}_i(X)Y = 1 | \bar{\lambda}_i(X) \neq 0, N(X) = k, X' = x_j, X' \in k) \times \\ &\quad \Pr(X' = x_j | \bar{\lambda}_i(X) \neq 0, N(X) = k, X' \in k) \times \Pr(N(X) = k | \bar{\lambda}_i(X) \neq 0). \end{aligned} \quad (5)$$

$\Pr(X' = x_j | \bar{\lambda}_i(X) \neq 0, N(X) = k, X' \in k)$ corresponds to our weighting rule, which here is equal to the conditional pdf $\Pr(X' = x_j | X' \in k)$. We now focus on the first term $\Pr(\bar{\lambda}_i(X)Y = 1 | \bar{\lambda}_i(X) \neq 0, N(X) = k, X' = x_j, X' \in k)$, which can be decomposed into the sum of four probabilities:

$$\begin{aligned} &\Pr(\bar{\lambda}_i(X)Y = 1 | \bar{\lambda}_i(X) \neq 0, N(X) = k, X' = x_j, X' \in k) \\ &= \Pr(\bar{\lambda}_i(X) = \lambda_i(X'), \lambda_i(X') = Y', Y' = Y | \bar{\lambda}_i(X) \neq 0, N(X) = k, X' = x_j, X' \in k) + \quad (6) \\ &\quad \Pr(\bar{\lambda}_i(X) \neq \lambda_i(X'), \lambda_i(X') = Y', Y' \neq Y | \bar{\lambda}_i(X) \neq 0, N(X) = k, X' = x_j, X' \in k) + \\ &\quad \Pr(\bar{\lambda}_i(X) \neq \lambda_i(X'), \lambda_i(X') \neq Y', Y' = Y | \bar{\lambda}_i(X) \neq 0, N(X) = k, X' = x_j, X' \in k) + \\ &\quad \Pr(\bar{\lambda}_i(X) = \lambda_i(X'), \lambda_i(X') \neq Y', Y' \neq Y | \bar{\lambda}_i(X) \neq 0, N(X) = k, X' = x_j, X' \in k). \end{aligned}$$

Each of these probabilities can be expressed using the chain rule. Taking the first line (6) as an example, we have

$$\begin{aligned} &\Pr(\bar{\lambda}_i(X) = \lambda_i(X'), \lambda_i(X') = Y', Y' = Y | \bar{\lambda}_i(X) \neq 0, N(X) = k, X' = x_j, X' \in k) \\ &= \Pr(\bar{\lambda}_i(X) = \lambda_i(X') | \lambda_i(X') = Y', Y' = Y, \bar{\lambda}_i(X) \neq 0, N(X) = k, X' = x_j, X' \in k) \quad (7) \\ &\quad \times \Pr(\lambda_i(X') = Y' | Y' = Y, \bar{\lambda}_i(X) \neq 0, N(X) = k, X' = x_j, X' \in k) \quad (8) \\ &\quad \times \Pr(Y' = Y | \bar{\lambda}_i(X) \neq 0, N(X) = k, X' = x_j, X' \in k). \quad (9) \end{aligned}$$

(7) is always equal to 1 according to our extension procedure. (8) describes the accuracy of the labeling function on x_j , and (9) describes the smoothness of the Y labels over X 's neighbors. Define

$$h(r) = \Pr(Y' \neq Y | \bar{\lambda}_i(X) \neq 0, X' \in \text{supp}(\lambda_i), d_{\mathcal{Z}}(X, X') \leq r),$$

and

$$a_i^j = \Pr(\lambda_i(X') = Y' | X' = x_j).$$

Then, since $X' \in \text{supp}(\lambda_i)$ and $d_{\mathcal{Z}}(X, X') \leq r$ are implied by $x' \in k$,

$$\Pr(\bar{\lambda}_i(X)Y = 1 | \bar{\lambda}_i(X) \neq 0, N(X) = k, X' = x_j, X' \in k) = a_i^j(1 - h(r)) + (1 - a_i^j)h(r).$$

The new accuracy per point is always worse than before; therefore, we can use this extension method applied on the entirety of $\text{supp}(\bar{\lambda}_i)$ to lower bound the extension method applied on only $B_r(\lambda_i)$ while retaining a_i^j over $\text{supp}(\lambda_i)$ without propagating X' . Next, (5) can be written as

$$\begin{aligned} \bar{a}_i &= \sum_{k \in \mathcal{K}} \sum_{x_j \in k} (a_i^j(1 - h(r)) + (1 - a_i^j)h(r)) \Pr(X' = x_j | X' \in k) \Pr(N(X) = k | \bar{\lambda}_i(X) \neq 0) \\ &= (1 - h(r)) \sum_{k \in \mathcal{K}} \sum_{x_j \in k} a_i^j \times \Pr(X' = x_j | X' \in k) \times \Pr(N(X) = k | \bar{\lambda}_i(X) \neq 0) + \\ &\quad h(r) \sum_{k \in \mathcal{K}} \sum_{x_j \in k} (1 - a_i^j) \times \Pr(X' = x_j | X' \in k) \times \Pr(N(X) = k | \bar{\lambda}_i(X) \neq 0). \end{aligned}$$

Moreover, since accuracies on each $N(X)$ on average are equal to a_i by assumption, our expression just becomes

$$\begin{aligned} \bar{a}_i &= (1 - h(r)) \sum_{k \in \mathcal{K}} a_i \times \Pr(N(X) = k | \bar{\lambda}_i(X) \neq 0) + \\ &\quad h(r) \sum_{k \in \mathcal{K}} a_i \times \Pr(N(X) = k | \bar{\lambda}_i(X) \neq 0) \bar{a}_i \\ &= (1 - h(r))a_i + h(r)(1 - a_i). \end{aligned}$$

Lastly, we aim to upper bound $h(r)$, which will lower bound \bar{a}_i if $a_i \geq 0.5$ (i.e. our labeling function is better than random). We write $h(r)$ in terms of $M_Y(r)$:

$$\begin{aligned} M_Y(r) &\geq \Pr(Y \neq Y' | d_{\mathcal{Z}}(X, X') \leq r) \\ &\geq \Pr(Y \neq Y' | d_{\mathcal{Z}}(X, X') \leq r, X \in \text{supp}(\bar{\lambda}_i), X' \in \text{supp}(\lambda_i)) \\ &\quad \times \Pr(X \in \text{supp}(\bar{\lambda}_i), X' \in \text{supp}(\lambda_i) | d_{\mathcal{Z}}(X, X') \leq r) \end{aligned}$$

Then,

$$\begin{aligned} h(r) &\leq \frac{M_Y(r)}{\Pr(X \in \text{supp}(\bar{\lambda}_i), X' \in \text{supp}(\lambda_i) | d_{\mathcal{Z}}(X, X') \leq r)} \\ &= M_Y(r) \frac{\Pr(d_{\mathcal{Z}}(X, X') \leq r)}{\Pr(d_{\mathcal{Z}}(X, X') \leq r | X \in \text{supp}(\bar{\lambda}_i), X' \in \text{supp}(\lambda_i)) \Pr(X \in \text{supp}(\bar{\lambda}_i), X' \in \text{supp}(\lambda_i))}. \end{aligned}$$

$\Pr(d_{\mathcal{Z}}(X, X') \leq r)$ is less than $\Pr(d_{\mathcal{Z}}(X, X') \leq r | X \in \text{supp}(\bar{\lambda}_i), X' \in \text{supp}(\lambda_i))$, since the condition limits the maximum distance between points. Then our bound becomes

$$\begin{aligned} h(r) &\leq \frac{M_Y(r)}{\Pr(X \in \text{supp}(\bar{\lambda}_i), X' \in \text{supp}(\lambda_i))} \\ &\leq \frac{M_Y(r)}{\Pr(X \in \text{supp}(\bar{\lambda}_i)) \Pr(X' \in \text{supp}(\lambda_i))} \leq \frac{M_Y(r)}{(1 + L_{\lambda'_i}(r)p_{d(r)})p_i^2}, \end{aligned}$$

where we have used Lemma 5 in the last inequality. Therefore, our final bound is

$$\bar{a}_i \geq a_i + (1 - 2a_i) \frac{M_Y(r)}{(1 + L_{\lambda'_i}(r)p_{d(r)})p_i^2}.$$

We can also compute $\tilde{a}_i = \Pr(\bar{\lambda}_i(X)Y = 1 | X \in B_r(\lambda_i))$ in terms of a_i and \bar{a}_i .

$$\begin{aligned} \bar{a}_i &= \Pr(\bar{\lambda}_i Y = 1 | \bar{\lambda}_i \neq 0) = \Pr(\bar{\lambda}_i Y = 1 | \lambda_i \neq 0) \Pr(X \in \text{supp}(\lambda_i) | X \in \text{supp}(\bar{\lambda}_i)) + \\ &\quad \Pr(\bar{\lambda}_i(X)Y = 1 | X \in B_r(\lambda_i)) \Pr(X \in B_r(\lambda_i) | X \in \text{supp}(\bar{\lambda}_i)) \\ &= a_i \frac{1}{1 + L_{\lambda'_i}(r)p_{d(r)}} + \tilde{a}_i \frac{L_{\lambda'_i}(r)p_{d(r)}}{1 + L_{\lambda'_i}(r)p_{d(r)}} \end{aligned}$$

Therefore,

$$\begin{aligned}\tilde{a}_i &= \frac{(1 + L_{\lambda'_i}(r)p_{d(r)})\bar{a}_i - a_i}{L_{\lambda'_i}(r)p_{d(r)}} = \frac{\bar{a}_i - a_i}{L_{\lambda'_i}(r)p_{d(r)}} + \bar{a}_i \\ &\leq \bar{a}_i + (1 - 2a_i) \frac{M_Y(r)}{L_{\lambda'_i}(r)p_{d(r)}(1 + L_{\lambda'_i}(r)p_{d(r)})p_i^2}\end{aligned}$$

C.2 Theorem 1 Risk Estimation Error

We first bound the estimation error $\mathbb{E}[\|\hat{a} - a\|_1]$ by analyzing the given WS parameter recovery method. Note that this approach also holds for EPOXY.

Lemma 3. *Denote M as the conditional second moment matrix over all observed variables, e.g. $M_{ij} = \mathbb{E}[\lambda_i \lambda_j | \lambda_i \neq 0, \lambda_j \neq 0]$ and assume that there are a sufficient number of samples such that all $\hat{M}_{ij} \neq 0$. Define $e_{\min} = \min\{\min_i |\hat{a}_i^E|, |a_i^E|\}$ and $c_1 = \min_{i,j} \{\mathbb{E}[\lambda_i \lambda_j | \lambda_i, \lambda_j \neq 0], \hat{\mathbb{E}}[\lambda_i \lambda_j | \lambda_i, \lambda_j \neq 0]\}$. Assume $\text{sign}(a_i^E) = \text{sign}(\hat{a}_i^E)$ for all a_i^E . Then, when the minimum overlap of labeling functions used in the parameter recovery is $o_{\min} \leq \Pr(X \in \text{supp}(\lambda_i) \cap \text{supp}(\lambda_j))$ for all i, j pairs used for parameter recovery, the estimation error of the accuracies is*

$$\mathbb{E}[\|\hat{a} - a\|_1] \leq \frac{81\sqrt{\pi}}{e_{\min}c_1^2} \cdot \frac{m}{\sqrt{n \cdot o_{\min}}}.$$

Proof. Suppose $\lambda_i, \lambda_j, \lambda_k$ make up a conditionally independent triplet, and in total let T be the set of triplets we need to recover all accuracies. Our estimate of a^E can be obtained with

$$|\hat{a}_i^E| = \left(\frac{|\hat{M}_{ij}||\hat{M}_{ik}|}{|\hat{M}_{jk}|} \right)^{\frac{1}{2}}.$$

Because we assume that signs are completely recoverable,

$$\|\hat{a}^E - a^E\|_1 = \|\hat{a}^E| - |a^E|\|_1 = \sum_{\{i,j,k\} \in T} \left| |\hat{a}_i^E| - |a_i^E| \right| + \left| |\hat{a}_j^E| - |a_j^E| \right| + \left| |\hat{a}_k^E| - |a_k^E| \right|. \quad (10)$$

Note that $|(\hat{a}_i^E)^2 - (a_i^E)^2| = |\hat{a}_i^E - a_i^E| |\hat{a}_i^E + a_i^E|$. By the reverse triangle inequality, $|\hat{a}_i^E| - |a_i^E| \leq |\hat{a}_i^E - a_i^E| = \frac{|(\hat{a}_i^E)^2 - (a_i^E)^2|}{|\hat{a}_i^E + a_i^E|} \leq \frac{1}{2e_{\min}} |(\hat{a}_i^E)^2 - (a_i^E)^2|$, because $|\hat{a}_i^E + a_i^E| = |\hat{a}_i^E| + |a_i^E| \geq 2e_{\min}$. Then

$$\begin{aligned}||\hat{a}_i^E| - |a_i^E|| &\leq \frac{1}{2e_{\min}} |(\hat{a}_i^E)^2 - (a_i^E)^2| = \frac{1}{2e_{\min}} \left| \frac{|\hat{M}_{ij}||\hat{M}_{ik}|}{|\hat{M}_{jk}|} - \frac{|M_{ij}||M_{ik}|}{|M_{jk}|} \right| \\ &= \frac{1}{2e_{\min}} \left| \frac{|\hat{M}_{ij}||\hat{M}_{ik}|}{|\hat{M}_{jk}|} - \frac{|\hat{M}_{ij}||\hat{M}_{ik}|}{|M_{jk}|} + \frac{|\hat{M}_{ij}||\hat{M}_{ik}|}{|M_{jk}|} - \frac{|\hat{M}_{ij}||M_{ik}|}{|M_{jk}|} + \frac{|\hat{M}_{ij}||M_{ik}|}{|M_{jk}|} - \frac{|M_{ij}||M_{ik}|}{|M_{jk}|} \right| \\ &\leq \frac{1}{2e_{\min}} \left(\left| \frac{\hat{M}_{ij}\hat{M}_{ik}}{\hat{M}_{jk}M_{jk}} \right| \left| |\hat{M}_{jk}| - |M_{jk}| \right| + \left| \frac{\hat{M}_{ij}}{M_{jk}} \right| \left| |\hat{M}_{ik}| - |M_{ik}| \right| + \left| \frac{M_{ik}}{M_{jk}} \right| \left| |\hat{M}_{ij}| - |M_{ij}| \right| \right) \\ &\leq \frac{1}{2e_{\min}} \left(\left| \frac{\hat{M}_{ij}\hat{M}_{ik}}{\hat{M}_{jk}M_{jk}} \right| |\hat{M}_{jk} - M_{jk}| + \left| \frac{\hat{M}_{ij}}{M_{jk}} \right| |\hat{M}_{ik} - M_{ik}| + \left| \frac{M_{ik}}{M_{jk}} \right| |\hat{M}_{ij} - M_{ij}| \right).\end{aligned}$$

Clearly, all elements of \hat{M} and M must be less than 1. We further know that elements of $|M|$ and $|\hat{M}|$ are at least c_1 . Define $\Delta_{ij} = \hat{M}_{ij} - M_{ij}$. Then

$$\begin{aligned}||\hat{a}_1^E| - |a_1^E|| &\leq \frac{1}{2e_{\min}} \left(\frac{1}{c_1^2} |\Delta_{jk}| + \frac{1}{c_1} |\Delta_{ik}| + \frac{1}{c_1} |\Delta_{ij}| \right) \\ &\leq \frac{1}{2e_{\min}} \sqrt{\Delta_{jk}^2 + \Delta_{ik}^2 + \Delta_{ij}^2} \sqrt{\frac{1}{c_1^4} + \frac{2}{c_1^2}}.\end{aligned}$$

(10) is now

$$\|\hat{a}^E - a^E\|_1 \leq \frac{3}{2e_{\min}} \sqrt{\frac{1}{c_1^4} + \frac{2}{c_1^2}} \sum_{\{i,j,k\} \in T} \sqrt{\Delta_{jk}^2 + \Delta_{ik}^2 + \Delta_{ij}^2}.$$

Note that the Frobenius norm of the error on the 3×3 submatrix of M defined over $\tau = \{i, j, k\}$ is

$$\|\hat{M}_\tau - M_\tau\|_F = \sqrt{2} \cdot \sqrt{\Delta_{ij}^2 + \Delta_{ik}^2 + \Delta_{jk}^2}.$$

Moreover, $\|\hat{M}_\tau - M_\tau\|_F \leq \sqrt{3} \|\hat{M}_\tau - M_\tau\|_2$. Putting everything together,

$$\|\hat{a}^E - a^E\|_1 \leq \frac{3\sqrt{3}}{2\sqrt{2}e_{\min}} \sqrt{\frac{1}{c_1^4} + \frac{2}{c_1^2}} \sum_{\tau \in T} \|\hat{M}_\tau - M_\tau\|_2,$$

and the expectation is

$$\mathbb{E} [\|\hat{a}^E - a^E\|_1] \leq \frac{3\sqrt{3}}{2\sqrt{2}e_{\min}} \sqrt{\frac{1}{c_1^4} + \frac{2}{c_1^2}} \sum_{\tau \in T} \mathbb{E} [\|\hat{M}_\tau - M_\tau\|_2]. \quad (11)$$

We use the matrix Hoeffding inequality as described in [50], which says

$$\Pr(\|\hat{M} - M\|_2 \geq \gamma) \leq 2m \exp\left(-\frac{n\gamma^2}{32m^2}\right).$$

For τ , we can integrate this to get

$$\begin{aligned} \mathbb{E}[\|\hat{M}_\tau - M_\tau\|_2] &= \int_0^\infty \Pr(\|\hat{M}_\tau - M_\tau\|_2 \geq \gamma) d\gamma \leq \int_0^\infty 2m \exp\left(-\frac{no_{\min}\gamma^2}{32m^2}\right) d\gamma \\ &= 2m \sqrt{(32m^2/(n \cdot o_{\min}))\pi} \int_0^\infty \frac{1}{\sqrt{(32m^2/(n \cdot o_{\min}))\pi}} \exp\left(-\frac{\gamma^2}{32m^2/(n \cdot o_{\min})}\right) d\gamma \\ &= m \sqrt{\frac{32m^2\pi}{n \cdot o_{\min}}}. \end{aligned}$$

Since $m = 3$ for M_τ , this is equal to $36\sqrt{\frac{2\pi}{n \cdot o_{\min}}}$. Substituting this back into (11), we get

$$\begin{aligned} \mathbb{E} [\|\hat{a}^E - a^E\|_1] &\leq \frac{3\sqrt{3}}{2\sqrt{2}e_{\min}} \sqrt{\frac{1}{c_1^4} + \frac{2}{c_1^2}} \sum_{\tau \in T} 36\sqrt{\frac{2\pi}{n \cdot o_{\min}}} \\ &\leq \frac{3\sqrt{3}}{e_{\min}} \sqrt{\frac{1}{c_1^4} + \frac{2}{c_1^2}} \sum_{\tau \in T} 18\sqrt{\frac{\pi}{n \cdot o_{\min}}}. \end{aligned}$$

At most $|T| = m$ if we were to do a separate triplet for each a_i , so our bound becomes

$$\begin{aligned} \mathbb{E} [\|\hat{a}^E - a^E\|_1] &\leq \frac{3\sqrt{3}}{e_{\min}} \sqrt{\frac{1}{c_1^4} + \frac{2}{c_1^2}} m \cdot 18\sqrt{\frac{\pi}{n \cdot o_{\min}}} \\ &\leq \frac{54\sqrt{3}}{e_{\min}} \sqrt{\frac{1}{c_1^4} + \frac{2}{c_1^2}} m \sqrt{\frac{\pi}{n \cdot o_{\min}}}. \end{aligned}$$

Finally, note that $\frac{1}{c_1^4} + \frac{2}{c_1^2} \leq \frac{3}{c_1^2}$, and that $\mathbb{E} [\|\hat{a} - a\|_1] = \frac{1}{2} \mathbb{E} [\|\hat{a}^E - a^E\|_1]$. Therefore, the sampling error for the accuracy is bounded by

$$\mathbb{E} [\|\hat{a} - a\|_1] \leq \frac{81\sqrt{\pi}}{e_{\min}c_1^2} \cdot \frac{m}{\sqrt{n \cdot o_{\min}}}.$$

□

Now, recall that $f_{WS}(X) = 2 \Pr_\mu(\tilde{Y} = 1|\lambda(X)) - 1$, where μ corresponds to the accuracies. Define $\hat{f}_{WS}(X) = 2 \Pr_{\hat{\mu}}(\tilde{Y} = 1|\lambda(X)) - 1$. We want to bound the gap between $\mathcal{R}(f_{WS})$ and $\mathcal{R}(\hat{f}_{WS})$.

$$\begin{aligned} \mathbb{E} \left[|\mathcal{R}(f_{WS}) - \mathcal{R}(\hat{f}_{WS})| \right] &\leq \mathbb{E} \left[\mathbb{E}_{X,Y \sim \mathcal{D}} \left[\left| \text{sign}(Y) \left(\Pr_\mu(\tilde{Y} = 1|\lambda(X)) - \Pr_{\hat{\mu}}(\tilde{Y} = 1|\lambda(X)) \right) \right| \right] \right] \\ &= \mathbb{E} \left[\mathbb{E}_{X,Y \sim \mathcal{D}} \left[\left| \frac{\Pr_\mu(\lambda(X)|Y=1)p}{\Pr(\lambda(X))} - \frac{\Pr_{\hat{\mu}}(\lambda(X)|Y=1)p}{\hat{\Pr}(\lambda(X))} \right| \right] \right] \\ &= \mathbb{E}_{X,Y \sim \mathcal{D}} \left[\mathbb{E} \left[\left| \frac{\Pr_\mu(\lambda(X)|Y=1)p}{\Pr(\lambda(X))} - \frac{\Pr_{\hat{\mu}}(\lambda(X)|Y=1)p}{\hat{\Pr}(\lambda(X))} \right| \right] \right]. \end{aligned}$$

Here, we have abbreviated $\Pr(\lambda = \lambda(X))$ as $\Pr(\lambda(X))$. Note that $\hat{\Pr}(\lambda(X))$ is observable. Let $|\Pr(\lambda(X)) - \hat{\Pr}(\lambda(X))| = \varepsilon$. Let I_+ be the event that $\frac{\Pr_\mu(\lambda(X)|Y=1)}{\Pr(\lambda(X))} \geq \frac{\Pr_{\hat{\mu}}(\lambda(X)|Y=1)}{\hat{\Pr}(\lambda(X))}$ and similarly I_- . Then, the risk gap becomes

$$\begin{aligned} \mathbb{E}_{X,Y \sim \mathcal{D}} \left[\mathbb{E}_{I_+} \left[\frac{\Pr_\mu(\lambda(X)|Y=1)p}{\Pr(\lambda(X))} - \frac{\Pr_{\hat{\mu}}(\lambda(X)|Y=1)p}{\hat{\Pr}(\lambda(X))} \right] \Pr(I_+) + \right. \\ \left. \mathbb{E}_{I_-} \left[\frac{\Pr_{\hat{\mu}}(\lambda(X)|Y=1)p}{\hat{\Pr}(\lambda(X))} - \frac{\Pr_\mu(\lambda(X)|Y=1)p}{\Pr(\lambda(X))} \right] \Pr(I_-) \right]. \quad (12) \end{aligned}$$

We can then bound $\hat{\Pr}(\lambda(X))$ with $\Pr(\lambda(X)) + \varepsilon$ in the case of I_+ and with $\Pr(\lambda(X)) - \varepsilon$ in the case of I_- . We can write (12) as being less than

$$\begin{aligned} &\mathbb{E}_{\mathcal{D}} \left[\mathbb{E}_{I_+} \left[\frac{\Pr_\mu(\lambda(X)|Y=1)p}{\Pr(\lambda(X))} - \frac{\Pr_{\hat{\mu}}(\lambda(X)|Y=1)p}{\Pr(\lambda(X)) + \varepsilon} \right] \Pr(I_+) + \right. \\ &\quad \left. \mathbb{E}_{I_-} \left[\frac{\Pr_{\hat{\mu}}(\lambda(X)|Y=1)p}{\Pr(\lambda(X)) - \varepsilon} - \frac{\Pr_\mu(\lambda(X)|Y=1)p}{\Pr(\lambda(X))} \right] \Pr(I_-) \right] \\ &= \mathbb{E}_{\mathcal{D}} \left[\mathbb{E}_{I_+} \left[\frac{\Pr(\lambda(X))(\Pr_\mu(\lambda(X)|Y=1) - \Pr_{\hat{\mu}}(\lambda(X)|Y=1)) + \varepsilon \Pr_\mu(\lambda(X)|Y=1)}{\Pr(\lambda(X))(\Pr(\lambda(X)) + \varepsilon)} \right] p \Pr(I_+) + \right. \\ &\quad \left. \mathbb{E}_{I_-} \left[\frac{\Pr(\lambda(X))(\Pr_{\hat{\mu}}(\lambda(X)|Y=1) - \Pr_\mu(\lambda(X)|Y=1)) + \varepsilon \Pr_\mu(\lambda(X)|Y=1)}{\Pr(\lambda(X))(\Pr(\lambda(X)) - \varepsilon)} \right] p \Pr(I_-) \right] \\ &\leq \mathbb{E}_{\mathcal{D}} \left[\mathbb{E} \left[\frac{\Pr(\lambda(X)) |\Pr_\mu(\lambda(X)|Y=1) - \Pr_{\hat{\mu}}(\lambda(X)|Y=1)| + \varepsilon \Pr_\mu(\lambda(X)|Y=1)}{\Pr(\lambda(X))(\Pr(\lambda(X)) - \varepsilon)} \right] \right] \cdot p \\ &= \mathbb{E}_{\mathcal{D}} \left[\mathbb{E} \left[\frac{|\Pr_\mu(\lambda(X)|Y=1) - \Pr_{\hat{\mu}}(\lambda(X)|Y=1)|}{\Pr(\lambda(X)) - \varepsilon} \right] + \frac{\Pr_\mu(\lambda(X)|Y=1)}{\Pr(\lambda(X))} \mathbb{E} \left[\frac{\varepsilon}{\Pr(\lambda(X)) - \varepsilon} \right] \right] \cdot p. \end{aligned}$$

We can apply Hoeffding's inequality on $\hat{\Pr}(\lambda(X)) - \Pr(\lambda(X))$. For any $\lambda(X)$, we have that $\Pr(|\hat{\Pr}(\lambda(X)) - \Pr(\lambda(X))| \geq \gamma) \leq 2 \exp(-2n\gamma^2)$. Therefore, with probability at least $1 - \delta$, $|\hat{\Pr}(\lambda(X)) - \Pr(\lambda(X))| \leq \sqrt{\frac{\log(2/\delta)}{2n}}$. Denote $\varepsilon_n = \sqrt{\frac{\log(2/\delta)}{2n}}$. Then with high probability,

$$\mathbb{E} \left[\frac{|\Pr_\mu(\lambda(X)|Y=1) - \Pr_{\hat{\mu}}(\lambda(X)|Y=1)|}{\Pr(\lambda(X)) - \varepsilon} \right] \leq \frac{\mathbb{E} [|\Pr_\mu(\lambda(X)|Y=1) - \Pr_{\hat{\mu}}(\lambda(X)|Y=1)|]}{\Pr(\lambda(X)) - \varepsilon_n}.$$

Similarly, $\mathbb{E} \left[\frac{\varepsilon}{\Pr(\lambda(X)) - \varepsilon} \right]$ can be written as $\mathbb{E} \left[\frac{\Pr(\lambda(X))}{\Pr(\lambda(X)) - \varepsilon} \right] - 1$. Under the same event that $\varepsilon \leq \varepsilon_n$, we have that $\mathbb{E} \left[\frac{\varepsilon}{\Pr(\lambda(X)) - \varepsilon} \right]$ is less than $\frac{\Pr(\lambda(X))}{\Pr(\lambda(X)) - \varepsilon_n} - 1 = \frac{\varepsilon_n}{\Pr(\lambda(X)) - \varepsilon_n}$. Therefore, with high

probability our expression is bounded by

$$\mathbb{E}_{\mathcal{D}} \left[\frac{\mathbb{E} [|\Pr_{\mu}(\boldsymbol{\lambda}(X)|Y=1) - \Pr_{\hat{\mu}}(\boldsymbol{\lambda}(X)|Y=1)|]}{\Pr(\boldsymbol{\lambda}(X)) - \varepsilon_n} + \frac{\Pr_{\mu}(\boldsymbol{\lambda}(X)|Y=1)}{\Pr(\boldsymbol{\lambda}(X))} \frac{\varepsilon_n}{\Pr(\boldsymbol{\lambda}(X)) - \varepsilon_n} \right] \cdot p \quad (13)$$

We now focus on the value of $|\Pr_{\mu}(\boldsymbol{\lambda}(X)|Y=1) - \Pr_{\hat{\mu}}(\boldsymbol{\lambda}(X)|Y=1)|$. Regardless of what X is, $\Pr_{\mu}(\boldsymbol{\lambda}(X)|Y=1)$ can be written as a product $\prod_{i=1}^m b_i$, where $b_i \in \{a_i, 1 - a_i\}$, and similarly, $\Pr_{\hat{\mu}}(\boldsymbol{\lambda}(X)|Y=1) = \prod_{i=1}^m \hat{b}_i$, where $\hat{b}_i \in \{\hat{a}_i, 1 - \hat{a}_i\}$. Then this difference of probabilities can be written as

$$\begin{aligned} & \left| \Pr_{\mu}(\boldsymbol{\lambda}(X)|Y=1) - \Pr_{\hat{\mu}}(\boldsymbol{\lambda}(X)|Y=1) \right| = \left| \prod_{i=1}^m b_i - \prod_{i=1}^m \hat{b}_i \right| \\ &= \left| b_1 \prod_{i=2}^m b_i - \hat{b}_1 \prod_{i=2}^m b_i + \hat{b}_1 \prod_{i=2}^m b_i - \hat{b}_1 \prod_{i=2}^m \hat{b}_i \right| \\ &= \left| (b_1 - \hat{b}_1) \prod_{i=2}^m b_i + \hat{b}_1 \left(\prod_{i=2}^m b_i - \prod_{i=2}^m \hat{b}_i \right) \right| \\ &\leq |b_1 - \hat{b}_1| \prod_{i=2}^m b_i + \hat{b}_1 \left| \prod_{i=2}^m b_i - \prod_{i=2}^m \hat{b}_i \right| \\ &\leq |b_1 - \hat{b}_1| + \left| \prod_{i=2}^m b_i - \prod_{i=2}^m \hat{b}_i \right|. \end{aligned}$$

Therefore, $|\Pr_{\mu}(\boldsymbol{\lambda}(X)|Y=1) - \Pr_{\hat{\mu}}(\boldsymbol{\lambda}(X)|Y=1)| \leq \sum_{i=1}^m |b_i - \hat{b}_i| = \sum_{i=1}^m |a_i - \hat{a}_i|$. (13) now becomes

$$\mathbb{E}_{X,Y \sim \mathcal{D}} \left[\frac{\mathbb{E} [\|a - \hat{a}\|_1] p}{\Pr(\boldsymbol{\lambda}(X)) - \varepsilon_n} \right] + \mathbb{E}_{X,Y \sim \mathcal{D}} \left[\Pr(Y=1|\boldsymbol{\lambda}(X)) \cdot \frac{\varepsilon_n}{\Pr(\boldsymbol{\lambda}(X)) - \varepsilon_n} \right].$$

Define c_p as the minimum value of $\Pr(\boldsymbol{\lambda}(X))$, e.g. the smallest “region” and define $c_2 = \mathbb{E}_{X,Y \sim \mathcal{D}} [\Pr(Y=1|\boldsymbol{\lambda}(X))]$. Then our risk gap is less than

$$\frac{\mathbb{E} [\|a - \hat{a}\|_1] p}{c_p - \varepsilon_n} + \frac{\varepsilon_n \cdot c_2}{c_p - \varepsilon_n}.$$

Using the accuracy estimation error result from Lemma 3, we have that with high probability,

$$\mathbb{E} [|\mathcal{R}(f_{WS}) - \mathcal{R}(\hat{f}_{WS})|] \leq \frac{81\sqrt{\pi}p}{e_{\min} c_1^2 (c_p - \varepsilon_n)} \cdot \frac{m}{\sqrt{n \cdot o_{\min}}} + \frac{\varepsilon_n \cdot c_2}{c_p - \varepsilon_n}.$$

Since the parameter recovery method is the same for EPOXY, we replace $n \cdot o_{\min}$ with $n \cdot o_{\min}(1 + L_{\min}(r_{\min}) \cdot p_{d(r_{\min})})$ using Lemma 6. Note that some of the constants will also be renamed. Our estimation error for EPOXY is then

$$\mathbb{E} [|\mathcal{R}(f_E) - \mathcal{R}(\hat{f}_E)|] \leq \frac{81\sqrt{\pi}p}{\bar{e}_{\min} \bar{c}_1^2 (\bar{c}_p - \varepsilon_n)} \cdot \frac{m}{\sqrt{n \cdot o_{\min}(1 + L_{\min}(r_{\min}) \cdot p_{d(r_{\min})})}} + \frac{\varepsilon_n \cdot \bar{c}_2}{\bar{c}_p - \varepsilon_n}.$$

C.3 Theorem 1 Generalization Lift

We now present proof of the asymptotic generalization lift result in Theorem 1, for which we compare label models parametrized by μ and $\hat{\mu}$.

$$\begin{aligned}
\mathcal{R}(f_{WS}) - \mathcal{R}(f_E) &= \mathbb{E}_{(X,Y) \sim \mathcal{D}} [\ell(f_{WS}(X), Y) - \ell(f_E(X), Y)] \\
&= \frac{1}{2} \mathbb{E}_{(X,Y) \sim \mathcal{D}} [|Y - 2 \Pr_{\mu}(\tilde{Y} = 1 | \boldsymbol{\lambda} = \boldsymbol{\lambda}(X)) + 1| - |Y - 2 \Pr_{\bar{\mu}}(\tilde{Y} = 1 | \bar{\boldsymbol{\lambda}} = \bar{\boldsymbol{\lambda}}(X)) + 1|] \\
&= \mathbb{E}_{X,Y \sim \mathcal{D}} \left[\text{sign}(Y) \left(\Pr_{\bar{\mu}}(\tilde{Y} = 1 | \bar{\boldsymbol{\lambda}} = \bar{\boldsymbol{\lambda}}(X), \lambda_{-i}(X)) - \Pr_{\mu}(\tilde{Y} = 1 | \boldsymbol{\lambda} = \boldsymbol{\lambda}(X), \lambda_{-i}(X)) \right) \right] \\
&= \mathbb{E}_{X,Y \sim \mathcal{D}} \left[\text{sign}(Y) \left(\frac{\Pr_{\bar{\mu}}(\tilde{Y} = 1, \bar{\boldsymbol{\lambda}} = \bar{\boldsymbol{\lambda}}(X), \lambda_{-i}(X))}{\Pr_{\bar{\mu}}(\bar{\boldsymbol{\lambda}} = \bar{\boldsymbol{\lambda}}(X), \lambda_{-i}(X))} - \frac{\Pr_{\mu}(\tilde{Y} = 1, \boldsymbol{\lambda} = \boldsymbol{\lambda}(X), \lambda_{-i}(X))}{\Pr_{\mu}(\boldsymbol{\lambda} = \boldsymbol{\lambda}(X), \lambda_{-i}(X))} \right) \right]. \tag{14}
\end{aligned}$$

We rewrite the probabilities:

$$\begin{aligned}
\mathbb{E}_{X,Y \sim \mathcal{D}} \left[\text{sign}(Y) \left(\frac{\Pr_{\bar{\mu}}(\bar{\boldsymbol{\lambda}} = \bar{\boldsymbol{\lambda}}(X), \lambda_{-i}(X) | Y = 1)p}{\Pr_{\bar{\mu}}(\bar{\boldsymbol{\lambda}} = \bar{\boldsymbol{\lambda}}(X), \lambda_{-i}(X) | Y = 1)p + \Pr_{\bar{\mu}}(\bar{\boldsymbol{\lambda}} = \bar{\boldsymbol{\lambda}}(X), \lambda_{-i}(X) | Y = -1)(1-p)} \right. \right. \\
\left. \left. - \frac{\Pr_{\mu}(\boldsymbol{\lambda} = \boldsymbol{\lambda}(X), \lambda_{-i}(X) | Y = 1)p}{\Pr_{\mu}(\boldsymbol{\lambda} = \boldsymbol{\lambda}(X), \lambda_{-i}(X) | Y = 1)p + \Pr_{\mu}(\boldsymbol{\lambda} = \boldsymbol{\lambda}(X), \lambda_{-i}(X) | Y = -1)(1-p)} \right) \right]. \tag{15}
\end{aligned}$$

Since all labeling functions are conditionally independent, we have that $\Pr_{\bar{\mu}}(\bar{\boldsymbol{\lambda}} = \bar{\boldsymbol{\lambda}}(X), \lambda_{-i}(X) | Y = 1) = \Pr_{\bar{\mu}}(\bar{\lambda}_i = \bar{\lambda}_i(X) | Y = 1) \times \prod_{j \neq i} \Pr(\bar{\lambda}_j = \lambda_j(X) | Y = 1)$. Define

$$\begin{aligned}
p(X) &= \Pr(Y = 1 | \lambda_{-i} = \lambda_{-i}(X)) \\
&= \frac{\prod_{j \neq i} \Pr(\bar{\lambda}_j = \lambda_j(X) | Y = 1)p}{\prod_{j \neq i} \Pr(\bar{\lambda}_j = \lambda_j(X) | Y = 1)p + \prod_{j \neq i} \Pr(\bar{\lambda}_j = \lambda_j(X) | Y = -1)(1-p)}.
\end{aligned}$$

Then (15) can be written as

$$\begin{aligned}
\mathbb{E} \left[\text{sign}(Y) \left(\frac{\Pr_{\bar{\mu}}(\bar{\lambda}_i = \bar{\lambda}_i(X) | Y = 1)p(X)}{\Pr_{\bar{\mu}}(\bar{\lambda}_i = \bar{\lambda}_i(X) | Y = 1)p(X) + \Pr_{\bar{\mu}}(\bar{\lambda}_i = \bar{\lambda}_i(X) | Y = -1)(1-p(X))} \right. \right. \\
\left. \left. - \frac{\Pr_{\mu}(\lambda_i = \lambda_i(X) | Y = 1)p(X)}{\Pr_{\mu}(\lambda_i = \lambda_i(X) | Y = 1)p(X) + \Pr_{\mu}(\lambda_i = \lambda_i(X) | Y = -1)(1-p(X))} \right) \right].
\end{aligned}$$

Now we look at the lift over three regions: $\text{supp}(\lambda_i)$, $B_r(\lambda_i)$, and $(\text{supp}(\lambda_i) \cup B_r(\lambda_i))^C$. When $X \in \text{supp}(\lambda_i)$, we choose to use the same label model parameters and votes as before, and therefore there is no improvement in the generalization error over this region. Similarly, when both λ_i and $\bar{\lambda}_i$ abstain, there is no improvement. Lastly, when $X \in B_r(\lambda_i)$, the original labeling function would have abstained, in which case $\Pr_{\mu}(\lambda_i = \lambda_i(X) | Y = 1) = \Pr_{\mu}(\lambda_i = 0 | Y = 1) = \Pr(\lambda_i = 0)$, but on the other hand the extended labeling function no longer abstains. Therefore, the lift comes from increased prediction accuracy over $B_r(\lambda_i)$, and we can write

$$\begin{aligned}
\mathcal{R}(f_{WS}) - \mathcal{R}(f_E) &= \Pr(X \in B_r(\lambda_i)) \times \\
&\mathbb{E}_{X \in B_r(\lambda_i)} \left[\text{sign}(Y) \left(\frac{\Pr_{\bar{\mu}}(\bar{\lambda}_i(X) | Y = 1)p(X)}{\Pr_{\bar{\mu}}(\bar{\lambda}_i(X) | Y = 1)p(X) + \Pr_{\bar{\mu}}(\bar{\lambda}_i(X) | Y = -1)(1-p(X))} - p(X) \right) \right]. \tag{16}
\end{aligned}$$

Now, we look at when $Y = 1$ and $Y = -1$ separately and use Lemma 1 to write the probabilities inside the expectation in terms of accuracies.

1. $X \in B_r(\lambda_i), Y = 1$:

This region contributes

$$\begin{aligned}
&\mathbb{E}_{Y=1} \left[\frac{\bar{a}_i p(X)}{\bar{a}_i p(X) + (1 - \bar{a}_i)(1 - p(X))} - p(X) \right] \Pr(X \in B_r(\lambda_i), Y = 1, \bar{\lambda}_i(X) = 1) + \\
&\mathbb{E}_{Y=-1} \left[\frac{(1 - \bar{a}_i)p(X)}{(1 - \bar{a}_i)p(X) + \bar{a}_i(1 - p(X))} - p(X) \right] \Pr(X \in B_r(\lambda_i), Y = 1, \bar{\lambda}_i(X) = -1).
\end{aligned}$$

We can write the probabilities in terms of accuracy:

$$\begin{aligned}
& \Pr(X \in B_r(\lambda_i), Y = 1, \bar{\lambda}_i(X) = 1) \\
&= \Pr(\bar{\lambda}_i(X) = 1 | Y = 1, X \in B_r(\lambda_i)) \Pr(Y = 1, X \in B_r(\lambda_i)) \\
&= \tilde{a}_i \Pr(Y = 1, X \in B_r(\lambda_i)) \\
& \Pr(X \in B_r(\lambda_i), Y = 1, \bar{\lambda}_i(X) = -1) \\
&= \Pr(\bar{\lambda}_i(X) = -1 | Y = 1, X \in B_r(\lambda_i)) \Pr(Y = 1, X \in B_r(\lambda_i)) \\
&= (1 - \tilde{a}_i) \Pr(Y = 1, X \in B_r(\lambda_i)),
\end{aligned}$$

where $\tilde{a}_i = \Pr(\bar{\lambda}_i(X)Y = 1 | X \in B_r(\lambda_i))$. It might not be immediately obvious that $\Pr(\bar{\lambda}_i(X) = 1 | Y = 1, X \in B_r(\lambda_i)) = \tilde{a}_i$, since we only assume that the pre-extension and post-extension labeling functions can be described using the binary Ising model. However, we can write $\Pr(\bar{\lambda}_i = 1 | Y = 1, \bar{\lambda}_i \neq 0)$ as $\Pr(\bar{\lambda}_i(X) = 1 | Y = 1, X \in \text{supp}(\lambda_i)) \Pr(X \in \text{supp}(\lambda_i) | \bar{\lambda}_i \neq 0) + \Pr(\bar{\lambda}_i(X) = 1 | Y = 1, X \in B_r(\lambda_i)) \Pr(X \in B_r(\lambda_i) | \bar{\lambda}_i \neq 0)$. Therefore, $\Pr(\bar{\lambda}_i(X) = 1 | Y = 1, X \in B_r(\lambda_i)) = \frac{\tilde{a}_i \Pr(\bar{\lambda}_i \neq 0) - \tilde{a}_i \Pr(X \in \text{supp}(\lambda_i))}{\Pr(X \in B_r(\lambda_i))}$, which is the definition of \tilde{a}_i .

Since conditioning on the value of $\bar{\lambda}_i(X)$ can be ignored if the expectation is already conditioned on Y , we are able to combine the sum into one expectation to get

$$\begin{aligned}
& \Pr(Y = 1, X \in B_r(\lambda_i)) \cdot \mathbb{E}_{X \in B_r(\lambda_i), Y=1} \left[\frac{\tilde{a}_i \tilde{a}_i p(X)}{\tilde{a}_i p(X) + (1 - \tilde{a}_i)(1 - p(X))} \right. \\
& \left. + \frac{(1 - \tilde{a}_i)(1 - \tilde{a}_i)p(X)}{(1 - \tilde{a}_i)p(X) + \tilde{a}_i(1 - p(X))} - p(X) \right]. \tag{17}
\end{aligned}$$

2. $X \in B_r(\lambda_i), Y = -1$:

This region contributes

$$\begin{aligned}
& \mathbb{E}_{Y=-1} \left[p(X) - \frac{\tilde{a}_i p(X)}{\tilde{a}_i p(X) + (1 - \tilde{a}_i)(1 - p(X))} \right] \Pr(X \in B_r(\lambda_i), Y = -1, \bar{\lambda}_i(X) = 1) + \\
& \mathbb{E}_{Y=-1} \left[p(X) - \frac{(1 - \tilde{a}_i)p(X)}{(1 - \tilde{a}_i)p(X) + \tilde{a}_i(1 - p(X))} \right] \Pr(X \in B_r(\lambda_i), Y = -1, \bar{\lambda}_i(X) = -1).
\end{aligned}$$

We can write the probabilities as $(1 - \tilde{a}_i) \Pr(X \in B_r(\lambda_i), Y = -1)$ and $\tilde{a}_i \Pr(X \in B_r(\lambda_i), Y = -1)$ respectively. Similarly, we note that the expectations can be combined since the behavior of λ_{-i} conditioned on Y does not depend on λ_i . Therefore, the lift in this region is equal to

$$\begin{aligned}
& \Pr(Y = -1, X \in B_r(\lambda_i)) \times \\
& \mathbb{E}_{Y=-1} \left[p(X) - \frac{(1 - \tilde{a}_i)\tilde{a}_i p(X)}{\tilde{a}_i p(X) + (1 - \tilde{a}_i)(1 - p(X))} - \frac{\tilde{a}_i(1 - \tilde{a}_i)p(X)}{(1 - \tilde{a}_i)p(X) + \tilde{a}_i(1 - p(X))} \right].
\end{aligned}$$

We can convert this expectation to an expectation conditioned on $Y = 1$. Define $S = \{-1, 1\}^{m-1}$. Then,

$$\begin{aligned}
& \mathbb{E}_{Y=-1} \left[p(X) - \frac{(1 - \tilde{a}_i)\tilde{a}_i p(X)}{\tilde{a}_i p(X) + (1 - \tilde{a}_i)(1 - p(X))} - \frac{\tilde{a}_i(1 - \tilde{a}_i)p(X)}{(1 - \tilde{a}_i)p(X) + \tilde{a}_i(1 - p(X))} \right] = \\
& \sum_{s \in S} \Pr(\lambda_{-i} = s | Y = -1, X \in B_r(\lambda_i)) \left(\Pr(Y = 1 | \lambda_{-i} = s) - \right. \\
& \frac{(1 - \tilde{a}_i)\tilde{a}_i \Pr(Y = 1 | \lambda_{-i} = s)}{\tilde{a}_i \Pr(Y = 1 | \lambda_{-i} = s) + (1 - \tilde{a}_i) \Pr(Y = -1 | \lambda_{-i} = s)} - \\
& \left. \frac{\tilde{a}_i(1 - \tilde{a}_i) \Pr(Y = 1 | \lambda_{-i} = s)}{(1 - \tilde{a}_i) \Pr(Y = 1 | \lambda_{-i} = s) + \tilde{a}_i \Pr(Y = -1 | \lambda_{-i} = s)} \right).
\end{aligned}$$

Note that $\Pr(\lambda_{-i} = s | Y = -1, X \in B_r(\lambda_i)) = \prod_{j \neq i} \Pr(\lambda_j Y = -s_j | X \in B_r(\lambda_i)) = \Pr(\lambda_{-i} = -s | Y = 1, X \in B_r(\lambda_i))$ by Lemma 1. Then we flip the sign of s in the above

expression to get

$$\sum_{s \in -S} \Pr(\lambda_{-i} = s | Y = 1, X \in B_r(\lambda_i)) \left(\Pr(Y = 1 | \lambda_{-i} = -s) - \frac{(1 - \tilde{a}_i) \bar{a}_i \Pr(Y = 1 | \lambda_{-i} = -s)}{\bar{a}_i \Pr(Y = 1 | \lambda_{-i} = -s) + (1 - \bar{a}_i) \Pr(Y = -1 | \lambda_{-i} = -s)} - \frac{\tilde{a}_i (1 - \bar{a}_i) \Pr(Y = 1 | \lambda_{-i} = -s)}{(1 - \bar{a}_i) \Pr(Y = 1 | \lambda_{-i} = -s) + \bar{a}_i \Pr(Y = -1 | \lambda_{-i} = -s)} \right).$$

Define $p(-X) = \Pr(Y = 1 | \lambda_{-i} = -\lambda_{-i}(X))$. Then the above becomes

$$\mathbb{E}_{X \in B_r(\lambda_i), Y=1} \left[p(-X) - \frac{(1 - \tilde{a}_i) \bar{a}_i p(-X)}{\bar{a}_i p(-X) + (1 - \bar{a}_i)(1 - p(-X))} - \frac{\tilde{a}_i (1 - \bar{a}_i) p(-X)}{(1 - \bar{a}_i) p(-X) + \bar{a}_i (1 - p(-X))} \right]. \quad (18)$$

Recall that $p = 0.5$. We claim that $p(-X) = 1 - p(X)$. To see this, we can write $p(-X)$ as

$$\begin{aligned} p(-X) &= \frac{\Pr(Y = 1, \lambda_{-i} = -\lambda_{-i}(X))}{\Pr(\lambda_{-i} = -\lambda_{-i}(X))} \\ &= \frac{\Pr(\lambda_{-i} = -\lambda_{-i}(X) | Y = 1)}{\Pr(\lambda_{-i} = -\lambda_{-i}(X) | Y = 1) + \Pr(\lambda_{-i} = -\lambda_{-i}(X) | Y = -1)}. \end{aligned}$$

From Lemma 1, this can be written as

$$\begin{aligned} &\frac{\Pr(\lambda_{-i} = \lambda_{-i}(X) | Y = -1)}{\Pr(\lambda_{-i} = \lambda_{-i}(X) | Y = -1) + \Pr(\lambda_{-i} = \lambda_{-i}(X) | Y = 1)} \\ &= 1 - \frac{\Pr(\lambda_{-i} = \lambda_{-i}(X) | Y = 1)}{\Pr(\lambda_{-i} = \lambda_{-i}(X) | Y = -1) + \Pr(\lambda_{-i} = \lambda_{-i}(X) | Y = 1)} \\ &= 1 - \frac{\Pr(\lambda_{-i} = \lambda_{-i}(X) | Y = 1) p}{\Pr(\lambda_{-i} = \lambda_{-i}(X))} = 1 - p(X). \end{aligned}$$

Plugging this back into (18), we have

$$\mathbb{E}_{X \in B_r(\lambda_i), Y=1} \left[(1 - p(X)) - \frac{(1 - \tilde{a}_i) \bar{a}_i (1 - p(X))}{\bar{a}_i (1 - p(X)) + (1 - \bar{a}_i) p(X)} - \frac{\tilde{a}_i (1 - \bar{a}_i) (1 - p(X))}{(1 - \bar{a}_i) (1 - p(X)) + \bar{a}_i p(X)} \right]. \quad (19)$$

We now show that (19) and the expectation in (17) are equal:

$$\begin{aligned} &(1 - p(X)) - \frac{(1 - \tilde{a}_i) \bar{a}_i (1 - p(X))}{\bar{a}_i (1 - p(X)) + (1 - \bar{a}_i) p(X)} - \frac{\tilde{a}_i (1 - \bar{a}_i) (1 - p(X))}{(1 - \bar{a}_i) (1 - p(X)) + \bar{a}_i p(X)} \\ &= (1 - \tilde{a}_i) + \tilde{a}_i - p(X) - \frac{(1 - \tilde{a}_i) \bar{a}_i (1 - p(X))}{\bar{a}_i (1 - p(X)) + (1 - \bar{a}_i) p(X)} - \frac{\tilde{a}_i (1 - \bar{a}_i) (1 - p(X))}{(1 - \bar{a}_i) (1 - p(X)) + \bar{a}_i p(X)} \\ &= (1 - \tilde{a}_i) \left(1 - \frac{\bar{a}_i (1 - p(X))}{\bar{a}_i (1 - p(X)) + (1 - \bar{a}_i) p(X)} \right) + \tilde{a}_i \left(1 - \frac{(1 - \bar{a}_i) (1 - p(X))}{(1 - \bar{a}_i) (1 - p(X)) + \bar{a}_i p(X)} \right) - p(X) \\ &= (1 - \tilde{a}_i) \left(\frac{(1 - \bar{a}_i) p(X)}{\bar{a}_i (1 - p(X)) + (1 - \bar{a}_i) p(X)} \right) + \tilde{a}_i \left(\frac{\bar{a}_i p(X)}{(1 - \bar{a}_i) (1 - p(X)) + \bar{a}_i p(X)} \right) - p(X) \end{aligned}$$

Therefore, combining (17) and (19) gives us

$$\begin{aligned} \mathcal{R}(f_{WS}) - \mathcal{R}(f_E) &= \Pr(X \in B_r(\lambda_i)) \mathbb{E}_{X \in B_r(\lambda_i), Y=1} \left[\frac{\tilde{a}_i \bar{a}_i p(X)}{\bar{a}_i p(X) + (1 - \bar{a}_i)(1 - p(X))} \right. \\ &\quad \left. + \frac{(1 - \tilde{a}_i)(1 - \bar{a}_i)p(X)}{(1 - \bar{a}_i)p(X) + \bar{a}_i(1 - p(X))} - p(X) \right]. \end{aligned}$$

The denominator of both fractions above is at most $\max\{p(X), 1 - p(X)\}$, so we can write

$$\begin{aligned} \mathcal{R}(f_{WS}) - \mathcal{R}(f_E) &\geq \Pr(X \in B_r(\lambda_i)) \mathbb{E}_{X \in B_r(\lambda_i), Y=1} \left[\frac{\tilde{a}_i \bar{a}_i p(X)}{\max\{p(X), 1 - p(X)\}} \right. \\ &\quad \left. + \frac{(1 - \tilde{a}_i)(1 - \bar{a}_i)p(X)}{\max\{p(X), 1 - p(X)\}} - p(X) \right]. \end{aligned}$$

We can split this expectation based on if $p(X) \geq 0.5$. Furthermore, the condition that $X \in B_r(\lambda_i)$ is no longer relevant when also conditioning on $Y = 1$, so the above expectation becomes

$$\begin{aligned} \mathbb{E}_{Y=1} &\left[\frac{\tilde{a}_i \bar{a}_i p(X)}{\max\{p(X), 1 - p(X)\}} + \frac{(1 - \tilde{a}_i)(1 - \bar{a}_i)p(X)}{\max\{p(X), 1 - p(X)\}} - p(X) \right] \\ &= (\tilde{a}_i \bar{a}_i + (1 - \tilde{a}_i)(1 - \bar{a}_i)) \cdot \Pr(p(X) \geq 0.5 | Y = 1) - \mathbb{E}_{Y=1} [p(X)] + \\ &\quad \mathbb{E}_{Y=1} \left[\frac{p(X)}{1 - p(X)} (\tilde{a}_i \bar{a}_i + (1 - \tilde{a}_i)(1 - \bar{a}_i)) \mid p(X) < 0.5 \right] \Pr(p(X) < 0.5 | Y = 1) \\ &\geq (\tilde{a}_i \bar{a}_i + (1 - \tilde{a}_i)(1 - \bar{a}_i)) \cdot \Pr(p(X) \geq 0.5 | Y = 1) - \mathbb{E}_{Y=1} [p(X)] + \\ &\quad \mathbb{E}_{Y=1} [p(X) | p(X) < 0.5] (\tilde{a}_i \bar{a}_i + (1 - \tilde{a}_i)(1 - \bar{a}_i)) \cdot \Pr(p(X) < 0.5 | Y = 1) \\ &= (\Pr(p(X) \geq 0.5 | Y = 1) + \mathbb{E}_{Y=1} [p(X) | p(X) < 0.5] \Pr(p(X) < 0.5 | Y = 1)) \times \\ &\quad (\tilde{a}_i \bar{a}_i + (1 - \tilde{a}_i)(1 - \bar{a}_i)) - \mathbb{E}_{Y=1} [p(X)]. \end{aligned} \quad (20)$$

For convenience, denote $p_{0.5} = \Pr(p(X) \geq 0.5 | Y = 1)$. We can write $\mathbb{E}_{Y=1} [p(X)]$ as

$$\mathbb{E}_{Y=1} [p(X)] = \mathbb{E}_{Y=1} [p(X) | p(X) < 0.5] (1 - p_{0.5}) + \mathbb{E}_{Y=1} [p(X) | p(X) \geq 0.5] p_{0.5}.$$

We can use this to substitute $\mathbb{E}_{Y=1} [p(X) | p(X) < 0.5] (1 - p_{0.5})$ into (20) to get

$$(p_{0.5} + \mathbb{E}_{Y=1} [p(X)] - \mathbb{E}_{Y=1} [p(X) | p(X) \geq 0.5] p_{0.5}) \cdot (\tilde{a}_i \bar{a}_i + (1 - \tilde{a}_i)(1 - \bar{a}_i)) - \mathbb{E}_{Y=1} [p(X)].$$

Because $\tilde{a}_i \bar{a}_i + (1 - \tilde{a}_i)(1 - \bar{a}_i)$ is at most 1, we can lower bound the above expression by replacing $\mathbb{E}_{Y=1} [p(X)]$ with $C := \mathbb{E}_{Y=1} [p(X) | p(X) \geq 0.5]$. The expression becomes

$$(p_{0.5} + C - C \cdot p_{0.5}) \cdot (\tilde{a}_i \bar{a}_i + (1 - \tilde{a}_i)(1 - \bar{a}_i)) - C. \quad (21)$$

The last step is to show that $p_{0.5} \geq 0.5$. Define $\mathcal{S} = \{-1, 0, 1\}^{m-1}$ to be all possible sets of votes for the remaining labeling functions. Then we can write

$$\begin{aligned} p_{0.5} &= \Pr(\Pr(Y = 1 | \lambda_{-i} = \lambda_{-i}(X)) \geq 0.5 | Y = 1) \\ &= \sum_{s \in \mathcal{S}} \Pr(\Pr(Y = 1 | \lambda_{-i} = s) \geq 0.5 | Y = 1, \lambda_{-i}(X) = s) \Pr(\lambda_{-i}(X) = s | Y = 1). \end{aligned} \quad (22)$$

Using the fact that $p = 0.5$, the event that $\Pr(Y = 1 | \lambda_{-i} = s) \geq 0.5$ is equivalent to

$$\begin{aligned} \frac{\Pr(\lambda_{-i} = s | Y = 1)p}{\Pr(\lambda_{-i} = s)} &\geq 0.5 \\ \Rightarrow \Pr(\lambda_{-i} = s | Y = 1) &\geq 0.5(\Pr(\lambda_{-i} = s | Y = 1) + \Pr(\lambda_{-i} = s | Y = -1)) \\ \Rightarrow \Pr(\lambda_{-i} = s | Y = 1) &\geq \Pr(\lambda_{-i} = s | Y = -1). \end{aligned}$$

For a given s , denote $s^+ = \{i : s_i = 1\}$ and $s^- = \{i : s_i = -1\}$. Then, since abstaining labeling functions cancel out, we can write the above condition as

$$\prod_{s^+} a_i \prod_{s^-} (1 - a_i) \geq \prod_{s^+} (1 - a_i) \prod_{s^-} a_i.$$

This is a condition we can check for each s ; let the set of s that satisfy this be $\mathcal{S}^+ = \{s \in \mathcal{S} : \prod_{s^+} a_i \prod_{s^-} (1 - a_i) \geq \prod_{s^+} (1 - a_i) \prod_{s^-} a_i\}$. We can now write (22) as

$$p_{0.5} = \sum_{s \in \mathcal{S}^+} \Pr(\lambda_{-i}(X) = s | Y = 1) = \sum_{s \in \mathcal{S}^+} \prod_{s^+} a_i \prod_{s^-} (1 - a_i). \quad (23)$$

In order to show that this value is greater than 0.5, we equivalently show that it is greater than $\Pr(p(X) < 0.5 | Y = 1)$. Using the same approach as before, this can be written as

$$\begin{aligned} & \sum_{s \in \mathcal{S}} \Pr(\Pr(Y = 1 | \lambda_{-i} = -s) < 0.5 | Y = 1, \lambda_{-i}(X) = -s) \Pr(\lambda_{-i}(X) = -s | Y = 1) \\ &= \sum_{s \in \mathcal{S}} \Pr(\Pr(\lambda_{-i} = -s | Y = 1) < \Pr(\lambda_{-i} = -s | Y = -1) | Y = 1, \lambda_{-i}(X) = -s) \times \\ & \quad \Pr(\lambda_{-i}(X) = -s | Y = 1). \end{aligned}$$

Using symmetry of our graphical model from Lemma 1, this becomes

$$\begin{aligned} & \sum_{s \in \mathcal{S}} \Pr(\Pr(\lambda_{-i} = s | Y = -1) < \Pr(\lambda_{-i} = s | Y = 1) | Y = 1, \lambda_{-i}(X) = -s) \prod_{s^+} (1 - a_i) \prod_{s^-} a_i \\ &= \sum_{s \in \mathcal{S}^+} \prod_{s^+} (1 - a_i) \prod_{s^-} a_i. \end{aligned}$$

We see this is clearly less than (23) by definition of \mathcal{S}^+ . Therefore $p_{0.5} \geq 0.5$. We plug this back into (21) and use Lemma 5 in multiplying by $\Pr(X \in B_r(\lambda_i))$ to get

$$\mathcal{R}(f_{WS}) - \mathcal{R}(f_E) \geq L_{\lambda'_i}(r) p_{d(r)} p_i \left(\frac{1}{2} (C + 1) (\tilde{a}_i \bar{a}_i + (1 - \tilde{a}_i)(1 - \bar{a}_i)) - C \right).$$

General cases This concludes our proof of Theorem 1. However, it is worth examining what the exact quantity is for the generalization lift when all labeling functions are extended. For each labeling function, we split up the embedding space into three regions by use of a *participation function* $v : \mathcal{X} \rightarrow \{0, 1, 2\}^m$ such that

$$v_i(X) = \begin{cases} 0 & \lambda_i(X) = \bar{\lambda}_i(X) = 0 \\ 1 & \lambda_i(X) = \bar{\lambda}_i(X) \neq 0 \\ 2 & \lambda_i(X) = 0, \bar{\lambda}_i(X) \neq 0 \end{cases}.$$

That is, the 0 case indicates that X will not be labeled by λ_i even after extension, the 1 case indicates $X \in \text{supp}(\lambda_i)$, and the 2 case indicates $X \in B_r(\lambda_i)$. We can now write $\mathcal{R}(f_{WS}) - \mathcal{R}(f_E)$ using this idea of participation in various regions. Let $V = \{0, 1, 2\}^m$.

$$\begin{aligned} \mathcal{R}(f_{WS}) - \mathcal{R}(f_E) &= \mathbb{E} \left[\text{sign}(Y) (\Pr_{\bar{\mu}}(Y = 1 | \bar{\lambda} = \bar{\lambda}(X)) - \Pr_{\mu}(Y = 1 | \lambda = \lambda(X))) \right] \\ &= \sum_{v \in V} \mathbb{E}_{v(X)=v} \left[\text{sign}(Y) (\Pr_{\bar{\mu}}(Y = 1 | \bar{\lambda} = \bar{\lambda}(X)) - \Pr_{\mu}(Y = 1 | \lambda = \lambda(X))) \right] \times \\ & \quad \Pr(v(X) = v). \end{aligned} \quad (24)$$

We can write $\Pr_{\bar{\mu}}(Y = 1 | \bar{\lambda} = \bar{\lambda}(X))$ as $\frac{\prod_{i=1}^m \Pr(\bar{\lambda}_i = \bar{\lambda}_i(X) | Y=1)p}{\prod_{i=1}^m \Pr(\bar{\lambda}_i = \bar{\lambda}_i(X) | Y=1)p + \prod_{i=1}^m \Pr(\bar{\lambda}_i = \bar{\lambda}_i(X) | Y=-1)(1-p)}$ and a similar expression for $\Pr_{\mu}(Y = 1 | \lambda = \lambda(X))$. Now for X such that $v(X) = v$, we split the participation function's output vector into three disjoint sets of indices $\{V_0, V_1, V_2\}$ where $V_j = \{i : v_i(X) = j\}$ for $j = 0, 1, 2$. Then the product of conditional probabilities across the labeling functions can be grouped in this way. For $\Pr_{\mu}(Y = 1 | \lambda = \lambda(X))$, $\Pr(\lambda_i = \lambda_i(X) | Y = 1)$ is equal to $\Pr(\lambda_i = 0)$ when $i \in V_0, V_1$. Therefore, we can denote $p_1(X)$ as

$$\begin{aligned} p_1(X) &= \Pr(Y = 1 | \lambda_{V_1} = \lambda_{V_1}(X)) \\ &= \frac{\prod_{i \in V_1} \Pr(\lambda_i = \lambda_i(X) | Y = 1)p}{\prod_{i \in V_1} \Pr(\lambda_i = \lambda_i(X) | Y = 1)p + \prod_{i \in V_1} \Pr(\lambda_i = \lambda_i(X) | Y = -1)(1-p)}. \end{aligned}$$

For $\Pr_{\bar{\mu}}(Y = 1 | \bar{\lambda} = \bar{\lambda}(X))$, $\Pr(\bar{\lambda}_i = \bar{\lambda}_i(X) | Y = 1)$ becomes $\Pr(\bar{\lambda}_i = 0)$ for $i \in V_0$, becomes $\Pr(\lambda_i = \lambda_i(X) | Y = 1)$ for $i \in V_1$, and stays the same for $i \in V_2$. Then we can write $\Pr_{\bar{\mu}}(Y = 1 | \bar{\lambda} = \bar{\lambda}(X))$ in terms of $p_1(X)$, and (24) becomes

$$\sum_{v \in V} \Pr(v(X) = v) \mathbb{E}_{v(X)=v} \left[\text{sign}(Y) \times \left(\frac{\prod_{i \in V_2} \Pr(\bar{\lambda}_i = \bar{\lambda}_i(X) | Y = 1) p_1(X)}{\prod_{i \in V_2} \Pr(\bar{\lambda}_i = \bar{\lambda}_i(X) | Y = 1) p_1(X) + \prod_{i \in V_2} \Pr(\bar{\lambda}_i = \bar{\lambda}_i(X) | Y = -1) (1 - p_1(X))} - p_1(X) \right) \right].$$

We can further write each $\Pr(\bar{\lambda}_i = \bar{\lambda}_i(X) | Y = 1)$ as \bar{a}_i or $1 - \bar{a}_i$ according to Lemma 1. Let V_2 be partitioned into $V_2^+ = \{i \in V_2 : \bar{\lambda}_i(X) = 1\}$ and $V_2^- = \{i \in V_2 : \bar{\lambda}_i(X) = -1\}$. Then our expression for generalization lift is now

$$\sum_{v \in V} \sum_{V_2^+, V_2^-} \Pr(v(X) = v, \bar{\lambda}_{V_2^+}(X) = 1, \bar{\lambda}_{V_2^-}(X) = -1) \mathbb{E}_{v(X)=v} \left[\text{sign}(Y) \times \left(\frac{\prod_{i \in V_2^+} \bar{a}_i \prod_{j \in V_2^-} (1 - \bar{a}_j) p_1(X)}{\prod_{i \in V_2^+} \bar{a}_i \prod_{j \in V_2^-} (1 - \bar{a}_j) p_1(X) + \prod_{i \in V_2^+} (1 - \bar{a}_i) \prod_{j \in V_2^-} \bar{a}_j (1 - p_1(X))} - p_1(X) \right) \right].$$

We now condition on $Y = 1$ and $Y = -1$ separately. Suppose $Y = 1$. Then the probability to evaluate is $\Pr(v(X) = v, \bar{\lambda}_{V_2^+}(X) = 1, \bar{\lambda}_{V_2^-}(X) = -1, Y = 1)$. This is equivalent to

$$\begin{aligned} & \Pr(X \in \text{supp}(\lambda_{V_1}), X \in B_r(\lambda_{V_2}), \bar{\lambda}_{V_0}(X) = 0, \bar{\lambda}_{V_2^+}(X) = 1, \bar{\lambda}_{V_2^-}(X) = -1, Y = 1) \\ &= \Pr(\bar{\lambda}_{V_2^+}(X) = 1, \bar{\lambda}_{V_2^-}(X) = -1 | Y = 1, X \in \text{supp}(\lambda_{V_1}), X \in B_r(\lambda_{V_2}), \bar{\lambda}_{V_0}(X) = 0) \times \\ & \Pr(Y = 1, X \in \text{supp}(\lambda_{V_1}), X \in B_r(\lambda_{V_2}), \bar{\lambda}_{V_0}(X) = 0). \end{aligned} \quad (25)$$

In the first probability, the fact that $X \in \text{supp}(\lambda_{V_1}), \bar{\lambda}_{V_0}(X) = 0$ does not matter since the probability is conditioned on Y . Then (25) becomes

$$\begin{aligned} & \Pr(\bar{\lambda}_{V_2^+}(X) = 1, \bar{\lambda}_{V_2^-}(X) = -1 | Y = 1, X \in B_r(\lambda_{V_2})) \times \\ & \Pr(X \in \text{supp}(\lambda_{V_1}), X \in B_r(\lambda_{V_2}), \bar{\lambda}_{V_0}(X) = 0 | Y = 1) p \\ &= \prod_{i \in V_2^+} \bar{a}_i \prod_{j \in V_2^-} (1 - \bar{a}_j) \prod_{i \in V_1} \Pr(X \in \text{supp}(\lambda_i)) \prod_{i \in V_2} \Pr(X \in B_r(\lambda_i)) \prod_{i \in V_0} \Pr(\bar{\lambda}_i(X) = 0) p. \end{aligned}$$

Define $\bar{A}(V_a, V_b) = \prod_{i \in V_a} \bar{a}_i \prod_{j \in V_b} (1 - \bar{a}_j)$, and similarly, $\tilde{A}(V_a, V_b) = \prod_{i \in V_a} \tilde{a}_i \prod_{j \in V_b} (1 - \tilde{a}_j)$. The amount of lift that the $Y = 1$ case contributes is then

$$\begin{aligned} & \sum_{v \in V} \sum_{V_2^+, V_2^-} \bar{A}(V_2^+, V_2^-) \prod_{i \in V_1} \Pr(X \in \text{supp}(\lambda_i)) \prod_{i \in V_2} \Pr(X \in B_r(\lambda_i)) \prod_{i \in V_0} \Pr(\bar{\lambda}_i(X) = 0) p \times \\ & \mathbb{E}_{v(X)=v, Y=1} \left[\frac{\bar{A}(V_2^+, V_2^-) p_1(X)}{\bar{A}(V_2^+, V_2^-) p_1(X) + \tilde{A}(V_2^-, V_2^+) (1 - p_1(X))} - p_1(X) \right]. \end{aligned} \quad (26)$$

Next, suppose $Y = -1$. The probability to evaluate, using the same approach as before, is just

$$\begin{aligned} & \Pr(v(X) = v, \bar{\lambda}_{V_2^+}(X) = 1, \bar{\lambda}_{V_2^-}(X) = -1, Y = -1) \\ &= \prod_{i \in V_2^+} (1 - \tilde{a}_i) \prod_{j \in V_2^-} \tilde{a}_j \prod_{i \in V_1} \Pr(X \in \text{supp}(\lambda_i)) \prod_{i \in V_2} \Pr(X \in B_r(\lambda_i)) \prod_{i \in V_0} \Pr(\bar{\lambda}_i(X) = 0) (1 - p), \end{aligned}$$

and the amount of lift that the $Y = -1$ case contributes is

$$\begin{aligned} & \sum_{v \in V} \sum_{V_2^+, V_2^-} \tilde{A}(V_2^-, V_2^+) \prod_{i \in V_1} \Pr(X \in \text{supp}(\lambda_i)) \prod_{i \in V_2} \Pr(X \in B_r(\lambda_i)) \prod_{i \in V_0} \Pr(\bar{\lambda}_i(X) = 0) (1 - p) \times \\ & \mathbb{E}_{v(X)=v, Y=-1} \left[p_1(X) - \frac{\tilde{A}(V_2^-, V_2^+) p_1(X)}{\bar{A}(V_2^+, V_2^-) p_1(X) + \tilde{A}(V_2^-, V_2^+) (1 - p_1(X))} \right]. \end{aligned} \quad (27)$$

Combining (26) and (27) gives an exact value for $\mathcal{R}(f_{WS}) - \mathcal{R}(f_E)$. Intuitively, in both quantities the terms $\prod_{i \in V_1} \Pr(X \in \text{supp}(\lambda_i)) \prod_{i \in V_2} \Pr(X \in B_r(\lambda_i)) \prod_{i \in V_0} \Pr(\bar{\lambda}_i(X) = 0)$ represent the size of the region corresponding to v . Then, the expectation represents the particular lift over that region depending on if $Y = 1$ or $Y = -1$; we see that when \bar{a}_i and \bar{a}_j are equal to 0.5, the value inside the expectation becomes 0, and there is no improvement in performance due to EPOXY. Otherwise, the lift for $Y = 1$ is positive when $\bar{A}(V_2^+, V_2^-) \geq \bar{A}(V_2^-, V_2^+)$, e.g. $\prod_{i \in V_2^+} \frac{\bar{a}_i}{1-\bar{a}_i} \geq \prod_{j \in V_2^-} \frac{\bar{a}_j}{1-\bar{a}_j}$, and vice versa when $Y = -1$. These positive and negative expectations are then weighted by $\tilde{A}(V_2^+, V_2^-)$ and $\tilde{A}(V_2^-, V_2^+)$, which allows for an overall positive lift.

C.4 Proof of Proposition 2

Next, we prove the result connecting risk to embedding quality.

Proof. First, consider

$$\mathbb{E}_{(X', Y') \sim \mathcal{D}} [\Pr(f(X) = Y | d(X, X') \leq r)].$$

We can rewrite this as

$$\mathbb{E}_{(X', Y') \sim \mathcal{D}} [\mathbb{E} [\mathbb{1}\{f(X) = Y\} | d(X, X') \leq r]].$$

From the tower law of expectation, we have that

$$\begin{aligned} & \mathbb{E}_{(X', Y') \sim \mathcal{D}} [\Pr(f(X) = Y | d(X, X') \leq r)] \\ &= \mathbb{E}_{(X', Y') \sim \mathcal{D}} [\mathbb{E} [\mathbb{1}\{f(X) = Y\} | d(X, X') \leq r]] \\ &= \mathbb{E} [\mathbb{1}\{f(X) = Y\}] \\ &= \Pr(f(X) = Y) \\ &= \mathcal{R}(f_z). \end{aligned} \tag{28}$$

We similarly have that

$$\mathbb{E}_{(X', Y') \sim \mathcal{D}} [\Pr(f(X') = Y' | d(X, X') \leq r)] = \mathcal{R}(f_z). \tag{29}$$

Recall that

$$\mathbb{E}_{(X', Y') \sim \mathcal{D}} [\Pr(f(X) = f(X') | d(X, X') \leq r)] \leq M(r). \tag{30}$$

Now, consider

$$\mathbb{E}_{(X', Y') \sim \mathcal{D}} [\Pr(f(X) = f(X') = Y = Y' | d(X, X') \leq r)].$$

We have that

$$\begin{aligned} & \mathbb{E}_{(X', Y') \sim \mathcal{D}} [\Pr(f(X) = f(X') = Y = Y' | d(X, X') \leq r)] \\ & \geq 1 - \mathbb{E}_{(X', Y') \sim \mathcal{D}} [\Pr(f(X) \neq f(X') | d(X, X') \leq r)] \\ & \quad - \mathbb{E}_{(X', Y') \sim \mathcal{D}} [\Pr(f(X) \neq Y | d(X, X') \leq r)] \\ & \quad - \mathbb{E}_{(X', Y') \sim \mathcal{D}} [\Pr(f(X') \neq Y' | d(X, X') \leq r)] \\ & = 1 - (M(r) + 2\mathcal{R}(f)). \end{aligned} \tag{31}$$

To see this, first, we used the fact that $\Pr(A = B = C = D) \geq 1 - \Pr(A \neq B) - \Pr(A \neq C) - \Pr(B \neq D)$. Then, using this decomposition, we applied (28), (30), and (29).

Finally, note that $\Pr(f(X) = f(X') = Y = Y' | d(X, X') \leq r) \leq \Pr(Y = Y' | d(X, X') \leq r)$. Then, we have that

$$\mathbb{E}_{(X', Y') \sim \mathcal{D}} [\Pr(Y = Y' | d(X, X') \leq r)] \geq 1 - (M(r) + 2\mathcal{R}(f_z)),$$

or,

$$\mathbb{E}_{(X', Y') \sim \mathcal{D}} [\Pr(Y \neq Y' | d(X, X') \leq r)] \leq M(r) + 2\mathcal{R}(f_z), \tag{32}$$

Next, we can write

$$\begin{aligned} \mathbb{E}_{(X', Y') \sim \mathcal{D}} [\Pr(Y \neq Y' | d(X, X') \leq r)] &= \int \Pr(X' = x) \Pr(X = x | d(x, x') \leq r) \mathbb{1}\{Y \neq Y'\} \\ &= \Pr(Y \neq Y' | d(X, X') \leq r), \end{aligned}$$

as desired. \square

C.5 Theorem 2 Proof

The proof proceeds in the following steps.

1. Show that risk is higher if nonoverlapping votes are used.
2. Bound the risk that results from nonoverlapping supports in terms of individual accuracies.
3. Use Proposition 2 to bound the risk in terms of $R(f_i)$.

We first show that given $\{\text{supp}(\lambda_1), \dots, \text{supp}(\lambda_m)\}$, there is a way to create nonoverlapping $\{\text{supp}'(\lambda_1), \dots, \text{supp}'(\lambda_m)\}$ such that the risk is always higher.

Lemma 4. *Suppose there exists a region formed by the intersection of some k labeling functions, $\lambda_1, \dots, \lambda_k$, such that $S_k = \bigcap_{i=1}^k \text{supp}(\lambda_i)$. Suppose that $a_1 \geq a_2 \geq \dots \geq a_k$. Then the risk of the label model over S_k increases if λ_1 decides to abstain in S_k .*

Proof. The risk of the label model is $\mathcal{R}(f_{WS}) = \mathbb{E}_{X, Y \sim \mathcal{D}} \left[\frac{1}{2} |Y - 2 \Pr(\tilde{Y} = 1 | \lambda = \lambda(X)) + 1| \right]$ (this also holds for $R(f_E)$ with $\bar{\lambda}$, but for simplicity we work with λ). Then the risk over the region S_k is $\mathcal{R}_{S_k}(f_{WS}) = \mathbb{E}_{X, Y \in S_k} \left[\frac{1}{2} |Y - 2 \Pr(\tilde{Y} = 1 | \lambda = \lambda(X)) + 1| \right]$. This can be written as

$$\mathcal{R}_{S_k}(f_{WS}) = \mathbb{E}_{S_k, Y=1} \left[1 - \Pr(\tilde{Y} = 1 | \lambda = \lambda(X)) \right] p + \mathbb{E}_{S_k, Y=-1} \left[\Pr(\tilde{Y} = 1 | \lambda = \lambda(X)) \right] (1 - p),$$

where we've used that $\Pr(Y = 1 | S_k) = \Pr(Y = 1)$ by Lemma 2. Recall that labeling functions are conditionally independent given Y , so the probabilities can be decomposed into the product of individual $\Pr(\lambda_i = \lambda_i(X) | Y = 1)$. Moreover, for $i > k$, this probability is equivalent to $\Pr(\lambda_i = 0 | Y = 1)$, which is just $\Pr(\lambda_i = 0)$. After canceling terms out, we have

$$\begin{aligned} \mathbb{E}_{S_k, Y=1} & \left[1 - \frac{\prod_{i=1}^k \Pr(\lambda_i = \lambda_i(X) | Y = 1)p}{\prod_{i=1}^k \Pr(\lambda_i = \lambda_i(X) | Y = 1)p + \prod_{i=1}^k \Pr(\lambda_i = \lambda_i(X) | Y = -1)(1 - p)} \right] p + \\ \mathbb{E}_{S_k, Y=-1} & \left[\frac{\prod_{i=1}^k \Pr(\lambda_i = \lambda_i(X) | Y = 1)p}{\prod_{i=1}^k \Pr(\lambda_i = \lambda_i(X) | Y = 1)p + \prod_{i=1}^k \Pr(\lambda_i = \lambda_i(X) | Y = -1)(1 - p)} \right] (1 - p). \end{aligned} \quad (33)$$

Following Lemma (1), we condition on the value of $\lambda_1(X)$ to write the risk using the accuracy a_1 . For ease of notation, define the following expression:

$$\begin{aligned} p(X) &= \frac{\prod_{i=2}^k \Pr(\lambda_i = \lambda_i(X) | Y = 1)p}{\prod_{i=2}^k \Pr(\lambda_i = \lambda_i(X) | Y = 1)p + \prod_{i=2}^k \Pr(\lambda_i = \lambda_i(X) | Y = -1)(1 - p)} \\ &= \Pr(Y = 1 | \lambda_{2:k} = \lambda_2(X), \dots, \lambda_k(X)). \end{aligned}$$

(33) can now be written as

$$\begin{aligned} & \mathbb{E}_{S_k, \lambda_1(X)=1, Y=1} \left[1 - \frac{a_1 p(X)}{a_1 p(X) + (1 - a_1)(1 - p(X))} \right] \Pr(\lambda_1(X) = 1, Y = 1 | S_k) + \\ & \mathbb{E}_{S_k, \lambda_1(X)=-1, Y=1} \left[1 - \frac{(1 - a_1)p(X)}{(1 - a_1)p(X) + a_1(1 - p(X))} \right] \Pr(\lambda_1(X) = -1, Y = 1 | S_k) + \\ & \mathbb{E}_{S_k, \lambda_1(X)=1, Y=-1} \left[\frac{a_1 p(X)}{a_1 p(X) + (1 - a_1)(1 - p(X))} \right] \Pr(\lambda_1(X) = 1, Y = -1 | S_k) + \\ & \mathbb{E}_{S_k, \lambda_1(X)=-1, Y=-1} \left[\frac{(1 - a_1)p(X)}{(1 - a_1)p(X) + a_1(1 - p(X))} \right] \Pr(\lambda_1(X) = -1, Y = -1 | S_k). \end{aligned} \quad (34)$$

We now describe what we want to show. We want to upper bound this expression by $\mathcal{R}_{S'_k}(f_{WS})$, which is the risk over S_k when λ_1 abstains. For this risk, we can consider abstaining as removing the a_1 term from (34) (equivalently, considering $a_1 = 0.5$) to get

$$\mathcal{R}_{S'_k}(f_{WS}) = \mathbb{E}_{S_k, Y=1} [1 - p(X)] p + \mathbb{E}_{S_k, Y=-1} [p(X)] (1 - p). \quad (35)$$

It is thus sufficient to compare across expectations over $Y = 1$, and apply a symmetry argument to $Y = -1$. Before we do that, note that $\Pr(\lambda_1(X) = 1, Y = 1|S_k) = \Pr(\lambda_1(X) = 1|Y = 1, S_k) \Pr(Y = 1|S_k) = a_i \cdot p$, and we have similar expressions for the other probabilities in (34). The inequality we want to show is thus

$$\begin{aligned} & \mathbb{E}_{S_k, Y=1} \left[1 - \frac{a_1 p(X)}{a_1 p(X) + (1-a_1)(1-p(X))} \right] a_1 p \\ & + \mathbb{E}_{S_k, Y=1} \left[1 - \frac{(1-a_1)p(X)}{(1-a_1)p(X) + a_1(1-p(X))} \right] (1-a_1)p \leq \mathbb{E}_{S_k, Y=1} [1-p(X)] p. \end{aligned} \quad (36)$$

Combining terms, this is equal to showing

$$\mathbb{E}_{S_k, Y=1} \left[\frac{a_1^2 p(X)}{a_1 p(X) + (1-a_1)(1-p(X))} + \frac{(1-a_1)^2 p(X)}{(1-a_1)p(X) + a_1(1-p(X))} \right] \geq \mathbb{E}_{S_k, Y=1} [p(X)].$$

We now claim that $\frac{a_1^2 p(X)}{a_1 p(X) + (1-a_1)(1-p(X))} + \frac{(1-a_1)^2 p(X)}{(1-a_1)p(X) + a_1(1-p(X))} \geq p(X)$. If we rename $x := a_1$ and $p = p(X)$, this becomes equivalent to showing that

$$\frac{x^2}{xp + (1-x)(1-p)} + \frac{(1-x)^2}{(1-x)p + x(1-p)} \geq 1.$$

Define a function $f(x) = \frac{x}{xp + (1-x)(1-p)}$. Then we want to show that

$$xf(x) + (1-x)f(1-x) \geq 1. \quad (37)$$

Note that $f(x)$ is convex and increasing on $x \in [0, 1]$. Then we know that $f(x^2 + (1-x)^2) \leq xf(x) + (1-x)f(1-x)$. The smallest value of $x^2 + (1-x)^2$ is $\frac{1}{2}$ when $x = \frac{1}{2}$, so we know that any $xf(x) + (1-x)f(1-x) \geq \frac{1/2}{p/2 + (1-p)/2} = 1$. Therefore, we have shown that (37) is true, and hence (36) is also true. Furthermore, (37) is sufficient to show that the expectations over $Y = -1$ also satisfy the same condition. We conclude that $\mathcal{R}_{S_k}(f_{WS}) \leq \mathcal{R}_{S'_k}(f_{WS})$. \square

An immediate result follows:

Corollary 1. *We set $\text{supp}'(\lambda_1), \dots, \text{supp}'(\lambda_m)$ such that for each S_k overlapping region, only one labeling function votes on it, and denote the resulting risk from this transformation as $\mathcal{R}_{\text{disjoint}}(f_{WS})$. Then $\mathcal{R}(f_{WS}) \leq \mathcal{R}_{\text{disjoint}}(f_{WS})$.*

We stress that $\mathcal{R}(f_{WS})$ and $\mathcal{R}_{\text{disjoint}}(f_{WS})$ use the same set of accuracies - the only change is that at the inference step, $\mathcal{R}_{\text{disjoint}}(f_{WS})$ involves more abstains. For convenience, denote $\mathcal{X}_i = \text{supp}'(\lambda_i) \subseteq \text{supp}(\lambda_i)$ and $\mathcal{X}_0 = \{X : \lambda_i(X) = 0 \ \forall i\}$, such that the distribution over $\mathcal{X} \setminus \mathcal{X}_0$ can be partitioned into $\mathcal{X}_1, \dots, \mathcal{X}_m$. We can bound the risk of EPOXY with $\mathcal{R}_{\text{disjoint}}(f_E)$, which simply replaces λ with $\bar{\lambda}$, combined with the risk on \mathcal{X}_0 . We have that

$$\begin{aligned} \mathcal{R}(f_E) &= \mathbb{E}_{X, Y \sim D} \left[\frac{1}{2} |Y - 2 \Pr_{\bar{\mu}}(\tilde{Y} = 1 | \bar{\lambda} = \bar{\lambda}(X)) + 1| \right] \\ &\leq \sum_{i=1}^m \mathbb{E}_{\mathcal{X}_i} \left[\frac{1}{2} |Y - 2 \Pr_{\bar{\mu}}(\tilde{Y} = 1 | \bar{\lambda} = \bar{\lambda}(X)) + 1| \right] \Pr(X \in \mathcal{X}_i) + \mathcal{R}_0 \\ &= \sum_{i=1}^m \left(\mathbb{E}_{\mathcal{X}_i, Y=1} \left[1 - \Pr_{\bar{\mu}}(\tilde{Y} = 1 | \bar{\lambda} = \bar{\lambda}(X)) \right] \Pr(Y = 1, X \in \mathcal{X}_i) + \right. \\ &\quad \left. \mathbb{E}_{\mathcal{X}_i, Y=-1} \left[\Pr_{\bar{\mu}}(\tilde{Y} = 1 | \bar{\lambda} = \bar{\lambda}(X)) \right] \Pr(Y = -1, X \in \mathcal{X}_i) \right) + \mathcal{R}_0, \end{aligned} \quad (38)$$

where \mathcal{R}_0 is the risk over \mathcal{X}_0 . We can use the fact that only λ_i votes in \mathcal{X}_i to simplify $\mathbb{E}_{\mathcal{X}_i, Y=\pm 1} [\Pr_{\bar{\mu}}(\tilde{Y} = 1 | \bar{\lambda} = \bar{\lambda}(X))]$.

$$\begin{aligned} & \mathbb{E}_{\mathcal{X}_i, Y=1} \left[1 - \Pr_{\bar{\mu}}(\tilde{Y} = 1 | \bar{\lambda} = \bar{\lambda}(X)) \right] \\ &= \mathbb{E}_{\mathcal{X}_i, Y=1} \left[1 - \frac{\Pr_{\bar{\mu}}(\bar{\lambda} = \bar{\lambda}(X) | Y = 1)p}{\Pr_{\bar{\mu}}(\bar{\lambda} = \bar{\lambda}(X) | Y = 1)p + \Pr_{\bar{\mu}}(\bar{\lambda} = \bar{\lambda}(X) | Y = -1)(1-p)} \right]. \end{aligned}$$

Again, we write $\Pr_{\bar{\mu}}(\bar{\lambda} = \bar{\lambda}(X) | Y = 1)$ as $\prod_{i=1}^m \Pr(\bar{\lambda}_i = \bar{\lambda}_i(X) | Y = 1)$, and since only λ_i votes on \mathcal{X}_i , all other terms are equal to $\Pr(\bar{\lambda}_j = 0)$ for $j \neq i$. After canceling terms in the numerator and denominator, we simply have that

$$\begin{aligned} & \mathbb{E}_{\mathcal{X}_i, Y=1} \left[1 - \Pr_{\bar{\mu}}(\tilde{Y} = 1 | \bar{\lambda} = \bar{\lambda}(X)) \right] \\ &= \mathbb{E}_{\mathcal{X}_i, Y=1} \left[1 - \frac{\Pr(\bar{\lambda}_i = \bar{\lambda}_i(X) | Y = 1)p}{\Pr(\bar{\lambda}_i = \bar{\lambda}_i(X) | Y = 1)p + \Pr(\bar{\lambda}_i = \bar{\lambda}_i(X) | Y = -1)(1-p)} \right] \\ &= \left(1 - \frac{\bar{a}_i p}{\bar{a}_i p + (1 - \bar{a}_i)(1-p)} \right) \Pr(\bar{\lambda}_i(X) = 1 | Y = 1, X \in \mathcal{X}_i) + \\ & \quad \left(1 - \frac{(1 - \bar{a}_i)p}{(1 - \bar{a}_i)p + \bar{a}_i(1-p)} \right) \Pr(\bar{\lambda}_i(X) = -1 | Y = 1, X \in \mathcal{X}_i). \end{aligned} \quad (39)$$

Similarly,

$$\begin{aligned} \mathbb{E}_{\mathcal{X}_i, Y=-1} \left[\Pr_{\bar{\mu}}(\tilde{Y} = 1 | \bar{\lambda} = \bar{\lambda}(X)) \right] &= \frac{\bar{a}_i p}{\bar{a}_i p + (1 - \bar{a}_i)(1-p)} \Pr(\bar{\lambda}_i(X) = 1 | Y = -1, X \in \mathcal{X}_i) + \\ & \quad \frac{(1 - \bar{a}_i)p}{(1 - \bar{a}_i)p + \bar{a}_i(1-p)} \Pr(\bar{\lambda}_i(X) = -1 | Y = -1, X \in \mathcal{X}_i). \end{aligned} \quad (40)$$

We now show that when $p \geq \frac{1}{2}$, we have that $1 - \frac{\bar{a}_i p}{\bar{a}_i p + (1 - \bar{a}_i)(1-p)} \leq \frac{(1 - \bar{a}_i)p}{(1 - \bar{a}_i)p + \bar{a}_i(1-p)}$, and vice versa for when $p \leq \frac{1}{2}$. To see this, note that both $\frac{\bar{a}_i p}{\bar{a}_i p + (1 - \bar{a}_i)(1-p)}$ and $\frac{(1 - \bar{a}_i)p}{(1 - \bar{a}_i)p + \bar{a}_i(1-p)}$ are increasing in p . Then for $p \geq \frac{1}{2}$, we have that $1 - \frac{\bar{a}_i p}{\bar{a}_i p + (1 - \bar{a}_i)(1-p)} \leq 1 - \frac{\bar{a}_i/2}{\bar{a}_i/2 + (1 - \bar{a}_i)/2} = 1 - \bar{a}_i$, and $\frac{(1 - \bar{a}_i)p}{(1 - \bar{a}_i)p + \bar{a}_i(1-p)} \geq \frac{(1 - \bar{a}_i)/2}{(1 - \bar{a}_i)/2 + \bar{a}_i/2} = 1 - \bar{a}_i$. Note that the opposite sequence of inequalities holds for $p \leq \frac{1}{2}$. Combining this observation with (39) and (40), we can write (38) as:

$$\begin{aligned} \mathcal{R}(f_E) &\leq \sum_{i=1}^m \frac{(1 - \bar{a}_i)p}{(1 - \bar{a}_i)p + \bar{a}_i(1-p)} \bar{a}_i \Pr(Y = 1, X \in \mathcal{X}_i) + \\ & \quad \frac{\bar{a}_i p}{\bar{a}_i p + (1 - \bar{a}_i)(1-p)} (1 - \bar{a}_i) \Pr(Y = 1, X \in \mathcal{X}_i) + \\ & \quad \frac{\bar{a}_i p}{\bar{a}_i p + (1 - \bar{a}_i)(1-p)} (1 - \bar{a}_i) \Pr(Y = -1, X \in \mathcal{X}_i) + \\ & \quad \frac{(1 - \bar{a}_i)p}{(1 - \bar{a}_i)p + \bar{a}_i(1-p)} \bar{a}_i \Pr(Y = -1, X \in \mathcal{X}_i) + \mathcal{R}_0, \end{aligned}$$

where we have used that $\Pr(\bar{\lambda}_i(X) = 1 | Y = 1, X \in \mathcal{X}_i) = \Pr(\bar{\lambda}_i(X) = 1 | Y = 1, \bar{\lambda}(X_i) \neq 0) = \bar{a}_i$. This is equivalent to

$$\begin{aligned} \mathcal{R}(f_E) &\leq \sum_{i=1}^m \frac{(1 - \bar{a}_i)\bar{a}_i p}{(1 - \bar{a}_i)p + \bar{a}_i(1-p)} \Pr(X \in \mathcal{X}_i) + \frac{\bar{a}_i(1 - \bar{a}_i)p}{\bar{a}_i p + (1 - \bar{a}_i)(1-p)} \Pr(X \in \mathcal{X}_i) + \mathcal{R}_0 \\ &= \sum_{i=1}^m \bar{a}_i(1 - \bar{a}_i)p \Pr(X \in \mathcal{X}_i) \left(\frac{1}{(1 - \bar{a}_i)p + \bar{a}_i(1-p)} + \frac{1}{\bar{a}_i p + (1 - \bar{a}_i)(1-p)} \right) + \mathcal{R}_0. \end{aligned}$$

The sum of fractions can be upper bounded by $\frac{2}{1-p}$, so our bound is now

$$\sum_{i=1}^m \bar{a}_i(1 - \bar{a}_i) \Pr(X \in \mathcal{X}_i) \frac{2p}{1-p} + \mathcal{R}_0 \leq \sum_{i=1}^m (1 - \bar{a}_i) \Pr(X \in \mathcal{X}_i) \frac{2p}{1-p} + \mathcal{R}_0.$$

We use Proposition 2 on the specialized models f_i on \mathcal{X}_i to get that

$$\begin{aligned} \mathcal{R}(f_E) &\leq \sum_{i=1}^m \left(1 - a_i + (2a_i - 1) \frac{M_{f_i}(r_i) + 2\mathcal{R}(f_i)}{p_i^2(1 + L_{\lambda'_i}(r_i)p_{d(r_i)})} \right) \frac{2p}{1-p} \Pr(X \in \mathcal{X}_i) + \mathcal{R}_0 \\ &= \frac{2p}{1-p} \mathbb{E}_{\mathcal{D}_i} \left[1 - a_i + (2a_i - 1) \frac{M_{f_i}(r_i) + 2\mathcal{R}(f_i)}{p_i^2(1 + L_{\lambda'_i}(r_i)p_{d(r_i)})} \right] + \mathcal{R}_0. \end{aligned}$$

Lastly, we compute \mathcal{R}_0 . This is just $\Pr(X \in \mathcal{X}_0) \mathbb{E}_{\mathcal{X}_0} \left[\frac{1}{2} |Y - 2\Pr_{\bar{\mu}}(\tilde{Y} = 1 | \bar{\lambda} = 0) + 1| \right] = \Pr(X \in \mathcal{X}_0) \mathbb{E}_{\mathcal{X}_0} \left[\frac{1}{2} |Y - 2p + 1| \right] = \Pr(X \in \mathcal{X}_0) 2p(1-p)$. Finally, we note that this entire derivation also holds for $p \leq \frac{1}{2}$, so we define the max odds to be $b = \max\{\frac{p}{1-p}, \frac{1-p}{p}\}$. Then our final bound becomes

$$\mathcal{R}(f_E) \leq 2b \cdot \mathbb{E}_{\mathcal{D}_i} \left[1 - a_i + (2a_i - 1) \frac{M_{f_i}(r_i) + 2\mathcal{R}(f_i)}{p_i^2(1 + L_{\lambda'_i}(r_i)p_{d(r_i)})} \right] + 2\Pr(X \in \mathcal{X}_0)p(1-p).$$

C.6 Controlling the minimum increases in support and overlaps from extensions

We want to lower bound $\Pr(X \in B_r(\lambda_i))$ and $\Pr(X \in \text{supp}(\bar{\lambda}_i \cap \bar{\lambda}_j))$ using $L_{\lambda'_i}(r)$ from our definition of probabilistic Lipschitzness.

Lemma 5. *For a labeling function λ_i with threshold radius r ,*

$$\Pr(X \in B_r(\lambda_i)) \geq L_{\lambda'_i}(r)p_{d(r)}p_i,$$

where $p_{d(r)} = \Pr(d_{\mathcal{Z}}(X, X') \leq r)$ and $p_i = \Pr(X \in \text{supp}(\lambda_i))$.

Proof. By conditioning on the event that $X' \in \text{supp}(\lambda_i)$, we have that

$$\begin{aligned} \Pr(X \in B_r(\lambda_i)) &\geq \Pr(X \in B_r(\lambda_i) | d_{\mathcal{Z}}(X, X') \leq r, X' \in \text{supp}(\lambda_i)) \times \\ &\quad \Pr(d_{\mathcal{Z}}(X, X') \leq r, X' \in \text{supp}(\lambda_i)). \end{aligned} \tag{41}$$

We focus on the first probability and aim to write it in terms of $L_{\lambda'_i}(r)$. By definition of $B_r(\lambda_i)$,

$$\begin{aligned} \Pr(X \in B_r(\lambda_i) | d_{\mathcal{Z}}(X, X') \leq r, X' \in \text{supp}(\lambda_i)) &= \Pr(\bar{\lambda}_i(X) \neq 0, \lambda_i(X) = 0 | d_{\mathcal{Z}}(X, X') \leq r, X' \in \text{supp}(\lambda_i)) \\ &= \Pr(\lambda_i(X) = 0 | d_{\mathcal{Z}}(X, X') \leq r, X' \in \text{supp}(\lambda_i)) \\ &= \Pr(\lambda_i(X) = 0, \lambda_i(X') \neq 0 | d_{\mathcal{Z}}(X, X') \leq r, X' \in \text{supp}(\lambda_i)). \end{aligned}$$

Notice that $\Pr(\lambda_i(X) = 0, \lambda_i(X') \neq 0 | d_{\mathcal{Z}}(X, X') \leq r) \leq \Pr(\lambda_i(X) = 0, \lambda_i(X') \neq 0 | d_{\mathcal{Z}}(X, X') \leq r, X \in \text{supp}(\lambda_i))$. This is because $\Pr(\lambda_i(X) = 0, \lambda_i(X') \neq 0, d_{\mathcal{Z}}(X, X') \leq r)$ is equivalent to $\Pr(\lambda_i(X) = 0, \lambda_i(X') \neq 0, d_{\mathcal{Z}}(X, X') \leq r, X \in \text{supp}(\lambda_i))$, and $\Pr(d_{\mathcal{Z}}(X, X') \leq r) \geq \Pr(d_{\mathcal{Z}}(X, X') \leq r, X \in \text{supp}(\lambda_i))$. By the definition of $L_{\lambda'_i}(r)$, (41) becomes

$$\Pr(X \in B_r(\lambda_i)) \geq L_{\lambda'_i}(r) \Pr(d_{\mathcal{Z}}(X, X') \leq r, X' \in \text{supp}(\lambda_i)).$$

If we suppose that the distribution of X in \mathcal{Z} is independent of an individual labeling function's support, this gives us

$$\Pr(X \in B_r(\lambda_i)) \geq L_{\lambda'_i}(r)p_{d(r)}p_i.$$

□

Lemma 6. Suppose that λ_i is extended r_i and λ_j is extended r_j , and λ_i, λ_j are used to estimate accuracy parameters. Let $r_{\min} = \min\{r_i, r_j\}$, and $L_{\min} = \min\{L_{\lambda'_i}(r_{\min}), L_{\lambda'_j}(r_{\min})\}$. Then,

$$\Pr(X \in \text{supp}(\bar{\lambda}_i) \cap \text{supp}(\bar{\lambda}_j)) \geq (1 + (2L_{\min} - L_{\min}^2) \times p_{d(r_{\min})})o_{\min}.$$

Proof. For notation, we use $\text{supp}(\lambda_i \cap \lambda_j)$ to refer to $\text{supp}(\lambda_i) \cap \text{supp}(\lambda_j)$. We want to look at how much the overlap between the labeling functions has increased after extending, e.g. $\text{supp}(\bar{\lambda}_i \cap \bar{\lambda}_j) \setminus \text{supp}(\lambda_i \cap \lambda_j)$.

$$\begin{aligned} & \Pr(X \in \text{supp}(\bar{\lambda}_i \cap \bar{\lambda}_j) \setminus \text{supp}(\lambda_i \cap \lambda_j)) \\ & \geq \Pr(X \in \text{supp}(\bar{\lambda}_i \cap \bar{\lambda}_j) \setminus \text{supp}(\lambda_i \cap \lambda_j) | d_{\mathcal{Z}}(X, X') \leq r_{\min}, X' \in \text{supp}(\lambda_i \cap \lambda_j)) \times \\ & \quad \Pr(d_{\mathcal{Z}}(X, X') \leq r_{\min}, X' \in \text{supp}(\lambda_i \cap \lambda_j)). \end{aligned} \quad (42)$$

We focus on the first term and split it into three cases:

$$\begin{aligned} & \Pr(X \in \text{supp}(\bar{\lambda}_i \cap \bar{\lambda}_j) \setminus \text{supp}(\lambda_i \cap \lambda_j) | d_{\mathcal{Z}}(X, X') \leq r_{\min}, X' \in \text{supp}(\lambda_i \cap \lambda_j)) \\ & = \Pr(\bar{\lambda}_i(X) \neq 0, \lambda_i(X) = 0, \bar{\lambda}_j(X) \neq 0, \lambda_j(X) = 0 | d_{\mathcal{Z}}(X, X') \leq r_{\min}, X' \in \text{supp}(\lambda_i \cap \lambda_j)) + \\ & \quad \Pr(\bar{\lambda}_i(X) \neq 0, \lambda_i(X) \neq 0, \bar{\lambda}_j(X) \neq 0, \lambda_j(X) = 0 | d_{\mathcal{Z}}(X, X') \leq r_{\min}, X' \in \text{supp}(\lambda_i \cap \lambda_j)) + \\ & \quad \Pr(\bar{\lambda}_i(X) \neq 0, \lambda_i(X) = 0, \bar{\lambda}_j(X) \neq 0, \lambda_j(X) \neq 0 | d_{\mathcal{Z}}(X, X') \leq r_{\min}, X' \in \text{supp}(\lambda_i \cap \lambda_j)). \end{aligned}$$

The probability $\Pr(\bar{\lambda}_i(X) \neq 0, \lambda_i(X) = 0, \bar{\lambda}_j(X) \neq 0, \lambda_j(X) = 0 | d_{\mathcal{Z}}(X, X') \leq r_{\min}, X' \in \text{supp}(\lambda_i \cap \lambda_j))$ means that X was previously in neither the support of λ_i or λ_j and now is in the support of both. This probability can be written as

$$\Pr(\lambda_i(X) = 0, \lambda_j(X) = 0 | d_{\mathcal{Z}}(X, X') \leq r_{\min}, X' \in \text{supp}(\lambda_i \cap \lambda_j)),$$

because X being within r_{\min} of the overlapping support automatically implies that $\bar{\lambda}_i(X), \bar{\lambda}_j(X) \neq 0$. Since $X' \in \text{supp}(\lambda_i \cap \lambda_j)$ is equivalent to $\lambda_i(X') \neq 0, \lambda_j(X') \neq 0$, we now have

$$\Pr(\lambda_i(X) = 0, \lambda_i(X') \neq 0, \lambda_j(X) = 0, \lambda_j(X') \neq 0 | d_{\mathcal{Z}}(X, X') \leq r_{\min}, X' \in \text{supp}(\lambda_i \cap \lambda_j)).$$

By logic from Lemma 5, this is at least

$$\begin{aligned} & \Pr(\lambda_i(X) = 0, \lambda_i(X') \neq 0, \lambda_j(X) = 0, \lambda_j(X') \neq 0 | d_{\mathcal{Z}}(X, X') \leq r_{\min}) \\ & = \Pr(\lambda_i(X) = 0, \lambda_i(X') \neq 0 | d_{\mathcal{Z}}(X, X') \leq r_{\min}) \Pr(\lambda_j(X) = 0, \lambda_j(X') \neq 0 | d_{\mathcal{Z}}(X, X') \leq r_{\min}). \end{aligned}$$

Similarly, the other two probabilities can be written as

$$\begin{aligned} & \Pr(\lambda_i(X) \neq 0, \lambda_i(X') \neq 0 | d_{\mathcal{Z}}(X, X') \leq r_{\min}) \Pr(\lambda_j(X) = 0, \lambda_j(X') \neq 0 | d_{\mathcal{Z}}(X, X') \leq r_{\min}), \\ & \Pr(\lambda_i(X) = 0, \lambda_i(X') \neq 0 | d_{\mathcal{Z}}(X, X') \leq r_{\min}) \Pr(\lambda_j(X) \neq 0, \lambda_j(X') \neq 0 | d_{\mathcal{Z}}(X, X') \leq r_{\min}). \end{aligned}$$

Adding these together and bounding by L_{\min} , (42) becomes

$$\begin{aligned} & \Pr(X \in \text{supp}(\bar{\lambda}_i \cap \bar{\lambda}_j) \setminus \text{supp}(\lambda_i \cap \lambda_j)) \\ & \geq (L_{\min}^2 + 2L_{\min}(1 - L_{\min})) \times \Pr(d_{\mathcal{Z}}(X, X') \leq r_{\min}, X' \in \text{supp}(\lambda_i \cap \lambda_j)) \\ & \geq (2L_{\min} - L_{\min}^2) \times \Pr(d_{\mathcal{Z}}(X, X') \leq r_{\min}, X' \in \text{supp}(\lambda_i \cap \lambda_j)) \\ & \geq (2L_{\min} - L_{\min}^2) \times p_{d(r_{\min})}o_{\min}. \end{aligned}$$

Therefore, the new overlap is at least

$$\Pr(X \in \text{supp}(\bar{\lambda}_i) \cap \text{supp}(\bar{\lambda}_j)) \geq (1 + (2L_{\min} - L_{\min}^2) \times p_{d(r_{\min})})o_{\min}.$$

□

Task (Embedding)	T	m/T	Prop	End Model	N_{train}	N_{dev}	N_{test}
Spam (BERT)	1	10	0.49	BERT-Base	1,586	120	250
Weather (BERT)	1	103	0.53	BERT-Base	187	50	50
Spouse (BERT)	1	9	0.07	LSTM	22,254	2,811	2,701
Basketball (RN-101)	8	4	0.12	ResNet-18	3,594	212	244
Commercial (RN-101)	6	4	0.32	ResNet-50	64,130	9,479	7,496
Tennis (RN-101)	14	6	0.34	ResNet-50	6,959	746	1,098
Basketball (BiT-M)	8	4	0.12	BiT-M-R50x1	3,594	212	244
Commercial (BiT-M)	6	4	0.32	BiT-M-R50x1	64,130	9,479	7,496
Tennis (BiT-M)	14	6	0.34	BiT-M-R50x1	6,959	746	1,098

Table 4: Details for each dataset. T : the number of related elements modeled by the weak supervision label model. m/T : the number of supervision sources per element. **Prop**: The proportion of positive examples in each dataset. **End Model**: The end model used for fully-trained deep network baselines (TS-FT, WS-FT, and EPOXY-FT). N_{train} : The size of the unlabeled training set. N_{dev} : The size of the labeled dev set. N_{test} : The size of the held-out test set.

D Experimental Details

We describe additional details about each task, including details about data sources (Section D.1), end models (Section D.2), supervision sources (Section D.3), and setting extension thresholds (Section D.4).

D.1 Dataset Details

Table 4 provides details on train/dev/test splits for each dataset, as well as statistics about the positive class proportion and the number of labeling functions. Additional details about each dataset are provided below.

Spam We use the dataset as provided by Snorkel² and those train/dev/test splits.

Weather, Spouse These datasets are used in [52] and [20] for evaluation, and we use the train/dev/test splits from those works (**Weather** is called **Crowd** in that work).

Basketball This dataset is a subset of ActivityNet and was used for evaluation in [57] and [20]. We use the train/dev/test splits from those works.

Commercial We use the dataset from [21] and [20] and the train/dev/test splits from those works.

Tennis We use the dataset from [20] and the train/dev/test splits from those works.

D.2 Task-Specific End Models

For **Spam** and **Weather**, we use BERT-Base for sequence classification as implemented by HuggingFace [68], and tune the learning rate and number of epochs with grid search (ultimately using 0.00005, 4 epochs for **Spam** and 0.00004, 40 epochs with early stopping for **Weather**). For **Spouse**, we use an LSTM as used in [52] and [20], and use the hyperparameters from [20]. For **Basketball**, **Commercial**, and **Tennis**, we use different end models depending on which embedding we are evaluating in order to provide a fair comparison. When using RN-101 pre-trained on ImageNet for embeddings, we use ResNet’s pre-trained on ImageNet, as in [20] (RN-18 for **Basketball**, RN-50 for **Commercial** and **Tennis**). For these end models, we use hyperparameters from the previous work [20]. When using BiT-M for the embeddings, we fine-tune BiT-M for the end model. We use the default hyperparameters from BiT-M using the BiT “hyperrule” as detailed in [33], but we resize frames to 256 by 256 and use batch size of 128 for memory. To adjust for the smaller batch size, we tune learning rate between 0.001 and 0.003, as recommended by the official BiT implementation. We end up using 0.003 for **Basketball**, and 0.001 for **Commercial** and **Tennis**.

²<https://www.snorkel.org/use-cases/01-spam-tutorial>

D.3 Supervision Sources

Supervision sources are expressed as short Python functions. Each source relied on different information to assign noisy labels:

Spam, Weather, Spouse For these tasks, we used the same supervision sources as used in previous work [52, 20]. These are all text classification tasks, so they rely on text-based heuristics such as the presence or absence of certain words, or particular regex patterns.

Basketball, Commercial, Tennis Again, we use sources from previous work [57, 20]. For **Basketball**, these sources rely on an off-the-shelf object detector to detect balls or people, and use heuristics based on the average pixel of the detected ball or distance between the ball and person to determine whether the sport being played is basketball or not. For **Commercial**, there is a strong signal for the presence or absence of commercials in pixel histograms and the text; in particular, commercials are book-ended on either side by sequences of black frames, and commercial segments tend to have mixed-case or missing transcripts (whereas news segments are in all caps). For **Tennis**, we use an off-the-shelf pose detector to provide primitives for the weak supervision sources. The supervision sources are heuristics based on the number of people on court and their positions. Additional supervision sources use color histograms of the frames (i.e., how green the frame is, or whether there are enough white pixels for the court markings to be shown).

D.4 Setting r_i

We tune r_i using the dev set in two steps. First, we set all the r_i to the same value r and use grid search over r . Then, we perform a series of small per-coordinate searches for a subset of the labeling functions to optimize individual r_i values. For labeling functions with full coverage, we set the threshold to have no extensions.

Now we report thresholds in terms of *cosine similarities* (note that this is a different presentation than in terms of distances). For **Spam**, all thresholds are set to 0.85, except for LF’s 4 and 7, which have thresholds 0.81 and 0.88. For **Weather**, all thresholds are set to 0.87, except for LF 0, which has threshold 0.88. For **Spouse**, thresholds are set to [0.955, 0.953, 0.95, 0.95, 0.951, 0.945, 0.95, 0.95, 0.95] for LF’s 0 – 8. For **Basketball**, thresholds are set to [1.0, 1.0, 0.1, 1.0] and [0.6, 1.0, 0.53, 1.0] for RN-101 and BiT-M embeddings, respectively. For **Commercial**, thresholds are set to [0.2, 1.0, 0.15, 0.15] and [0.63, 1.0, 0.4, 0.565] for RN-101 and BiT-M embeddings, respectively. For **Tennis**, thresholds are set to [1.0, 1.0, 1.0, 0.25, 1.0, 0.4] and [1.0, 1.0, 1.0, 0.8, 1.0, 0.9] for RN-101 and BiT-M embeddings, respectively.

E Additional Evaluation

We provide additional evaluation. We present synthetic experiments validating our theoretical insights (Section E.1); additional interactive-speed baseline methods including other label models and other methods for transfer learning without fine-tuning (Section E.2); more detailed metrics including standard deviations of training runs and precision/recall breakdowns for label models (Section E.3); measurements of how fine-tuning changes embeddings (Section E.4); details and results for our ablation studies (Section E.5); and measurements of one-time preprocessing cost (Section E.6).

E.1 Synthetics

We evaluate our method of extending one labeling function on synthetic data in two experiments to confirm the insights about accuracy, embedding smoothness, and choice of threshold radius from Theorem 1. We create an embedding space over 10000 uniformly sampled points in $[0, 1]^2$ with a fixed class balance $\Pr(Y)$ and $m = 3$ labeling functions, where only λ_1 is extended. To understand the impact of a labeling function’s accuracy, we fix a task distribution by assigning Y labels in a 10×10 “checkerboard” pattern and run our algorithm on four versions of λ_1 with varying accuracy, keeping λ_1 ’s support consistent. In Figure 2 (left), we extend λ_1 based on r for each of the four versions of the labeling function. This confirms that extending a highly accurate labeling function results in greater generalization lift. To understand the impact of Lipschitzness of the task distribution, we produce four distributions of Y over the embedding space, three of which follow a checkerboard

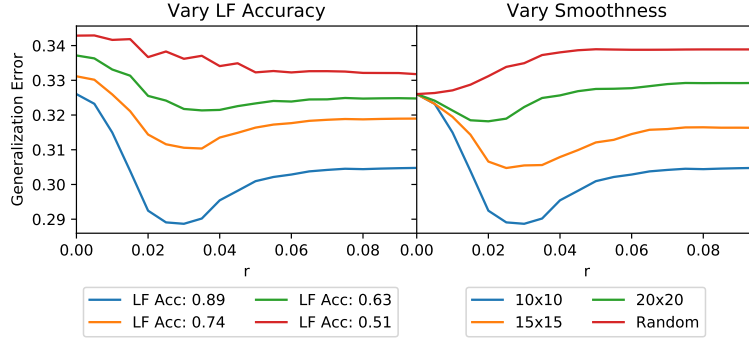


Figure 2: Reduction in generalization error from extending labeling functions of varying accuracies (left), and on embedding spaces of varying smoothness (right).

		Label Models				NFT Baselines			
	Task (Embedding)	EPOXY	MV-LM	DP-LM	WS-LM	TS-NFT	WS-NFT	TS-KNN	WS-KNN
NLP	Spam (BERT)	89.6	84.0	86.0	83.6	78.5	87.2	49.2	48.4
	Weather (BERT)	82.0	78.0	78.0	78.0	71.6	74.4	64.0	58.0
	Spouse (BERT)	48.4	46.6	42.3	47.0	17.7	17.5	0.0	4.9
Video	Basketball (RN-101)	31.3	17.7	14.0	27.9	18.8	16.8	0.0	0.0
	Commercial (RN-101)	90.1	83.7	83.7	88.4	73.6	75.5	30.7	30.3
	Tennis (RN-101)	82.9	80.8	80.7	82.0	76.7	79.5	43.5	52.6
	Basketball (BiT-M)	42.5	17.7	14.0	27.9	22.8	23.2	5.6	10.2
	Commercial (BiT-M)	91.8	83.7	83.7	88.4	71.7	73.8	29.3	45.3
	Tennis (BiT-M)	83.1	80.8	80.7	82.0	75.5	79.0	50.1	52.1

Table 5: EPOXY performance compared to additional label models and TL without fine-tuning baselines. MV-LM is majority vote over labeling function outputs; DP-LM is the label model from [52]; WS-LM is the label model from [20]. TS-NFT and WS-NFT train a single fully-connected layer over pretrained embeddings using dev set labels or WS labels over the training set; TS-KNN and WS-KNN train a nearest neighbors classifier over pretrained embeddings using dev set labels or WS labels over the training set.

clustering pattern (such that more divisions mean less smoothness), and one that spatially distributes the values of Y at random. In Figure 2 (right), each curve represents performance of the same high-accuracy labeling function ($a_1 = 0.89$) over embeddings of varying Lipschitzness. This confirms that the greatest improvement due to an extension occurs for the smoothest embedding. Lastly, both of these graphs illustrate the tradeoff in setting a threshold radius, confirming the theoretical insight that over-extending a labeling function can yield worse performance.

Note that our synthetic experiments reflect the observations from Theorem 1. This suggests selecting a threshold radius by maximizing the performance of the lower bound $\mathcal{R}(f_{WS}) - \mathcal{R}(f_E)$ from the theorem. We sketch the process. All elements of the bound can be estimated or are already known. We can use \hat{a}_i and \hat{C} as estimates of the accuracies in standard WS, and p_i , $p_{d(r)}$, and $L_{\chi'_i}(r)$ are directly estimatable. The only other term left to approximate is $M_Y(r)$. There are two ways to do this: first, we can use the development set to directly compute the Lipschitzness upper bound. Alternatively, we can use Proposition 2 and estimate $M_{f_z}(r) + 2\mathcal{R}(f_z)$ instead by choosing a simple model f_z on the given embedding. Using these values, it is possible to select a threshold radius for λ_i to optimize the lower bound on the generalization lift.

E.2 Additional Baselines

Table 5 shows additional interactive-speed baselines that we compared against. In addition to the label model from [20], which we compare against in Section 5 (WS-LM), we also compare against the label model from Snorkel [52] (DP-LM) and a majority vote baseline (MV-LM). We also report results from another method of using pretrained embeddings without fine-tuning—KNN search. TS-KNN reports the performance of using the embeddings for a KNN classifier trained with labels

	Task (Embedding)	TS-NFT	WS-NFT	TS-FT	WS-FT	EPOXY-FT
NLP	Spam (BERT)	78.5 (10.8)	87.2 (4.2)	76.7 (17.1)	90.0 (4.1)	94.1 (1.8)
	Weather (BERT)	71.6 (1.7)	74.4 (5.5)	71.2 (10.1)	85.6 (2.2)	86.8 (3.0)
	Spouse (BERT)	17.7 (7.5)	17.5 (2.8)	20.4 (0.2)	49.6 (2.4)	51.3 (0.9)
Video	Basketball (RN-101)	18.8 (8.5)	16.8 (4.7)	26.8 (1.3)	35.8 (1.5)	36.7 (1.3)
	Commercial (RN-101)	73.6 (2.6)	75.5 (1.3)	90.9 (1.0)	92.5 (0.3)	93.0 (0.3)
	Tennis (RN-101)	76.7 (3.3)	79.5 (7.1)	57.6 (3.4)	82.9 (1.0)	83.1 (0.5)
	Basketball (BiT-M)	22.8 (7.5)	23.2 (3.6)	29.1 (5.4)	33.8 (7.3)	45.8 (5.2)
	Commercial (BiT-M)	71.7 (2.0)	73.8 (2.8)	93.2 (0.4)	93.7 (0.3)	94.4 (0.2)
	Tennis (BiT-M)	75.5 (3.1)	79.0 (1.6)	47.5 (7.4)	83.7 (0.1)	83.8 (0.4)

Table 6: Average and standard deviation in parentheses of methods trained with SGD, taken over five random seeds.

Task (Embedding)	Metric	EPOXY	WS-LM
Spam (BERT)	Precision	88.3	86.7
	Recall	89.8	77.1
	F1	89.1	81.6
Weather (BERT)	Precision	91.3	90.5
	Recall	75.0	67.9
	F1	82.4	77.6
Spouse (BERT)	Precision	41.6	37.5
	Recall	57.8	58.3
	F1	48.4	45.7
Basketball (RN-101)	Precision	26.1	26.7
	Recall	39.0	29.3
	F1	31.3	27.9
Commercial (RN-101)	Precision	91.1	89.9
	Recall	89.0	86.8
	F1	90.1	88.3
Tennis (RN-101)	Precision	79.6	79.8
	Recall	86.5	85.7
	F1	82.9	82.7
Basketball (BiT-M)	Precision	27.8	26.7
	Recall	89.4	29.3
	F1	42.5	27.9
Commercial (BiT-M)	Precision	90.7	89.9
	Recall	93.0	86.8
	F1	91.8	88.3
Tennis (BiT-M)	Precision	80.0	79.8
	Recall	86.5	85.7
	F1	83.1	82.7

Table 7: Precision, Recall, and F1 scores for EPOXY and WS-LM for all tasks. In most cases, the lift from EPOXY is largely due to improvement in recall.

over the dev set, while WS-KNN reports the performance of a KNN classifier trained over labels generated by WS-LM over the unlabeled training set.

E.3 Detailed Metrics

We provide more details about our experimental results. First, we report measures of variance for non-deterministic methods. Table 6 reports the means and standard deviations for the results from Table 1 that required training layers of a deep network using SGD. We report results from runs with five random seeds. All other methods (label models) are deterministic.

Next, we discuss lift of EPOXY over WS-LM in more detail, in terms of both precision and recall. As Table 2 from Section 5 suggests, EPOXY primarily improves over WS-LM by improving coverage of the labeling functions. Table 7 shows precision, recall, and F1 scores for all tasks for EPOXY and WS-LM. In most tasks, the performance lift of EPOXY over WS-LM is primarily reflected in the increase in recall—exposing the mechanism through which increased coverage results in improved performance.

	BERT			RN-101 ImageNet			BiT-M RN-50x1		
	Spam	Weather	Spouse	Basketball	Commercial	Tennis	Basketball	Commercial	Tennis
min. pre-pool similarity	0.313	0.293	-0.061	0.481	-0.023	0.323	-0.061	-0.092	-0.069
$1 - d(PT, DN)$	0.735	0.677	0.248	0.562	0.284	0.113	0.907	0.559	0.408
WS-FT vs. WS-NFT	+2.8	+11.2	+32.1	+19.0	+17.0	+3.4	+10.6	+19.9	+4.7

Table 8: min. pre-pool similarity is the minimum similarity between pretrained and fine-tuned embeddings before the pooling step (tokens for text, spatial areas for visual). Fine-tuning can change the embeddings in ways that are not reflected in the overall embedding distance ($1 - d(PT - DN)$) but still move the features—resulting in a gap between WS-FT and WS-NFT.

Task	EPOXY-fixed- r	EPOXY
Spam (BERT)	88.0	89.6
Weather (BERT)	80.0	82.0
Spouse (BERT)	43.9	48.4
Basketball (RN-101)	23.8	31.3
Commercial (RN-101)	89.1	90.1
Tennis (RN-101)	82.6	82.9
Basketball (RN-101)	34.5	42.5
Commercial (RN-101)	90.5	91.8
Tennis (RN-101)	82.7	83.1

Table 9: EPOXY performance degrades when setting a fixed threshold for all labeling functions.

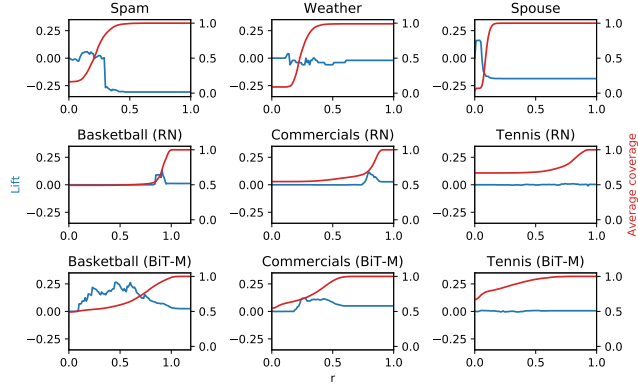


Figure 3: Lift (blue, left Y axis) and coverage (red, right Y axis) for different thresholds (same threshold for all labeling sources).

E.4 Measuring Changes from Fine-Tuning

As discussed in Section 5, the similarity between pretrained and fine-tuned embeddings $1 - d(PT, DN)$ is a good predictor for how much lift EPOXY can provide over WS-LM. However, it is not a good predictor of the relative performance of transfer learning without fine-tuning. We investigated this phenomenon, and found that a major cause of this gap is that fine-tuning can change the embeddings in ways that are reflected in a distance metric.

Table 8 demonstrates this phenomenon and reports *min. pre-pool similarity*, an additional metric demonstrating that embeddings can be changed significantly during fine-tuning without the differences being reflected in an overall similarity metric. This metric looks at similarity one step before the final embeddings are generated. In both NLP and video applications, the pre-trained networks generate many descriptors for each dataset; BERT generates an embedding for each token in the sentence, while ResNet’s and BiT-M generate embeddings over convolutional windows of each frame. Normally, these embeddings are pooled to generate a single embedding for the data point. min. pre-pool similarity reports the minimum similarity between matching descriptors *before* this pooling step. For example, for a sentence, it compares embeddings of the first token generated by the pre-trained and fine-tuned network, embeddings of the second token, and so on, and takes the minimum similarity. For the ResNet’s, it compares matching convolutional windows for the same data point. For each of the datasets, this metric is *low*, demonstrating that the embeddings before the pooling step are changing significantly. This helps explain why there can be a gap between fine-tuned and pre-trained performance, even though the overall (pooled) similarity between fine-tuned and pre-trained embeddings is high.

E.5 Ablations

We report the results of two ablation studies. In the first, we use a single fixed threshold for extension for each labeling function in a given task, instead of tuning different thresholds for different labeling functions. The results are shown in Table 9 in the EPOXY-fixed- r column. Second, we report the effects of sweeping a fixed threshold for each task. Figure 3 shows relative lift and average coverage

of labeling functions for different values of a fixed threshold r . For each task, there is a region where lift increases as r increases (corresponding to an increase in average coverage), but lift decreases if the threshold is set too large (corresponding to the region where the extended labeling functions become too inaccurate).

E.6 Pre-Processing Time

Task (Embedding)	Embedding pre-processing time (s)
Spam (BERT)	21.3
Weather (BERT)	6.1
Spouse (BERT)	417.6
Basketball (RN-101)	71.1
Commercial (RN-101)	329.5
Tennis (RN-101)	47.1
Basketball (BiT-M)	85.6
Commercial (BiT-M)	401.9
Tennis (BiT-M)	91.5
Average	163.5

Table 10: One-time pre-processing cost in seconds to compute embeddings and pairwise distances for each dataset.

Both EPOXY and the baseline transfer learning without fine-tuning methods require running inference over the datasets with pre-trained deep networks as a pre-processing step. Table 10 reports this one-time pre-processing cost for each dataset. On average, pre-processing the data requires less than three minutes.